Utilizing High-throughput Phenotyping to dissect Plant Genetic Resources of Wheat and Chickpea under Drought Stress

Kumulative Dissertation
zur Erlangung des Doktorgrades
der Agrarwissenschaften (Dr. agr.)

der

Naturwissenschaftlichen Fakultät III
Agrar- und Ernährungswissenschaften,
Geowissenschaften und Informatik
der Martin-Luther-Universität Halle-Wittenberg

vorgelegt von
Frau Madita Maria Lauterberg

Erster Gutachter: Prof. Dr. Klaus Pillen
Zweiter Gutachter: Prof. Dr. Achim Walter (ETH, Zürich)
verteidigt am 24.02.2025

Outline

Summary

According to United Nations estimates, the world population will continue to grow and the climate will become more unpredictable over the next decades. On the one hand, this places high demands on agricultural production and, on the other hand, challenges for stable production under unstable growing conditions. Plant breeding is crucial to provide cultivars that produce high yields under unstable conditions such as drought stress. Climate require adaptation to unstable conditions. Therefore, it is a valuable approach to consider plant genetic resources (PGR) and deciding on the choice of crop. PGR are necessary to provide a basis of genetic variation for plant breeding. High-throughput phenotyping (HTP) is a useful tool for testing PGR for drought tolerance. Although the costs of genotyping have fallen in recent decades, phenotyping is still costly and time-consuming. With HTP, plants are imaged repeatedly in the greenhouse or in the field without being destroyed. These images are evaluated for traits characteristics such as biomass (estimated biovolume), plant height, mean color value or even the yellow to green color ratio. HTP can be supplemented with an imaging system for photosynthesis using chlorophyll fluorescence, so that physiological traits can also be precisely recorded.

The PGR of wheat also includes wild emmer. Genotypes of wild emmer were selected to integrate the advantageous phenotypes for drought stress in elite cultivars. With targeted backcrossing it takes several generation cycles to create the Near-isogenic lines (NIL). These carry only a quantitative trait locus (QTL) from wild emmer wheat and are otherwise the elite cultivar. This means that the disadvantages of wild emmer wheat, such as spindle brittleness, were excluded. An HTP experiment was conducted to test this material over its entire life cycle. This confirmed the effect of the QTLs, which had already been documented in field experiments, and provided further insights. One QTL causes the stay-green effect, i.e. delayed ripening and thus a longer grain-filling phase, which in turn led to an increased thousand-kernel weight during the drought stress. This effect could be determined exclusively via color traits with HTP for single days.

Chickpea is a protein-rich, robust crop that can fix nitrogen from the air. Currently, chickpea production is focused on India and Australia. As a result of climate change and increased demand, the cultivation of chickpeas in southern Europe is becoming more attractive. In the usual growing regions in India and Australia, drought stress is prevalent during the final growth phase. However, with unpredictable climatic conditions, tolerance to drought stress in the vegetative development phase is essential. 60 genotypes of chickpea PGR were tested for the first time on an HTP system in drought stress with subsequent rewatering. Phenotypic variation was observed. In addition, the two types of chickpea, *desi* and *kabuli*, were compared. *Desi* is the predominant commercial type in India, with black, green or beige seeds. In addition, the plants and chickpeas are smaller and have a rough surface. *Kabuli* is the type marketed in Europe. The chickpeas and plants are larger and have an exclusively beige, smooth seed coat. Genotypes of the *desi* type were significantly more tolerant than *kabuli* genotypes under drought stress and showed more dynamic growth when rewatering.

Chlorophyll fluorescence measurements most often include the maximum quantum yield (F_v/F_m) and the operating efficiency of photosystem II (ΦPSII), as these traits are practical to measure. The heat emission of photosynthesis, non-photochemical quenching (NPQ), is rarely measured. To measure

NPQ, fully dark adaptation is necessary, as well as a phase in which the plants re-adapt to the light, followed by a further dark adaptation. Since the first measurement point for dark-adapted plants is the very constant value F_v/F_m for healthy plants, it can be measured once for the plants in the experiment and does not have to be measured every time for NPQ. Furthermore, further adaptation to darkness can be accelerated by applying far-red light (700-750nm wavelength). Far-red light ensures that the electrons move from photosystem II to the next electron acceptor, plastoquinone. These aspects bring a temporal advantage. An adapted measurement protocol for theoretical NPQ ($NPQ_{(T)}$) was successfully implemented for HTP with the 60 genotypes of chickpeas. NPQ has recently been put in a new light by two publications with tobacco and soybeans. It was found that the plants had significantly higher yields and biomass production if they were able to quickly shut down the NPQ protective mechanism during the transition from high light to low light. The tolerance of the *desi* genotypes to drought stress could also be further dissected using $NPQ_{(T)}$. A more efficient release of excess energy and a higher plasticity of *desi* for NPQ could contribute to the better tolerance under drought stress.

HTP can be engaged to screen PGR for breeding under drought stress. It was shown how chickpeas can be selected for drought stress tolerance. Furthermore, NPQ was measured for the first time with HTP and further highlighted the drought tolerance of *desi* chickpeas. There will always be challenges when combining or comparing two experiments. This applies to field as well as greenhouse studies. Therefore, experiments in different environments should complement each other and be conducted in accordance with good scientific practice. HTP can be used to screen for PGR or to examine advanced breeding material NIL or contrasting genotypes precisely and with traits from daily image recordings. In addition, HTP studies in controlled environments are leading the way, as studies can be conducted in simulations of future climate conditions.

Zusammenfassung

In den nächsten Jahrzehenten wird die Weltbevölkerung laut Schätzungen der Vereinten Nationen weiter zunehmen und das Klima unbeständiger werden. Das stellt zum einen hohe Anforderungen an die landwirtschaftliche Produktion und andererseits Herausforderungen an eine stabile Produktion bei unsteten Bedingungen. Pflanzenzüchtung ist entscheidend um Sorten bereitzustellen, die hohe Erträge unter unsteten Bedingungen wie Dürre bringen. Die klimatischen Anbaubedingungen fordern Anpassungen an unstete Bedingungen. Daher ist es ein wertvoller Ansatz, Pflanzen Genetische Ressourcen (PGR) in Betracht zu ziehen und auch über die Wahl der Kulturpflanze zu entscheiden. PGR sind notwendig um eine Grundlage an genetischer Variation für die Pflanzenzüchtung zu geben. Um die PGR hinsichtlich ihrer Dürretoleranz zu testen, bietet sich High-throughput Phenotyping (HTP) an. Zwar sind die Kosten für Genotypisierung in den letzten Jahrzehnten gesunken, Phänotypiserung ist immer noch kostenintensiv und zeitaufwändig. Mit HTP werden im Gewächshaus oder im Feld Pflanzen zerstörungsfrei und wiederholt fotografiert. Diese Bilder werden für zahlreiche Merkmale wie die Biomasse, das geschätzte Biovolumen, Pflanzenhöhe, den mittleren Farbwert oder auch das gelb zu grün Farbverhältnis ausgewertet. Ergänzt werden kann HTP mit einem Bildgebungssystem für Photosynthese mittels Chlorophyll Fluoreszenz, sodass auch physiologische Merkmale präzise erfasst werden.

Zu den PGR von Weizen gehört auch der wilde Emmer. Genotypen vom wilden Emmer wurden ausgewählt, um die vorteilhaften Phänotypen während Dürre in Elitesorten zu integrieren. Bei einer gezielten Rückkreuzung dauert es mehrere Generationen, bis die Near-isogenic Lines (NIL) entstehen. Diese tragen nur einen Quantitativen Trait Loci (QTL) von wildem Emmer und sind ansonsten die Elitesorte. Das bedeutet, das Nachteile vom wilden Emmer, wie zum Beispiel Spindelbrüchigkeit ausgeschlossen werden. Um dieses Material über den gesamten Lebenszyklus zu testen wurde ein HTP Experiment durchgeführt. Damit konnte der Effekt der QTLs, welcher in Feldexpeimenten bereits dokumentiert wurde, bestätigt und weiter aufgeklärt werden. So bewirkt der eine QTL den stay-green effect, also eine verspätete Abreife und damit längere Kornfüllungsphase, die wiederum zu einem erhöhten Tausendkorngewicht während der Dürre geführt hat. Diesen Effekt konnte man ausschließlich über Farbmerkmale mit HTP für vereinzelte Tage bestimmen.

Kichererbsen sind eine proteinreiche, robuste Kulturpflanze, die Stickstoff aus der Luft binden kann. Derzeit fokussiert sich der Anbau auf Indien und Australien. Im Zuge der klimatischen Veränderungen und erhöhten Nachfrage wird der Anbau von Kichererbsen in Südeuropa interessant. In den üblichen Anbauregionen in Indien und Australien ist Trockenstress während der finalen Wachstumsphase vorherrschend. Mit unsteten klimatischen Bedingungen, ist jedoch eine Toleranz zu Trockenstress in der vegetativen Entwicklungsphase essentiell. Sechzig Genotypen der PGR der Kichererbse wurden erstmals auf einem HTP System im Trockenstress mit anschließender Wiederbewässerung getestet. Es konnte eine phänotypische Variation festgestellt werden. Zudem wurden die beiden Typen der Kichererbse *desi* und *kabuli* verglichen. *Desi* ist der vorherrschende Vermarktungstyp in Indien, hat schwarz, grün oder beige Körner. Zudem sind die Pflanzen und Kichererbsen kleiner und haben eine raue Oberfläche. *Kabuli* ist der Typ der in Europa vermarktet wird. Die Kichererbsen und Pflanzen sind größer und besitzt eine ausschließlich beige glatte Samenschale. Genotypen des Typen *desi*

waren signifikant toleranter als Genotypen von *kabuli* im Trockenstress und zeigte ein dynamischeres Wachstum bei der Wiederbewässerung.
Mit Chlorophyll Fluoreszenz werden meistens die maximale Quantenausbeute (F_v/F_m) und die Nutzungseffizienz des Photosystem II (operating efficiency ΦPSII) gemessen, da diese Merkmale praktikabel zu messen sind. Die Wärmeabgabe der Photosynthese, das non-photochemical quenching (NPQ) wird selten gemessen. Um NPQ zu messen, ist vollkommene dunkel-adaptation notwendig sowie eine Phase in der sich die Pflanzen wieder an das Licht adaptiert, gefolgt von einer weiteren dunkel-adaption. Da der erste Messpunkt bei dunkeladaptierten Pflanzen der sehr konstanter Wert für F_v/F_m für gesunde Pflanzen ist, kann dieser auch einmal für die Pflanzen des Experimentes gemessen werden und muss nicht jedes Mal für NPQ gemessen werden. Zudem kann die weitere Adapation an Dunkelheit mit der Applikation von Far-red light (700-750nm Wellenlänge) beschleunigt werden. Far-red light sorgt dafür, dass die Elektronen sich von dem Photosystem II weiter zum nächsten Elektronenakzeptor, dem Plastoquinone bewegen. Diese Aspekte bringen einen zeitlichen Vorteil. Ein angepasstes Messprotokoll für theoretischen NPQ ($NPQ_{(T)}$) wurde für HTP mit den sechzig Genotypen der Kichererbsen erfolgreich umgesetzt. NPQ wurde erst kürzlich durch zwei Publikationen mit Tabak und Sojabohnen in neues Licht gerückt. Es konnte festgestellt werden, dass die Pflanzen einen deutlich höheren Ertrag und Biomasse Produktion haben, sofern sie den Schutzmechanismus NPQ beim Übergang von viel Licht zu wenig Licht schnell wieder runterfahren konnten. Auch für Trockenstress konnte die Tolerance von den *desi* Genotypen mittels $NPQ_{(T)}$ weiter aufgeschlüsselt werden. Eine effizientere Abgabe der überflüssigen Energie und eine höhere Plastizität von *desi* für NPQ könnten zu der besseren Toleranz unter Trockenstress beitragen.

HTP kann angewendet werden um PGR für die Züchtung unter Trockenstress zu untersuchen. Es konnte gezeigt werden, wie Kichererbsen für Trockenstresstoleranz selektiert werden können. Darüber hinaus wurde NPQ das erste Mal mit HTP gemessen und hat die Toleranz von *desi* Kichererbsen gegenüber Trockenstess weiter herausgestellt. Es wird immer Herausforderungen geben, wenn zwei Experimente kombiniert oder miteinander verglichen werden sollen. Das gilt für Feld- sowie Gewächshausstudien. Daher sollten Experimente in unterschiedlichen Umwelten einander ergänzen und im Sinne der guten fachlichen Praxis durchgeführt werden. HTP kann verwendet werden, um PGR zu sichten oder um gezielt Zuchtlinien wie NIL oder kontrastierende Genotypen präzise und mit Merkmalen aus täglichen Bildaufnahmen zu untersuchen. Zudem sind HTP Studien in kontrollierten Umwelten wegweisen, da Studien in der Simulation von zukünftigen Klimabedingungen durchgeführt werden können.

1. General Introduction

1.1 Agriculture in a changing climate

Modern civilization was founded on agriculture. Today, agricultural and horticultural products are used for food, in the pharmaceutical industry, as a source of energy in industry, as animal feed and as fiber. Ensuring sustainable and equitable production to feed nourish a growing population is a global challenge for agriculture in a changing climate (Godfray et al., 2010).

Drought and the unpredictability of precipitation constitute a particular challenge. Globally, an increase in days without precipitation and the duration of drought stress periods as well as an increase in the intensity and frequency of wet extremes is expected (Giorgi et al., 2019). Along with an increase in temperature, that less precipitation is to be expected in Europe and the Mediterranean area (Figure 1) (Shiogama et al., 2022; Spinoni et al., 2018).

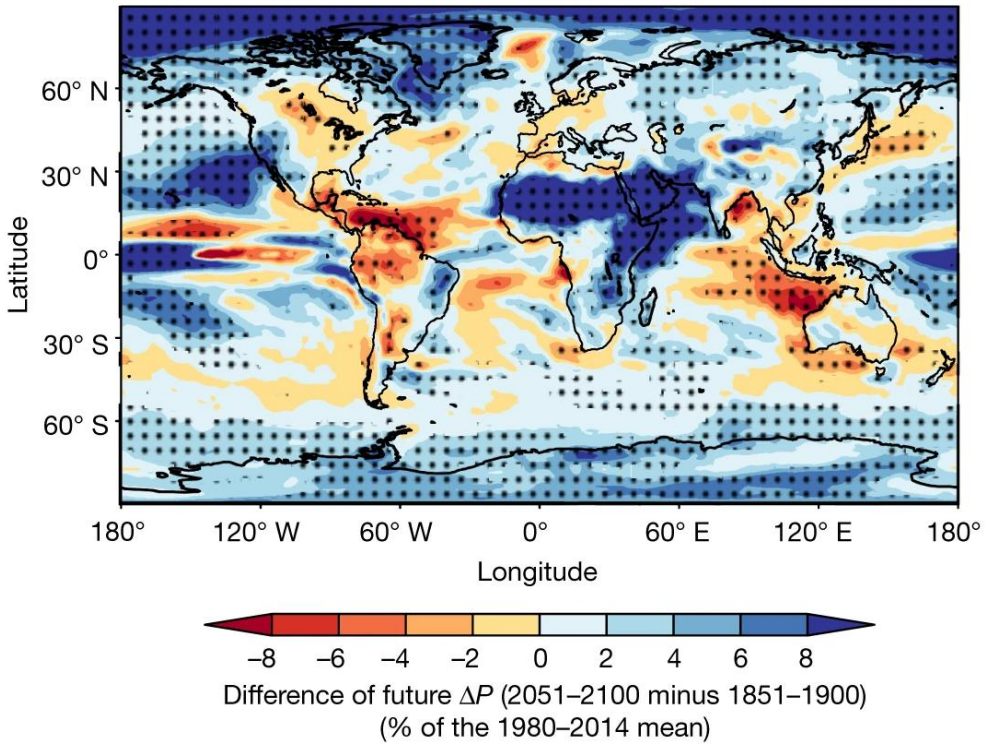

Figure 1: Spatial patterns of differences in future temperature and precipitation changes. Differences in future temperature changes (2051– 2100 minus 1851–1900 of hist+4.5, °C) between the OWM and the CWM of CMIP5 and CMIP66–8 (OWM minus CWM). The black hatches indicate that differences are significant at the ±10% level based on Welch's t-test. Figure adapted from figure 3b in reference (Shiogama et al., 2022)

It was estimated that global wheat production falls by 6% with each degree of warming (Asseng et al., 2015). A yield increase would be necessary, but in the recent decades yield stagnation in major production areas for wheat has been documented (Ray et al., 2012). This is due to socio-economic or political reasons, due to climate change and the genetic yield potential. It essential to adapt crops to

upcoming environmental conditions (Tester & Langridge, 2010). To increase the production of high-quality food under challenging conditions, legumes should be considered (Cullis & Kunert, 2016). Due to limited economic supply chain and other dominant crops, legumes, such as chickpea, received little attention of researchers, breeder, producers and consumers (Cullis & Kunert, 2016). Since they are more tolerant to harsh conditions and harbor valuable nutrients, it is time to investigate and improve their potential and give them the attention they deserve (Bellucci et al., 2021).

1.2 Chickpea – orphaned legume with potential

Next to soybean (*Glycine max*), common bean (*Phaseolus vulgaris*) and common pea (*Pisum sativum*), chickpea (*Cicer arietinum* L.) is the fourth most important legume (Semba et al., 2021).
Legumes, also known as pulses, are rich in protein and minerals and can play an important role in intercropping or crop rotations as they are capable to fix nitrogen from the air (López-Bellido et al., 2011). They are a part of the global diet and are gaining in importance as an alternative to reduced meat consumption (Foyer et al., 2016). This could be seen in the increase in the global production of legumes by 548.6 % between 1961/63 – 2014/16 (Nigam et al., 2021). The production of chickpea increased from 7.7 mio t in 1961 to 18.2 mio t in 2022 of which 13.5 mio t were produced in India (FAOSTAT, 2024) (Figure 2). Furthermore, chickpeas are produced in East and North Africa. In Europe, production is mainly located in Russia, Spain, Italy and the Balkan. In Europe, the cultivation of chickpeas was higher in the in the 1960s or 1990s. Cultivation declined due to falling demand and the difficult growing conditions caused by pathogen *Ascochyta rabiei* or *Ascochytes blight* (Bretag et al., 2008; Fanning et al., 2022; Singh et al., 2022).

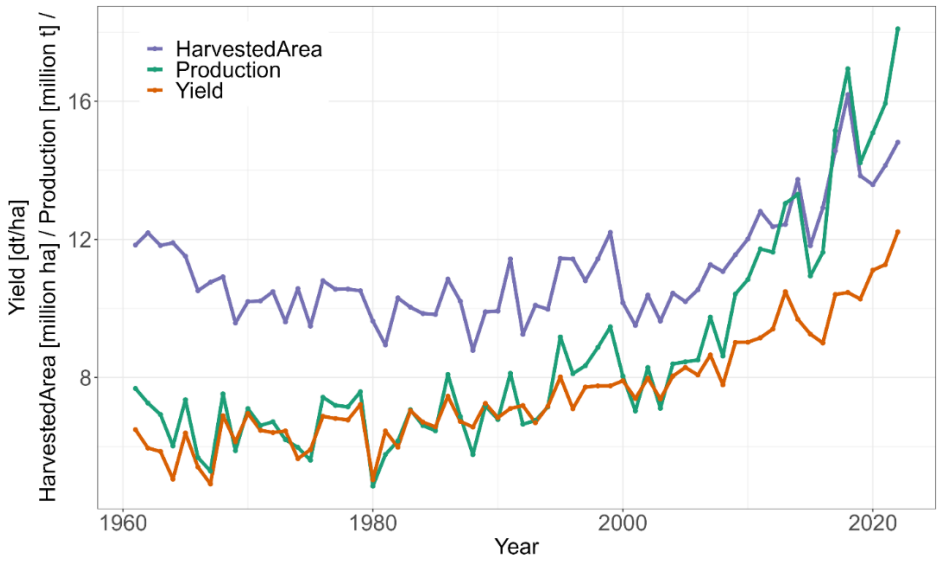

Figure 2: Harvested area, production and yield of chickpea worldwide. FAO STAT, 19.02.2024

Chickpea have the wild ancestor *C .reticulatum* and originate from the fertile crescent around 7,000 to 8,000 years ago (Gupta et al., 2016; Tanno & Willcox, 2006; Varshney et al., 2019). During

domestication, loss of seed dormancy, larger and more erected growing plants, larger seed sizes and reduced pod shattering were changed subsequently.
Chickpea is an annual and self-pollinating crop and reach a height of 0.2 – 0.5m with a bushy growth type, needs no vernalization and a minimum temperature of 12 °C for growth (Duarte, 2022). The yield components include the plant per square meter, the pods per plant, the number of seeds per pod and the seed weight. There is usually one seed per pod, but sometimes two seeds per pod, called double podding (Eker et al., 2022; Rubio et al., 2004). It is not certain whether double podding leads to higher yields.
Nowadays, two types of chickpea are differentiated: *desi* and *kabuli*. *Desi* is multi-colored and has less biomass and yield than *kabuli*, but is more tolerant to drought. Seeds of *kabuli* are of beige color with a larger size. Plants tend to be bigger. Based on the growth and seed morphology, *desi* is closer to the wild type *C. reticulatum* than *kabuli* (Gupta et al., 2016). One could assume, that crossing the two types of chickpea would lead to an improved intermediate type (Bayahi & Rezgui, 2018). Problematic is that an intermediate type is not requested by the consumers.
The genome of chickpea and the super-pangenome, based on eight annual *Cicer* wild species, have been published (Khan et al., 2024; Varshney, Song, et al., 2013). The chickpea genome is diploid (2n = 2x = 16), has a size of 738 Mbp and about 28,269 estimated genes. This published genome of chickpea and super-pangenome of *Cicer* wild species can be helpful for a more targeted crop improvement for challenging climate conditions.

1.3 Wheat – feeding the world population

Bread wheat (*Triticum aestivum*) and durum wheat (*T. durum*) are one of the most important crops worldwide. They provide feed and food for billions of people every day. In 2022, the worldwide production of wheat was 808 million tonnes and wheat was consumed mainly in baked goods such as bread or in pasta (FAOSTAT, 2024). Wheat is grown worldwide, with India and China being the main producers.
Wheat belongs to the family of *Poacea* and originates from the fertile crescent. Bread wheat and durum wheat developed through allopolyploidization 10,000 years ago (Avni et al. 2017).
Allotetraploid wild emmer (*T. turgidum* ssp*. diccocoides*, BBAA) originates from a hybridization of *T. urartu* (AA) and a now extinct, closely related species of *Aegilops speltoides* (B-like genome) (Avni et al. 2017). Domesticated emmer (*T. turgidum* ssp*. dicoccum*, BBAA) was developed by selecting spontaneous hulled seed mutants from wild emmer. Further selection for free-threshability during the domestication led to durum wheat (*T. turgidum* ssp*. durum*, BBAA). In addition, a hybridization of domesticated emmer and diploid *Aegilops tauschii* (DD) resulted in bread wheat (*T. aestivum*, BBAADD).
Besides, it was selected for grain size and a non-fragile rachis was one of the most important traits of domestication (Charmet, 2011).

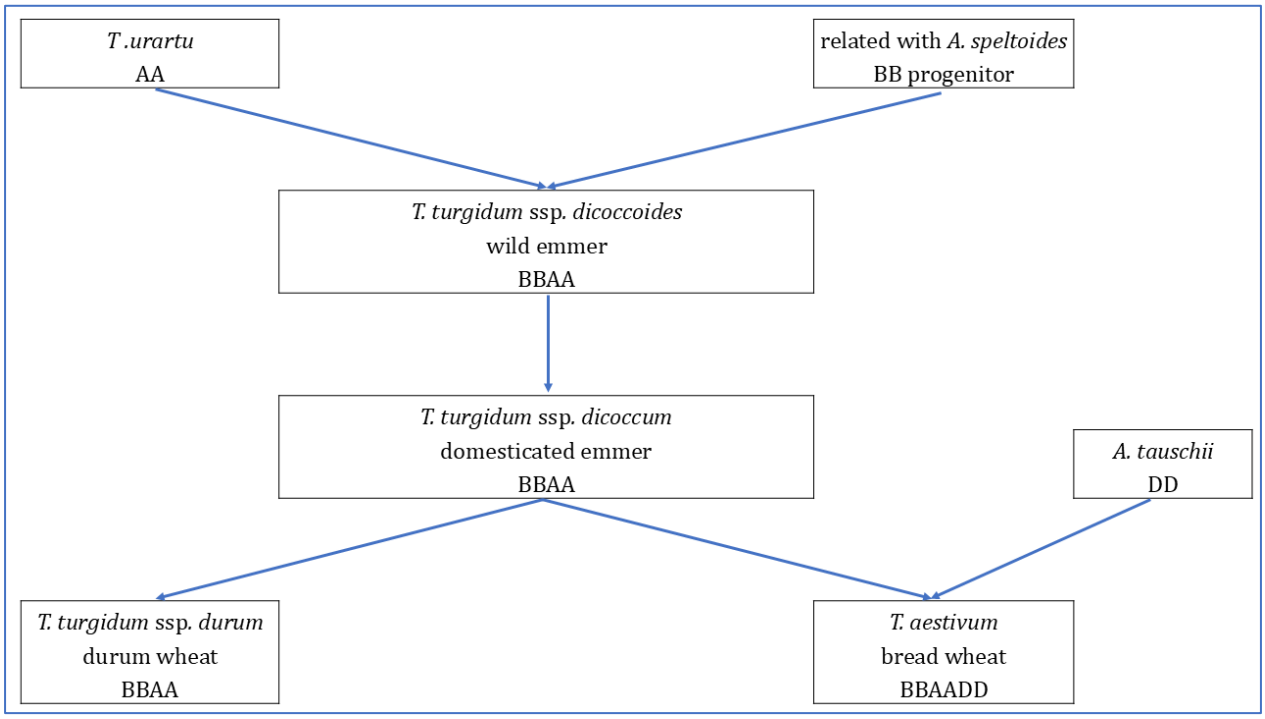

Figure 3: Model of evolution of *Triticum*. Modified after Avni et al. 2017.

This complex evolution of bread wheat resulted in a 14.1 gigabases genome with 107,891 high-confidence genes (The International Wheat Genome Sequencing Consortium (IWGSC) et al., 2018). The genome of durum wheat is smaller than the one of bread wheat (Maccaferri et al., 2019). The size of the reference genome of the cultivar Svevo is 10.45 gigabases and contains about 133,741 genes.
The close genetic distance among the species of *Triticum* makes it possible to transfer quantitative trait loci (QTL) across the genepool of *Triticum* and has the potential to improve the adaptation and tolerance to stress factors (Nevo & Chen, 2010; Sahrawat et al., 2003).

1.4 Plant Genetic Resources to enrich the narrowed genetic diversity of crops

Plant genetic resources (PGR) have been defined by the Food and Agriculture Organization (FAO) as the diversity of genetic material that includes everything from field-grown cultivars to landraces, wild relatives of crops and other wild plant species (FAO, 1998). All this material provides the raw material for breeding new cultivars.
Genetic diversity is influenced by recombination, mutation, genetic drift and gene flow. Recombination of selected genotypes is the base for breeding programs. Careful selection for many traits and over generations determines the best genotypes. As the best available cultivars are used for recombination in breeding programs, breeding narrowed the genetic base of modern cultivars (Tanksley & McCouch, 1997). Therefore, the exploitation, evaluation, conversation (*in situ*, *ex situ*) and utilization is of most importance for breeding cultivars resilient to upcoming climate scenarios (Zamir, 2001).
There is a classification of gene pools that reflect interspecies hybridization and evolutionary distance (Feuillet et al., 2008; Schoen et al., 2024). The species in the primary and secondary genepool share

homology in their genome and are sexually compatible. However, the crossing of species from the primary gene pool with the secondary gene pool is less successful than with species within the primary gene pool (Feuillet et al., 2008; Schoen et al., 2024). Examples for the primary genepool would be *T. aestivum* (AABBDD) and *T. turgidum* (AABB) and of the secondary it would be *T. monococcum* (AA) or *Ae.speltoides* (SS) (Figure 3). Species of the tertiary genepool would be rye (*Secale cereale*; RR) or barley (*Hordeum vulgare*; HH).

Another reason for a narrowed genetic diversity of crops is the founder effect associated with domestication for major traits such as non-brittle rachis in wheat, and the replacement of locally evolving landraces by elite cultivars (Abbo et al., 2003; Charmet, 2011). For chickpea, there are two factors which eroded the diversity: the limited distribution of the wild progenitor *C. reticulatum* and the early shift from winter to spring sowing, which was conducted to use the residual soil moisture instead of the rainfall. In fact, when resequencing 429 chickpea genotypes, of which 268 were landraces, 100 elite line, 44 breeding lines and 7 wild genotypes, based on the distribution of nucleotide diversity per kb, an 80% reduction in genetic diversity between wild genotypes and landraces and breeding lines has been revealed (Varshney et al., 2019). In addition, 122 candidate regions with 204 genes were identified and selected for post-domestication diversification and plant breeding. As these are associated with stress response, DNA repair, protein kinase activity, seed development, germination and flower development, they suggest a selection for stress resistance and phenological traits. This genotypic data has been combined with phenotypic data for drought and heat tolerance of 272 genotypes tested in 6 locations and 262 marker-trait associations have been detected by genome wide association study (GWAS), which highlighted the value of PGR for breeding for future climate scenario.

1.5 High-throughput Phenotyping with chlorophyll fluorescence

Genotyping has become an affordable technology in the recent years. However, a genotype (G) exhibits different phenotypes (P) which are dependent on environmental influences (E; P = G + E). Testing the plasticity of a genotype's phenotype in different environments is more complex than genotyping (Furbank et al., 2019; Walter et al., 2015). In the last decade, phenotyping has evolved with High-throughput Phenotyping (HTP) (Fiorani & Schurr, 2013; Furbank & Tester, 2011; Tardieu et al., 2017).

There are indoor and outdoor phenotyping systems. For outdoor imaging unmanned aerial vehicle (UAV) can be used (Khan et al., 2018). UAV-based systems can image plants in field conditions, but are limited by the size and weight of sensors and by the weather conditions. A permanently installed imaging system, is less dependent on the weather and can document the development of the plants with numerous sensors (Kirchgessner et al., 2017). Furthermore, there are several indoor HTP systems with different imaging set-up. Single plants are planted in one pot and on a daily basis transported to am imaging and watering system. The infested leaf area was determined using small HTP systems or three-dimensional imaging was also carried out (Hinterberger et al., 2022; Jahnke et al., 2016). Several imaging systems have been constructed to investigate large populations of small size plants such as lettuce to large plants, like maize (Amitrano et al., 2022; Cabrera-Bosquet et al., 2016). Usually the shoot is investigated, but root phenotyping systems are available, too (Shi et al.,

2023). Based on image analysis software, the shoot biomass, color ratios or color mean values are calculated (Das Choudhury et al., 2019; Klukas et al., 2014). The Digital Biomass or the Estimated Biovolume are proxies for the biomass, calculated of images from three different side views (Dhanagond et al., 2019; Shi et al., 2023). More advanced, plant organs, like the maize ear and silks can be captured and described by HTP (Brichet et al., 2017). HTP systems have been equipped with pulse amplitude modulation (PAM) fluorometers to measure chlorophyll fluorescence (Schreiber et al., 1986; Tschiersch et al., 2017). Chlorophyll fluorescence is used to measure photosynthetic activity of photosystem II (Murchie & Lawson, 2013).

An advantage of HTP in glasshouses with one-plant-per-pot experiments is that environmental factors can be changed to simulate different environments. For example, studies were carried out with salinity stress and 245 accessions of chickpea, to reveal vegetative growth of 477 spring-canola accessions or to dissect drought stress tolerance of 100 barley accessions (Atieno et al., 2017; Knoch et al., 2021; Meyer et al., 2023). These studies showed that HTP was useful to study the spatio-temporal effects in different stress conditions of PGR.

1.6 Impact of drought stress on plant development

Drought stress means that less water than necessary is available for the plants (Farooq et al., 2018; Tardieu et al., 2018). A plant's drought stress tolerance can be measured by whether biomass and yield are maintained despite the stress (Tardieu et al., 2018). The impact of drought stress on plants differs in terms of at which developmental stage the drought stress starts and how long it lasts.

There are several effects of drought stress (Nadeem et al., 2019). First of all, drought stress can inhibit germination and thus, reduce the germination rate. Depending on the humidity the stomata close to avoid further water losses, but this means the CO_2 is limited and photosynthesis inhibited (Buckley & Mott, 2013). The osmotic pressure in the cells decrease, causing osmotic stress, disturbed ion balance, reactive oxygen species can form and damage of cell membrane and large molecules (Buckley & Mott, 2013; Farquhar & Sharkey, 1982). Drought stress reduced the operating efficiency of photosystem II (ΦPSII) and has an impact on non-photochemical quenching (NPQ) (Saglam et al., 2011; Zait et al., 2024). Dried out soil and a missing transpiration lead to decrease in water and nutrient uptake (Barzana et al., 2021). Taken together, limited water availability leads to a reduction in shoot biomass, root growth, flowering and finally limited yield (Nadeem et al., 2019).

The response of plants to drought stress is various. The hormone abscisic acid (ABA) is an important signaling hormone for drought stress and is involved in gene expression induction (Aslam et al., 2022; Fàbregas & Fernie, 2019). There is a decrease in leaf expansion and increase in antioxidant enzymes (Nadeem et al., 2019; Saglam et al., 2011). In particular primary metabolites accumulate under drought stress (Fàbregas & Fernie, 2019). During drought stress, there is initially an increase in sugars, followed by antioxidants such as ascorbate and dehydroascorbate and amino acids such as proline at a later stage of drought stress.

Various strategies for drought resistance have been discussed (Kooyers, 2015). When annual plants often suffer from terminal drought stress, rapid growth and early flowering are important for escaping drought. To avoid drought, high water-use efficiency, low stomatal conductance and high

root-to-shoot ratio or epicuticular waxes on leaves are associated phenotypes (Barzana et al., 2021; Kosma et al., 2009). Osmotic adjustments, the accumulation of sugars and osmoprotectants are important in the event of more frequent and more severe droughts.

A deeper and more extensive root system is relevant for drought resistance (Lynch, 2013; Uga et al., 2013). However, investing in root growth for water and nutrient uptake is a trade-off because it could limit shoot growth (Kurepa & Smalle, 2022; Tardieu et al., 2018).

The effects of drought stress and a plant's response or tolerance are a complex topic that requires a precise and comprehensive investigation.

1.7 Objectives

The present dissertation aims to find answers for four questions about High-throughput phenotyping of Plant Genetic Resources under drought stress. Firstly, the use of HTP for breeding for drought stress tolerance. Secondly, to demonstrate the use of HTP to adapt chickpeas to other cultivation areas. Thirdly, to discuss how HTP pot experiments and field experiments complement or contradict each other. And finally, how chlorophyll fluorescence imaging with HTP is indicative for yield potential.

Therefore, the present dissertation is based on three parts:

I. Application of HTP to validate and specify the spatio-temporal effects of wild emmer wheat QTLs on growth and drought resistance across the life cycle

Near-Isogenic Lines of wheat, carrying a QTL f wild emmer wheat has been tested under drought stress with HTP. Image-derived and yield traits have been compared to field experiments and the effect of the QTLs was further examined in a spatio-temporal manner (Lauterberg et al., 2022; Chapter 2.1).

II. Identify superior genotypes of chickpea plant genetic resources under drought stress by HTP

Sixty genotypes of chickpea have been tested under drought stress during vegetative growth phase with HTP. The impact of drought stress and recovery on biomass development, changes in color, photosynthesis traits and water-use efficiency have been investigated and approved for evaluate plant genetic resources of chickpea (Lauterberg et al., 2023; Chapter 2.2).

III. Implementing theoretical non-photochemical quenching $NPQ_{(T)}$ to further decipher drought tolerance with HTP

A new promising protocol for non-photochemical quenching has been implemented for HTP. Genetic resources of chickpea have been precisely phenotyped under drought stress and the image-derived traits have been combined with yield traits and for the first time with non-photochemical quenching (Lauterberg et al., 2024; Chapter 2.3).

2. Peer-reviewed Scientific Publications

2.1 HTP of NILs across the entire crop lifecycle

"Precision phenotyping across the life cycle to validate and decipher drought-adaptive QTLs of wild emmer wheat (*Triticum turgidum* ssp. *dicoccoides*) introduced into elite wheat varieties"

by

Madita Lauterberg, Yehoshua Saranga, Mathieu Deblieck, Christian Klukas, Tamar Krugman, Dragan Perovic, Frank Ordon, Andreas Graner and Kerstin Neumann

Published in
Frontiers in Plant Science; 12. October 2022
https://www.frontiersin.org/journals/plant-science/articles/10.3389/fpls.2022.965287/full

frontiers | Frontiers in Plant Science

TYPE Original Research
PUBLISHED 12 October 2022
DOI 10.3389/fpls.2022.965287

OPEN ACCESS

EDITED BY
Nadine Töpfer,
University of Cologne,
Germany

REVIEWED BY
Filippo Maria Bassi,
International Center for Agricultural Research in the Dry Areas (ICARDA), Morocco
Ana M. Casas,
Aula Dei Experimental Station (CSIC), Spain

*CORRESPONDENCE
Kerstin Neumann
neumannk@ipk-gatersleben.de

SPECIALTY SECTION
This article was submitted to Plant Systems and Synthetic Biology, a section of the journal Frontiers in Plant Science

RECEIVED 09 June 2022
ACCEPTED 29 August 2022
PUBLISHED 12 October 2022

CITATION
Lauterberg M, Saranga Y, Deblieck M, Klukas C, Krugman T, Perovic D, Ordon F, Graner A and Neumann K (2022) Precision phenotyping across the life cycle to validate and decipher drought-adaptive QTLs of wild emmer wheat (*Triticum turgidum* ssp. *dicoccoides*) introduced into elite wheat varieties. *Front. Plant Sci.* 13:965287. doi: 10.3389/fpls.2022.965287

Precision phenotyping across the life cycle to validate and decipher drought-adaptive QTLs of wild emmer wheat (*Triticum turgidum* ssp. *dicoccoides*) introduced into elite wheat varieties

Madita Lauterberg[1], Yehoshua Saranga[2], Mathieu Deblieck[3], Christian Klukas[4], Tamar Krugman[5], Dragan Perovic[3], Frank Ordon[3], Andreas Graner[1] and Kerstin Neumann[1]*

[1]Leibniz Institute of Plant Genetics and Crop Plant Research (IPK), Gatersleben, Germany, [2]The Robert H. Smith Institute of Plant Sciences and Genetics in Agriculture, The Hebrew University of Jerusalem, Rehovot, Israel, [3]Institute for Resistance Research and Stress Tolerance, Julius Kühn-Institute, Quedlinburg, Germany, [4]Digitalization in Research and Development (ROM), BASF SE, Ludwigshafen am Rhein, Germany, [5]Institute of Evolution, University of Haifa, Haifa, Israel

Drought events or the combination of drought and heat conditions are expected to become more frequent due to global warming, and wheat yields may fall below their long-term average. One way to increase climate-resilience of modern high-yielding varieties is by their genetic improvement with beneficial alleles from crop wild relatives. In the present study, the effect of two beneficial QTLs introgressed from wild emmer wheat and incorporated in the three wheat varieties BarNir, Zahir and Uzan was studied under well-watered conditions and under drought stress using non-destructive High-throughput Phenotyping (HTP) throughout the life cycle in a single pot-experiment. Plants were daily imaged with RGB top and side view cameras and watered automatically. Further, at two time points, the quantum yield of photosystem II was measured with a top view FluorCam. The QTL carrying near isogenic lines (NILs) were compared with their corresponding parents by *t*-test for all non-invasively obtained traits and for the manually determined agronomic and yield parameters. Data quality of phenotypic traits (repeatability) in the controlled HTP experiment was above 85% throughout the life cycle and at maturity. Drought stress had a strong effect on growth in all wheat genotypes causing biomass reduction from 2% up to 70% at early and late points in the drought period, respectively. At maturity, the drought caused 47–55% decreases in yield-related traits grain weight, straw weight and total biomass and reduced TKW by 10%, while water use efficiency (WUE) increased under drought by 29%. The yield-enhancing effect of the introgressed QTLs under drought conditions that were previously demonstrated under field/screenhouse conditions in Israel, could be mostly confirmed in a greenhouse pot experiment using HTP. Daily precision phenotyping enabled to decipher the mode of action of the

QTLs in the different genetic backgrounds throughout the entire wheat life cycle. Daily phenotyping allowed a precise determination of the timing and size of the QTLs effect (s) and further yielded information about which image-derived traits are informative at which developmental stage of wheat during the entire life cycle. Maximum height and estimated biovolume were reached about a week after heading, so experiments that only aim at exploring these traits would not need a longer observation period. To obtain information on different onset and progress of senescence, the CVa curves represented best the ongoing senescence of plants. The QTL on 7A in the BarNir background was found to improve yield under drought by increased biomass growth, a higher photosynthetic performance, a higher WUE and a "stay green effect."

KEYWORDS

high-throughput phenotyping, wild emmer wheat, near-isogenic lines, drought resilience, stay green, stay-green effect

Introduction

Wheat is one of the three most important staple foods worldwide and is consumed daily in the form of baked goods or pasta. Baked goods such as bread and flat bread are an important source of carbohydrates and protein for a large part of the human population (Shiferaw et al., 2013). The ongoing climate change threatens wheat yields, as with every degree of temperature, world wheat production decreases by 6% (Asseng et al., 2015). In 2020 the global wheat production was 760 million tons according to the FAOSTAT (2020), a warming of 1.5°C would mean a loss of 68 million tons. As the climate warms, droughts or dry and hot conditions are expected to become the norm by mid-century in major growing regions such as parts of Europe, the USA and Canada, and wheat production will accordingly fall below its long-term average (Leng and Hall, 2019; Toreti et al., 2019).

Drought is an extreme, prolonged condition in which less water or precipitation is available than is necessary for the plants' needs. Due to the parched soil, transpiration needs are not met, so less water and nutrients can be taken up by mass flow or diffusion and development processes are severely impaired (Barzana et al., 2020). Photosynthesis requires CO_2 as well as water and light. CO_2 flows through the stomata into the mesophyll at a rate described by stomatal conductance, which is related to turgor pressure and osmotic potential (Buckley and Mott, 2013). Plants close their stomata with increasing drought stress to reduce water loss. If dry conditions prevail, water is lost through the stomata openings due to physical compensation. The osmotic pressure within the plant cell decreases and the resulting osmotic stress, a disturbance of the ion balance, damages the cell membrane and large molecules. Strategies to osmotically adjust or open stomata regulate intercellular solute levels under water limitation, promoting maintenance of turgor and integrity of metabolic functions (Blum, 2017).

In Mediterranean climates, of which Israel is one, water deficit and high temperatures are common during the final stage of wheat growth, hence the grain filling phase is mainly affected (Saranga et al., 2008). Escape from drought is a common strategy to prevent the effects of such terminal drought. The strategy involves rapid plant development with a high metabolic rate. The stomata are open to allow the necessary high gas exchange. This leads to a moderate but effective photosynthetic rate, low water use efficiency (WUE) and rapid expansion and division of cells (Wang et al., 2017).

Phenotyping is known to be a time-consuming and partly subjective procedure. Non-invasive high-throughput phenotyping (HTP) offers a precise and rapid way to study genotypes in an objective and standardized manner (Chen et al., 2014). It can be carried out in the field or in the greenhouse, with greenhouse experiments under controlled conditions being particularly suitable for climate change scenarios such as drought stress (Langstroff et al., 2022). Modern phenotyping technology provides better experimental opportunities to identify key loci and mechanisms for the complex stress response (Langridge and Reynolds, 2021). Precision phenotyping has allowed a deep characterisation of individual drought tolerance components in barley with high phenotypic data quality even under drought and thus the breakdown of their genetic architecture (Neumann et al., 2015; Dhanagond et al., 2019; Pham et al., 2019).

However, up to now, HTP experiments have only been conducted until about flowering time. Insight into the senescence phase could previously be obtained by mobile field phenotyping from flowering to final maturity (Christopher et al., 2016) during some days between anthesis and final maturity (Kipp et al., 2014; Christopher et al., 2016). Nevertheless, the entire life cycle from plant establishment to final maturity has not yet been assessed by non-destructive phenotyping.

Wild species represent an important genetic resource to identify beneficial alleles from landraces and wild relatives and incorporate these into modern varieties (Mascher et al., 2019).

Wild emmer wheat is the ancestor of bread and durum wheat. It is well adapted to the dry climate of the levant and thus represents a valuable source of genetic diversity to improve drought resilience (Nevo and Beiles, 1989; Peleg et al., 2005; Krugman et al., 2018).

In a recombinant inbred line (RIL) population derived from a cross between durum wheat (cv. Langdon) and wild emmer wheat (acc. G18-16), two beneficial QTLs originating from wild emmer wheat were identified (Peleg et al., 2009; Fatiukha et al., 2021). A QTL on chromosome 2B confers higher grain yield under drought stress and control conditions and a QTL on chromosome 7A confers higher total and spike dry matter under drought stress, referred to hereafter as higher productivity (Merchuk-Ovnat et al., 2016a). Near isogenic lines (NILs) carrying these QTL regions have been developed for the 2B and 7A QTLs by marker assisted breeding backcross procedure to three Israeli cultivars. The advantageous effect on yield components in the elite cultivar background has been confirmed previously under well-watered and drought conditions (Merchuk-Ovnat et al., 2016a,b).

In the current study, we investigated the NILs carrying the two wild emmer QTLs along with the parental cultivars in an HTP experiment using the previously established protocol to simulate drought stress (Dhanagond et al., 2019). For the first time, a HTP experiment captured the whole plant life cycle. The study aimed to validate the QTL effects during drought stress observed in the field/screenhouse, in a pot experiment and to specify the spatio-temporal effects of wild emmer wheat QTLs on growth and drought resilience across the entire life cycle.

Materials and methods

Plant material

A marker-assisted backcross program was employed for the introgression of the wild donor (*T. turgidum* ssp. *dicoccoides*, acc. G18-16) alleles in selected QTL regions into durum and bread wheat cultivar., as described previously by Merchuk-Ovnat et al. (2016a). All the recurrent parents were elite Israeli cultivars, widely used commercially and well adapted to the Israeli semi-arid condition. The parental lines have very similar heading times, with only few days differences (Merchuk-Ovnat et al., 2016a). We studied three Near-Isogenic Lines (NIL) at a stage of BC_3F_7 and their recurrent parental cultivars: NIL-B-7A-2 and NIL-Z-7A-5 both carrying the 7A QTL with a size of 46 cM in the background of bread wheat cultivars BarNir and Zahir, respectively, and NIL-U-2B-3 carrying the 2B QTL comprises 43,5 cM the background of durum wheat cultivar Uzan (Table 1). In a new genetic map generated by 15 K SNP array (TraitGenetics, Gatersleben) the 7A QTL is designated as *QVegdm.huj. uh-7A* and the 2B QTL is designated as *QGy.huj. uh-2B.1* (Fatiukha et al., 2021). Furthermore, the size of the QLT on chromosome B7A in BarNir measures 115Mbp (Deblieck et al., 2020).

The name of the NIL is derived from the first letter of the parental variety, the number of the chromosome containing the introgression, and the line number.

These lines were previously evaluated in two consecutive years, under contrasting water regimes in a field/screenhouse experiment in Israel and were found advantageous under drought for the respective traits (Merchuk-Ovnat et al., 2016a).

HTP system

The High-throughput Phenotyping (HTP) system (LemnaTec-Scanalyzer 3D) used in the current study is installed in an environmentally controlled greenhouse at IPK Gatersleben (51°49′23″ N, 11°17′13″ E, altitude 112 m). On this system, each plant is transported by conveyor belts to the imaging chambers equipped with top and side view RGB and fluorescence cameras, where the lifter allows imaging from different angles in side view. The balance-watering station enables controlled watering and thereby defined drought setups. The system has been upgraded

TABLE 1 Overview of used plant material.

Name	Generation	Recurrent parents	Location of QTL introgression	Associated traits	Flanking markers
BarNir *T. aestivum*	Israeli cultivar				
NIL-B-7A-2 *T. aestivum*	BC_3F_7	BarNir	7A	Total & Spike Dry Matter under Drought	Xgwm60, Xwmc422
Zahir *T. aestivum*	Israeli cultivar				
NIL-Z-7A-5 *T. aestivum*	BC_3F_7	Zahir	7A	Total & Spike Dry Matter under Drought	Xgwm60, Xwmc596
Uzan *T. durum*	Israeli cultivar				
NIL-U-2B-3 *T. durum*	BC_3F_7	Uzan	2B	Grain Yield & Harvest Index	Xgwm1128, Xgwm1177

Modified after (Merchuk-Ovnat et al., 2016a).

with a chlorophyll fluorescence camera (FluorCam) from PSI to measure photosynthetic performance from top view (Tschiersch et al., 2017).

HTP experiment

All wheat lines were phenotyped on the HTP platform under contrasting water supply with 10 biological replicates per line in each treatment. The HTP experiment took place from July 2019 to November 2019 and covered the entire life cycle of the wheat plants from sowing until maturity. Seeds were provided by Prof. Y. Saranga, the Hebrew University of Jerusalem, Israel. To ensure the presence of one plant in each pot even, two seeds per pot were sown and thinned after germination to leave one seedling per pot. Each pot (18.5 cm height × 14.9 cm diameter) was filled in with Klasman substrate no. 2 and supplemented with 7 g fertilizer, containing 19% total nitrogen, 9% P_2O_5, and 10% K_2O. Below each pot is a container to collect water in case not all water during automated watering can be fully absorbed immediately. Since the growing conditions are not homogenous within a greenhouse, all pots were randomized by the modus "Random 208," which exchanges randomly positions of 208 plants with the position of another plant, included in the operating software of the commercial system, several times a week. Plants were imaged and watered daily, imaging was performed from three side view angles (0, 45 and 90°) and top view. In the well-watered treatment, plants were always watered to 90% plant available water content according to Dhanagond et al. (2019). The day length of supplementary greenhouse lights was set to 15 h per day during the whole experiment. The chosen temperature and watering setup during the HTP experiment aimed to mimic the Israeli field situation where temperatures increase over time and a drought period is slowly establishing and progressing. However, it should be noted that technical limitations of the greenhouse climatization prevent to match the exact temperatures as in Merchuk-Ovnat et al. (2016a) or the daily temperature gradients. Here, maximal temperatures of around 47 degrees were achieved in the field/screenhouse, which is not feasible in a greenhouse. Until 30 days after sowing (DAS), plants grew without any stress for plant establishment. The temperature during this first phase was 12°C at night and 16°C during the day. To induce drought stress, the irrigation of the plants in stress treatment was reduced to 30% plant available water content on DAS 31. This level that does not cause plant wilting or visual stress symptoms, but results in reduced growth and is therefore considered a mild drought level. With the onset of drought, the temperature was increased to 20°C during the day and 16°C at night. At DAS 62 (about a week after heading), a further temperature increase was made to 24°C during the day and 20°C at night. From DAS 64 onwards, irrigation was further reduced to 20% plant available water content to induce severe drought in the grain filling phase based on the barley threshold from Dhanagond et al. (2019). Drought level and temperature regime were persisted until maturity.

Measurements of chlorophyll fluorescence were made with the FluorCam at two time points during severe drought stress (DAS 69 and 74). Regular plant recordings and irrigation were carried out at night, starting at midnight. The first saturating light flash (4,000 µmol/m²/s) is used to measure the working efficiency of photosystem two under strong light influence (800µmo/m²/s), shortly followed by a second light flash to measure the quantum yield after a lower light intensity (80 µmol/m²/s) (Grieco et al., 2020). If the quantum yields of the second and the first light flash are put in relation to each other, one can measure how the photosystem can adapt to the changing light flashes, i.e., what plasticity it possesses.

Several additional traits were measured during the HTP experiment. Number of tillers were counted at DAS 28 before the drought, at DAS 53 (about 3 weeks of mild drought) and at DAS 70 about one week after the onset of severe drought (Supplementary material 1). Heading time (BBCH55) was determined by visual inspection of the raw images, when half of the first developing ear protrudes from the flag leaf (Witzenberger et al., 1989). At DAS 67 flag leaf of the main tiller from each plant was measured for length and width at the widest point to calculate flag leaf area (length*width*0.75 = area). Then the distal half of the same flag leaf was sampled to determine osmolality (Osmotic Potential MPa; Table 2) using a vapor pressure osmometer (model 5520; Wescor Inc., Logan, UT, USA) as described by Merchuk-Ovnat et al. (2016a).

At the ripening phase, plants were inspected and taken off the system for harvest when having reached full maturity. The first plants were removed from the system at DAS 96, while the last mature plants were removed at DAS 121. The day of final maturity, called final estimated biovolume (EB), was considered to be the day when, for the last time, seven out of ten biological replicas were still on the platform. As plant appearance only slowly changed in the ripening period, images were only taken every 2 days from DAS 96 onwards, while watering was still continued daily. At plant maturity, several growth and yield parameters were recorded manually (Table 2). We determined plant height (PH) without awns, culm length (CL) was from the soil surface to the base of the three first spikes, ear length, peduncle length and the length of the last internode below the flag leaf. In addition, the total number of spikes and the number of fertile spikes were counted. The above-ground plant biomass, the grain, and the straw weight were determined, and the harvest index (HI) was calculated. The main ear was harvested separately. Thousand kernel weight (TKW) was determined for the seeds of the main ear and for the seeds from the rest of the plant. Since the water sum for each pot is recorded by the system, the water use efficiency (WUE) for the entire biomass was calculated from the ratio of final biomass to water sum.

Comparison of the HTP experiment with the screenhouse/field experiment

In order to evaluate to what extent, the data from the HTP studies correspond to the results in the two field/screenhouse

TABLE 2 Non-imaging traits measured before and at maturity.

Traits measured before maturity	Traits measured at maturity
TN DAS28	Main Ear Awn Length (cm)
TN DAS53	Ear Length (cm)
TN DAS70	Culm Length (cm)
Gain of TN DAS28 and 53	Peduncle length (cm)
Gain of TN DAS53 and 70	Last Internode length (cm)
Gain of TN DAS28 and 70	Plant height (cm)
BBCH55 in DAS	Number of Spikes
Flag Leaf Width (mm)	Number of fertile Spikes
Flag Leaf Length (cm)	Plant Biomass (g)
Flag Leaf Area (cm²)	Plant Grain Weight (g)
Osmotic Potential (MPa)	Plant Straw Weight (g)
QY-H DAS 69	Plant Harvest Index
QY-H DAS 74	Biomass WUE (g/l)
QY-L DAS 69	Plant TKW (g)
QY-L DAS 74	Plant Seed area (mm²)
QY-LH Ratio DAS 69	Plant Seed width (mm)
QY-LH Ratio DAS 74	Plant Seed length (mm)
	Plant Grain Number
	Grains per Ear
	Main Ear Spikelet Number
	Main Ear Grain Number
	Main Ear Grains per Spikelet
	Main Ear Biomass (g)
	Main Ear Grain Weight (g)
	Main Ear Straw (g)
	Main Ear Harvest Index
	Main Ear TKW (g)
	Main Ear Seed Area (mm²)
	Watersum(l)

TN, tiller number; QY-H, quantum yield of photosystem II under high-light and QY-L under low light; QY-LH, ratio of QY-L to QY-H; DAS, days after sowing.

experiments, the comparable traits were used: Culm Length (cm; CL), Days Planting to Heading (here referred to BBCH55), Grains per Ear, Grain Yield (g), Harvest Index, Osmotic Potential (Mia), Number of Spikes per Plant, TKW and Plant Biomass (g; Merchuk-Ovnat et al., 2016a). The absolute values with significance between the parents and the NIL were compared. Additionally, the average value of each individual NIL was compared to the corresponding parent in percentage (NIL/Parent*100).

Image analysis

The image analysis was carried out with the Integrated Analysis Platform (IAP; Klukas et al. 2014). Due to the long observation time, the data set was more than two Terabyte and could initially not be handled by IAP. This problem was overcome with the release of IAP version 2.3.0. The FluorCam data were analyzed using the manufacturer's software.

Our focus in image data processing was on parameters from the RGB camera: the EB [voxel], plant height (PH) [mm] and the mean color value (CVa) [hue] from the side view. This average color value is part of the HSV color space, which is described by the hue, saturation and value of a color. To simplify the analysis of colors, different hue values are combined in a 20-bin model. Based on this model, an average hue of 0.23 corresponds to an image of a green plant. The EB is calculated based on images from top view and three different angles of side view.

$$\text{Estimated Biovolume}[\text{voxel}] = \sqrt{\text{average pixel side area}^2 * \text{top area}}$$

Statistical analysis

For the statistical analysis of the HTP experimental data, R Studio was used as described by Dhanagond et al. (2019). For the estimation of variance components and Best Linear Unbiased Estimations (BLUEs), the R package ASReml was used and consequently a mixed model with Residual Maximum Likelihood applied. In terms of plant establishment, all plants grew under identical conditions until DAS 31. Consequently, there was still no stress or control treatment, so all 20 biological replicates for each parent and each corresponding NIL were considered for subsequent data analysis. From DAS 31, the start of the mild drought treatment, the two treatments drought and well-watered were analyzed separately.

The outlier test was performed according to the Tukey method (Anscombe and Tukey, 1963). BLUE values were calculated for each day and treatment separately using the model $Y=(\mu+G+e)$, where Y is the vector of observed phenotypic values, μ is the intercept, G is the effect of genotype and e is the residual value for each plant. μ and G were treated as fixed effects.

The variance components were calculated using the mixed linear model $Y=G+e$, where G is the effect of genotype and e is that of residual. There is also the assumption that all effects are random effects. Since this is a single experiment, repeatability is calculated from the variance of the genotype the error variance and ten biological replicates.

$$R = \frac{v_G}{v_G + \frac{v_e}{nRep}}$$

R Repeatability
V_G genotypic variance
V_e error variance
$nRep$ number of biological replicates.

Values for the EB were analyzed with the downscaling factor of 10^6 during all calculations. Further, due to a management error,

the FluorCam was forgotten to pull back and therefore blocked the view of the RGB top view camera from DAS 28 to 32. Therefore, these days were excluded for EB that is calculated from side and top view areas but could be analyzed for PH (from side view images) and side view CVa. As FluorCam measurement on the first time point before the onset of drought was not successful, we did not consider this day in the analysis and only used the data from DAS 69 and 74.

Results

High repeatability of biomass related traits under drought stress

Data quality, represented by repeatability, was very high throughout the life cycle for PH and EB, i.e., above 85%. Except for a few days between DAS 60 and 80, repeatability was also higher than 80% for CVa (Figure 1).

To determine how well EB predicts the true value of plant biomass and its components, final EB was correlated with straw weight, grain weight, and biomass parameters measured manually at maturity (Figure 2). With a coefficient of determination of 92%, the correlation of EB with total plant biomass was the highest, closely followed by the correlation with straw weight, where the coefficient of determination was 91%. For Grain weight (GW), the correlation was slightly lower than the other two parameters, i.e.85%.

Impact of drought stress on evaluated traits

Drought stress treatment had a strong effect on growth in all wheat lines. Regarding EB and PH significant differences between the control and the stress treatment were observed after one week of drought, from DAS 38 to harvest (Supplementary material 2). The reduction of the traits varied for selected days during mild stress (DAS 33, 40, 47 and 54) and severe stress (DAS 70, 80 and 90) from 4 to70% (Supplementary material 3). The CVa differed between treatments only during the maturation period from DAS 67 to harvest, indicating a faster maturation under drought stress (Supplementary material 2). At maturity, drought-induced losses were most severe, amounting to 47–55% decreases in biomass-related traits such as total biomass, grain weight and straw weight (Supplementary material 4).

The mean time to reach BBCH55 under stress conditions was DAS 48, 2 days earlier compared to control (Supplementary materials 4, 5). BarNir, NIL-U-2B-3, and Uzan showed a slightly but significantly earlier heading under stress conditions than under control conditions. However, significant differences between the NILs and the parental lines within the stress treatment were only present for BarNir and NIL-B-7A-2 which headed significantly 1 day later than BarNir.

The effect of drought stress was also evident for the trait "time to maturity." The stressed plants matured on average 18 days earlier than control plants with larger variation in stress treatment compared to control (Supplementary material 6).

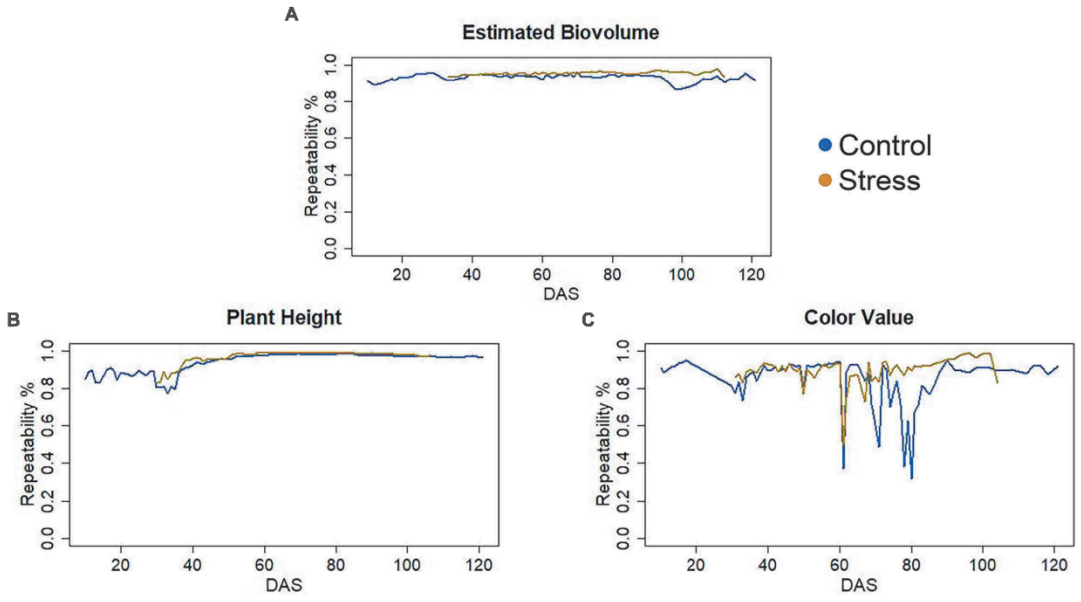

FIGURE 1
(A) Repeatability of the Estimated Biovolume. **(B)** Repeatability of the Plant Height. **(C)** Repeatability of the Color Value.

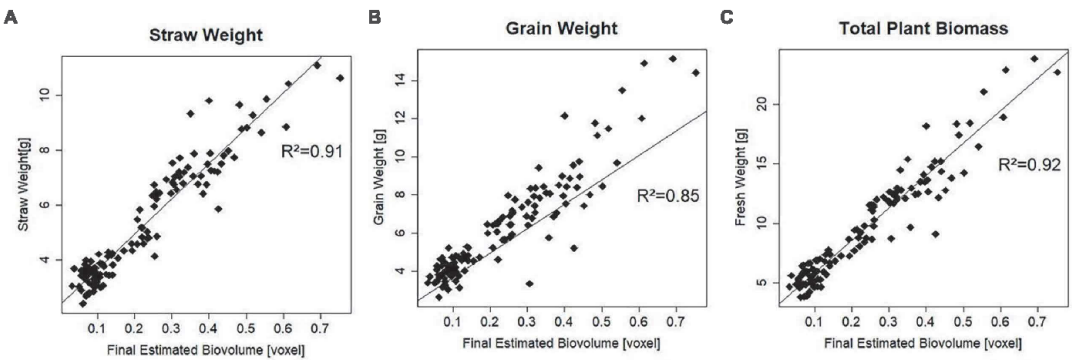

FIGURE 2
Coefficient of determination (R^2) of manually measured traits at maturity with final estimated biovolume for all 120 plants. **(A)** Coefficient of determination with plant straw weight. **(B)** Coefficient of determination with plant grain weight. **(C)** Coefficient of determination with plant biomass.

QTL effects on traits measured before and at maturity

Effect of QTL on chromosome 7A

For the traits recorded before maturity, significant differences were found between the parents and the corresponding NILs in a few traits (Table 3). Against the background of BarNir, the QTL on chromosome 7A in NIL-B-7A-2 proved to be superior in terms of flag leaf size both under control conditions with an increase of 18% and under drought conditions with 12%. Moreover, the 7A QTL in BarNir background improved the efficiency of photosystem II in both treatments under high light conditions (Quantum Yield under High light QY-H) on both time points under severe drought (DAS 69 and 74), while the QY in the transition to low light conditions (Quantum Yield under Low light QY-L), was only higher in the NIL on DAS 74 in the well-watered treatment. The QY-LH ratio, which describes the plasticity of photosystem II, was lower on both days, indicating a lower stress effect in the NIL. However, NIL-Z-7A-5 containing the same QTL in the background of Zahir, showed no difference compared to Zahir for all these traits. In both backgrounds, no influence of the 7A-QTL on the osmotic potential was detected.

The treatment has a significant effect on the time of heading (BBCH55; Table 3, Supplementary material 5). For the control treatment, the median of all six lines is at DAS 48 and for the stress treatment at DAS 50. However, this effect also depended on the genetic background and the treatment. NIL-B-7A-2 showed a significantly later heading of 1 day under stress conditions (Table 3). In contrast, in the NIL-Z-7A-5, also carrying the QTL 7A but in the Zahir background, a significantly earlier heading was observed in the control treatment. In the line NIL-U-2B-3 a significantly earlier heading under stress was detected compared to Uzan. For the osmotic potential, no significant differences were found for any of the lines (Table 3).

The 7A-QTL segment introduced in BarNir, NIL-B-7A-2, conferred significantly 25% higher plant biomass in the control and 33% higher plant biomass in the drought stress treatment at maturity (Table 4). In addition to increased PH, the 7A QTL in BarNir background increased also awn length, peduncle length and the length of the last internode in both treatments, while the ear length was decreased in well-watered conditions. In the Zahir background, no effect of the 7A QTL on height, awn length and ear length was detected, while the peduncle was longer only in well-watered conditions but the last internode was longer only in drought conditions in the respective NIL. In the BarNir background, the QTL caused increased grain and straw weight in both treatments, while HI was unaffected. These traits were not affected in the Zahir background (Table 4). Moreover, in the BarNir background, the 7A QTL significantly improved WUE, TKW and seed size parameters in both treatments. In the Zahir background improved WUE and TKW was observed only under drought stress, the higher TKW resulted from a higher seed area, or seed length.

Effect of QTL on chromosome 2B

The wild emmer wheat QTL on chromosome 2B in NIL-U-2B-3 caused a more pronounced tiller number of 35% more tillers under stress compared to the recurrent parent Uzan (Table 3). Furthermore, a small effect on heading was found, the NIL-U-2B-3 headed about 1 day earlier under drought stress compared to Uzan. No effect of the 2B QTL was detected for the osmotic potential. At maturity, the NIL-U-2B-3 plants were smaller in both treatments (Table 4). In accordance with the higher tillering during growth, a higher number of fertile spikes was also observed under drought stress, along with an improved WUE. Besides, a higher HI in both treatments was obtained. However, the higher number of tillers was linked with a lower TKW and its components and a lower grain number per ear.

TABLE 3 Averages and standard deviation and significant differences (*t*-test) between parents and corresponding NIL of traits measured before maturity.

	BarNir	NIL-B-7A-2	*p*-value	Zahir	NIL-Z-7A-5	*p*-value	Uzan	NIL-U-2B-3	*p*-value
Control									
TN DAS28	3.00 ± 0.67	2.90 ± 1.10	0.81	2.30 ± 0.48	2.10 ± 0.57	0.41	2.90 ± 0.32	2.90 ± 0.74	1.00
TN DAS53	6.30 ± 1.25	5.90 ± 1.60	0.54	3.40 ± 0.52	3.00 ± 0.47	0.09	3.70 ± 1.06	4.50 ± 1.27	0.14
TN DAS70	6.60 ± 1.07	7.10 ± 1.60	0.42	3.80 ± 0.79	3.80 ± 0.63	1.00	5.70 ± 0.95	7.40 ± 2.32	**0.05**
Gain of TN DAS28 and 53	3.30 ± 1.06	3.00 ± 1.05	0.53	1.10 ± 0.57	0.90 ± 0.57	0.44	0.80 ± 1.14	1.60 ± 1.26	0.15
Gain of TN DAS53 and 70	0.30 ± 0.48	1.20 ± 0.79	**0.01**	0.40 ± 0.70	0.80 ± 0.63	0.20	2.00 ± 1.49	2.90 ± 2.42	0.33
Gain of TN DAS28 and 70	3.60 ± 0.97	4.20 ± 1.03	0.20	1.50 ± 0.85	1.70 ± 0.67	0.57	2.80 ± 0.92	4.50 ± 1.84	**0.02**
BBCH55 in DAS	46.60 ± 0.97	47.00 ± 1.49	0.49	55.60 ± 2.99	54.00 ± 2.87	0.24	50.00 ± 0.67	49.80 ± 1.40	0.69
Flag Leaf Width (mm)	14.50 ± 0.53	15.80 ± 1.75	**0.04**	18.20 ± 1.14	18.00 ± 0.82	0.66	18.00 ± 1.15	18.10 ± 1.66	0.88
Flag Leaf Length (cm)	32.28 ± 1.40	33.89 ± 3.40	0.18	24.76 ± 2.53	25.60 ± 2.17	0.44	26.45 ± 1.94	25.40 ± 1.39	0.18
Flag Leaf Area (cm^2)	156.53 ± 6.12	188.03 ± 26.44	**0.00**	244.13 ± 20.29	242.93 ± 14.08	0.88	239.93 ± 21.03	241.88 ± 31.82	0.87
Osmotic Potential (MPa)	−1.53 ± 0.08	−1.52 ± 0.09	0.76	−1.34 ± 0.13	−1.38 ± 0.13	0.45	−1.54 ± 0.14	−1.58 ± 0.13	0.57
QY-H DAS 69	0.44 ± 0.01	0.47 ± 0.01	**0.00**	0.46 ± 0.01	0.47 ± 0.01	0.50	0.47 ± 0.01	0.47 ± 0.01	0.86
QY-H DAS 74	0.44 ± 0.01	0.46 ± 0.02	0.09	0.46 ± 0.01	0.46 ± 0.01	0.74	0.46 ± 0.01	0.46 ± 0.01	1.00
QY-L DAS 69	0.51 ± 0.01	0.51 ± 0.01	0.57	0.51 ± 0.01	0.51 ± 0.01	0.18	0.53 ± 0.02	0.53 ± 0.01	0.66
QY-L DAS 74	0.52 ± 0.01	0.53 ± 0.02	**0.04**	0.51 ± 0.02	0.51 ± 0.01	0.88	0.52 ± 0.02	0.53 ± 0.01	0.16
QY-LH Ratio DAS 69	1.15 ± 0.03	1.09 ± 0.02	**0.00**	1.09 ± 0.04	1.10 ± 0.03	0.70	1.12 ± 0.04	1.12 ± 0.02	0.75
QY-LH Ratio DAS 74	1.17 ± 0.03	1.16 ± 0.03	0.98	1.12 ± 0.04	1.12 ± 0.04	0.90	1.13 ± 0.04	1.15 ± 0.03	0.18
Stress									
TN DAS28	2.60 ± 0.52	2.80 ± 0.42	0.36	2.20 ± 0.79	2.00 ± 0.67	0.55	2.40 ± 0.52	3.30 ± 0.48	**0.00**
TN DAS53	4.10 ± 0.99	4.40 ± 1.07	0.53	2.70 ± 0.48	2.80 ± 0.63	0.70	3.00 ± 0.47	3.80 ± 0.42	**0.00**
TN DAS70	4.40 ± 0.97	4.60 ± 1.26	0.70	3.00 ± 0.67	3.00 ± 0.47	1.00	3.30 ± 0.48	5.10 ± 0.88	**0.00**
Gain of TN DAS28 and 53	1.50 ± 0.97	1.60 ± 0.97	0.82	0.50 ± 0.53	0.80 ± 0.92	0.38	0.60 ± 0.70	0.50 ± 0.53	0.72
Gain of TN DAS53 and 70	0.30 ± 0.48	0.20 ± 1.03	0.78	0.30 ± 0.67	0.20 ± 0.42	0.70	0.30 ± 0.82	1.30 ± 1.06	**0.03**
Gain of TN DAS28 and 70	1.80 ± 0.92	1.80 ± 1.32	1.00	0.80 ± 0.79	1.00 ± 082	0.58	0.90 ± 0.74	1.80 ± 1.03	**0.04**
BBCH55 in DAS	45.20 ± 0.63	46.20 ± 0.92	**0.01**	52.60 ± 1.84	52.80 ± 2.39	0.84	48.30 ± 0.67	47.50 ± 1.27	0.10
Flag Leaf Width (mm)	15.00 ± 1.15	15.70 ± 1.16	0.19	16.50 ± 1.72	15.90 ± 1.37	0.40	16.60 ± 0.97	16.40 ± 2.07	0.78
Flag Leaf Length (cm)	31.46 ± 1.05	35.78 ± 1.81	**0.00**	16.28 ± 3.43	17.55 ± 5.30	0.53	23.28 ± 0.67	22.96 ± 3.21	0.76
Flag Leaf Area (cm^2)	168.53 ± 15.57	189.98 ± 26.62	**0.04**	204.60 ± 22.68	189.83 ± 25.46	0.19	213.08 ± 22.28	182.66 ± 72.86	0.22
Osmotic Potential (MPa)	−1.86 ± 0.14	−1.89 ± 0.11	0.52	−1.73 ± 0.22	−1.72 ± 0.18	0.93	−1.82 ± 0.07	−1.89 ± 0.12	0.15
QY-H DAS 69	0.42 ± 0.02	0.46 ± 0.01	**0.00**	0.45 ± 0.02	0.44 ± 0.02	0.57	0.44 ± 0.02	0.43 ± 0.02	0.11
QY-H DAS 74	0.41 ± 0.01	0.45 ± 0.01	**0.00**	0.44 ± 0.01	0.44 ± 0.01	0.82	0.42 ± 0.02	0.39 ± 0.07	0.14
QY-L DAS 69	0.49 ± 0.02	0.51 ± 0.02	0.16	0.50 ± 0.02	0.50 ± 0.01	0.45	0.51 ± 0.02	0.49 ± 0.01	0.18
QY-L DAS 74	0.49 ± 0.03	0.51 ± 0.02	0.18	0.50 ± 0.02	0.50 ± 0.02	0.85	0.48 ± 0.03	0.47 ± 0.01	0.17
QY-LH Ratio DAS 69	1.18 ± 0.03	1.12 ± 0.04	**0.00**	1.11 ± 0.03	1.14 ± 0.05	0.20	1.14 ± 0.04	1.16 ± 0.05	0.43
QY-LH Ratio DAS 74	1.20 ± 0.06	1.14 ± 0.05	**0.02**	1.14 ± 0.05	1.15 ± 0.04	0.72	1.15 ± 0.04	1.29 ± 0.43	0.31

The mean followed by the standard deviation is shown. TN, tiller number; QY-H, quantum yield of photosystem II under high-light and QY-L under low light; QY-LH, ratio of QY-L to QY-H; DAS, days after sowing, for both = for control and stress treatment. A *t*-test with a significance level of $p < 0.05$ was used to detect significant differences between lines and has been highlighted here in bold.

Comparison of HTP experiment with the field/screenhouse experiment

The QTL effects for common traits between the HTP study and the field/screenhouse experiments from Merchuk-Ovnat et al. (2016a) were compared by calculating the relative percentage difference of the respective NIL and the corresponding parent in the HTP and each of the two field/screenhouse experiments and by looking at the phenotypic mean values in HTP and the two field/screenhouse experiments (Supplementary material 7; Table 5). Mostly, the advantageous effect of the QTL was visible in HTP and in at least one of the field/screenhouse experiments. However, the magnitude of the effects differed, sometimes the effect was more pronounced in the HTP experiment, in some cases more in the field/screenhouse. Most consistent were the results of both studies for the QTL effect in NIL-B-7A-2 compared to BarNir, while for the 7A QTL in the background of Zahir, more significant differences for yield-related traits were found in the field/screenhouse that were not detected in the HTP experiment. Notably, also the QTL effects between the 2 years of field/screenhouse experiments varied. Considering the absolute values, the BBCH55 stage occurred 10–15 days earlier in the controlled

TABLE 4 Averages and standard deviation and significant differences (t-test) between parents and corresponding NIL of traits manually measured at maturity.

	BarNir	NIL-B-7A-2	*p*-value	Zahir	NIL-Z-7A-5	*p*-value	Uzan	NIL-U-2B-3	*p*-value
Control									
Plant height (cm)	47.68 ± 1.58	72.61 ± 2.85	**0.00**	72.74 ± 3.27	74.78 ± 3.12	0.17	62.48 ± 1.86	54.74 ± 3.42	**0.00**
Main Ear Awn Length (cm)	6.26 ± 0.59	8.35 ± 0.70	**0.00**	6.35 ± 0.52	6.71 ± 0.23	0.07	11.71 ± 0.91	11.15 ± 1.07	0.22
Ear Length (cm)	10.23 ± 0.45	8.60 ± 3.06	0.11	10.17 ± 0.59	9.88 ± 0.47	0.24	5.20 ± 1.08	5.01 ± 0.30	0.60
Culm Length (cm)	37.45 ± 1.49	64.24 ± 4.39	**0.00**	62.37 ± 2.75	64.90 ± 2.99	0.09	57.28 ± 1.92	49.73 ± 3.15	**0.00**
Peduncle length (cm)	6.70 ± 1.26	13.16 ± 5.28	**0.00**	10.47 ± 1.91	13.20 ± 2.14	**0.01**	19.18 ± 12.23	11.64 ± 2.30	0.07
Last Internode length (cm)	16.09 ± 0.60	18.54 ± 7.00	0.28	17.25 ± 0.72	17.83 ± 0.59	0.07	11.62 ± 12.24	14.35 ± 0.77	0.49
Number of Spikes	6.80 ± 1.14	6.90 ± 1.73	0.88	4.00 ± 1.05	3.90 ± 0.57	0.79	5.30 ± 0.67	6.30 ± 1.25	**0.04**
Number of fertile Spikes	6.50 ± 1.08	6.90 ± 1.73	0.54	4.00 ± 1.05	3.90 ± 0.57	0.79	4.90 ± 0.99	5.80 ± 1.40	0.11
Plant Biomass (g)	1,251 ± 2.02	16.94 ± 5.89	**0.04**	13.27 ± 4.00	11.76 ± 1.85	0.29	11.69 ± 1.83	12.51 ± 3.22	0.49
Plant Grain Weight (g)	7.60 ± 1.24	10.50 ± 3.95	**0.04**	8.70 ± 2.34	7.50 ± 1.08	0.15	6.90 ± 1.70	7.40 ± 1.99	0.54
Plant Straw Weight (g)	6.35 ± 1.02	8.42 ± 2.24	**0.02**	7.61 ± 1.80	6.97 ± 1.00	0.33	6.86 ± 0.59	6.97 ± 1.56	0.84
Plant Harvest Index	0.51 ± 0.04	0.51 ± 0.05	0.88	0.46 ± 0.04	0.45 ± 0.05	0.48	0.44 ± 0.07	0.46 ± 0.05	0.36
Biomass WUE (g/l)	1.53 ± 0.09	1.66 ± 0.26	0.14	1.46 ± 0.20	1.43 ± 0.14	0.73	1.27 ± 0.13	1.33 ± 0.19	0.42
Plant TKW (g)	37.30 ± 2.16	44.60 ± 6.55	**0.00**	47.43 ± 4.75	47.55 ± 2.18	0.95	50.05 ± 570	48.32 ± 3.05	0.41
Plant Seed area (mm^2)	13.92 ± 0.54	15.94 ± 1.61	**0.00**	16.29 ± 0.93	16.69 ± 0.49	0.24	18.66 ± 0.97	17.47 ± 0.71	**0.01**
Plant Seed width (mm)	3.25 ± 0.10	3.48 ± 0.20	**0.00**	3.73 ± 0.13	3.68 ± 0.05	0.31	3.82 ± 0.13	3.76 ± 0.11	0.31
Plant Seed Length (mm)	5.94 ± 0.10	6.32 ± 0.25	**0.00**	6.07 ± 0.23	6.29 ± 0.14	**0.02**	6.92 ± 0.16	6.54 ± 0.11	**0.00**
Plant Grain Number	204.90 ± 34.01	227.80 ± 65.98	0.34	182.50 ± 45.45	156.30 ± 23.19	0.12	136.10 ± 27.32	152.00 ± 37.74	0.29
Grains per Ear	31.80 ± 4.47	32.98 ± 5.10	0.59	46.47 ± 8.29	40.34 ± 4.92	0.06	28.35 ± 6.30	26.55 ± 4.24	0.46
Main Ear Spikelet Number	18.10 ± 0.99	18.80 ± 1.03	0.14	23.80 ± 1.62	22.60 ± 1.35	0.09	14.80 ± 0.42	14.20 ± 0.79	**0.05**
Main Ear Grain Number	32.20 ± 6.71	34.80 ± 4.16	0.31	52.80 ± 6.66	45.40 ± 4.74	**0.01**	32.90 ± 2.13	31.00 ± 3.53	0.16
Main Ear Grains per Spikelet	56.92 ± 11.80	67.16 ± 5.82	**0.02**	119.24 ± 13.26	104.21 ± 13.16	**0.02**	89.21 ± 5.99	84.64 ± 9.84	0.23
Main Ear Biomass (g)	1.48 ± 0.17	2.01 ± 0.29	**0.00**	3.08 ± 0.52	2.73 ± 0.29	0.08	2.09 ± 0.28	1.90 ± 0.24	0.11
Main Ear Grain Weight (g)	1.21 ± 0.16	1.65 ± 0.26	**0.00**	2.55 ± 0.43	2.26 ± 0.25	0.08	1.72 ± 0.28	1.58 ± 0.18	0.19
Main Ear Straw (g)	0.27 ± 0.06	0.36 ± 0.08	**0.01**	0.54 ± 0.10	0.48 ± 0.05	0.10	0.37 ± 0.04	0.32 ± 0.07	0.06
Main Ear Harvest Index	0.82 ± 0.04	0.82 ± 0.04	0.89	0.83 ± 0.01	0.83 ± 0.01	0.94	0.82 ± 0.04	0.83 ± 0.02	0.36
Main Ear TKW (g)	38.16 ± 4.60	47.26 ± 4.61	**0.00**	48.04 ± 3.60	49.87 ± 4.44	0.32	52.29 ± 7.97	50.92 ± 2.23	0.61
Main Ear Seed Area (mm^2)	14.38 ± 0.95	16.53 ± 1.18	**0.00**	16.17 ± 0.92	16.72 ± 0.95	0.21	18.95 ± 1.16	17.71 ± 0.55	**0.01**
Watersum (l)	8.14 ± 0.99	9.91 ± 2.25	**0.04**	8.96 ± 1.68	8.20 ± 0.71	0.21	9.21 ± 1.10	9.28 ± 1.62	0.91
Stress									
Plant height (cm)	44.82 ± 0.99	67.21 ± 2.54	**0.00**	68.72 ± 1.79	67.83 ± 2.47	0.39	58.08 ± 1.29	48.03 ± 2.25	**0.00**
Main Ear Awn Length (cm)	6.16 ± 0.59	8.06 ± 0.72	**0.00**	5.67 ± 0.48	5.62 ± 0.56	0.83	11.46 ± 1.09	10.65 ± 0.88	0.09
Ear Length (cm)	10.57 ± 0.42	8.18 ± 3.88	0.07	8.76 ± 3.20	9.23 ± 3.28	0.75	4.84 ± 1.71	4.63 ± 1.66	0.78
Culm Length (cm)	34.25 ± 0.8	59.03 ± 4.09	**0.00**	59.82 ± 3.30	58.47 ± 3.57	0.39	52.10 ± 2.26	43.70 ± 3.25	**0.00**

(Continued)

TABLE 4 (Continued)

	BarNir	NIL-B-7A-2	*p*-value	Zahir	NIL-Z-7A-5	*p*-value	Uzan	NIL-U-2B-3	*p*-value
Peduncle length (cm)	4.98 ± 0.97	14.86 ± 3.90	**0.00**	10.42 ± 3.84	6.10 ± 20.73	0.53	14.45 ± 5.12	9.83 ± 4.10	**0.04**
Last Internode length (cm)	15.37 ± 0.37	19.21 ± 0.94	**0.00**	12.65 ± 21.33	15.70 ± 0.54	0.66	10.01 ± 11.14	11.45 ± 4.08	0.71
Number of Spikes	3.60 ± 0.84	4.10 ± 0.88	0.21	2.50 ± 0.53	2.40 ± 0.52	0.67	3.00 ± 0.00	3.80 ± 0.42	**0.00**
Number of fertile Spikes	3.33 ± 0.50	4.10 ± 0.88	**0.03**	2.40 ± 0.52	2.40 ± 0.52	1.00	3.00 ± 0.00	3.80 ± 0.42	**0.00**
Plant Biomass (g)	5.42 ± 0.55	8.09 ± 1.39	**0.00**	4.97 ± 0.76	5.12 ± 0.86	0.69	5.66 ± 0.75	6.43 ± 1.16	0.10
Plant Grain Weight (g)	4.00 ± 0.34	5.70 ± 0.91	**0.00**	4.00 ± 0.62	4.00 ± 0.63	0.88	3.90 ± 0.55	4.40 ± 0.78	0.18
Plant Straw Weight (g)	3.02 ± 0.31	4.48 ± 0.60	**0.00**	3.34 ± 0.32	3.39 ± 0.30	0.69	3.63 ± 0.35	3.69 ± 0.53	0.78
Plant Harvest Index	0.50 ± 0.03	0.49 ± 0.04	0.37	0.41 ± 0.06	0.41 ± 0.05	0.88	0.42 ± 0.03	0.46 ± 0.03	**0.01**
Biomass WUE (g/l)	1.93 ± 0.20	2.17 ± 0.25	**0.03**	1.70 ± 0.21	1.79 ± 0.19	0.34	1.70 ± 0.11	1.91 ± 0.19	**0.01**
Plant TKW (g)	33.05 ± 3.33	39.29 ± 2.11	**0.00**	38.17 ± 6.32	44.01 ± 5.27	**0.04**	46.85 ± 4.21	46.71 ± 3.48	0.94
Plant Seed area (mm^2)	13.17 ± 0.67	14.71 ± 0.73	**0.00**	13.88 ± 1.47	15.42 ± 1.20	**0.02**	17.48 ± 0.74	16.75 ± 0.53	**0.02**
Plant Seed width (mm)	3.08 ± 0.11	3.30 ± 0.08	**0.00**	3.39 ± 0.20	3.52 ± 0.13	0.09	3.69 ± 0.13	3.64 ± 0.09	0.24
Plant Seed Length (mm)	5.94 ± 0.10	6.18 ± 0.20	**0.00**	5.67 ± 0.34	6.06 ± 0.26	**0.01**	6.68 ± 0.11	6.49 ± 0.10	**0.00**
Plant Grain Number	120.30 ± 16.23	140.60 ± 26.67	**0.05**	105.90 ± 17.38	90.80 ± 21.29	0.10	81.20 ± 9.66	92.60 ± 17.30	0.09
Grains per Ear	35.01 ± 4.80	34.57 ± 2.84	0.81	44.73 ± 4.89	38.00 ± 5.73	**0.01**	28.17 ± 3.17	24.25 ± 3.11	**0.01**
Main Ear Spikelet Number	18.70 ± 0.48	18.70 ± 1.06	1.00	22.40 ± 1.17	22.20 ± 1.62	0.76	14.80 ± 0.92	13.60 ± 1.17	**0.02**
Main Ear Grain Number	37.60 ± 5.68	39.70 ± 6.91	0.47	51.40 ± 3.92	41.10 ± 7.78	**0.00**	30.20 ± 2.62	27.90 ± 2.33	**0.05**
Main Ear Grains per Spikelet	67.13 ± 10.19	73.73 ± 11.94	0.20	121.98 ± 13.69	90.19 ± 17.93	**0.00**	80.11 ± 6.65	74.25 ± 8.03	0.10
Main Ear Biomass (g)	1.62 ± 0.09	2.06 ± 0.22	**0.00**	2.37 ± 0.25	2.23 ± 0.17	0.18	1.91 ± 0.23	1.62 ± 0.17	**0.00**
Main Ear Grain Weight (g)	1.31 ± 0.10	1.71 ± 0.19	**0.00**	1.95 ± 0.23	1.82 ± 0.16	0.17	1.56 ± 0.21	1.36 ± 0.13	**0.02**
Main Ear Straw (g)	0.31 ± 0.03	0.35 ± 0.06	**0.04**	0.42 ± 0.06	0.41 ± 0.06	0.74	0.35 ± 0.04	0.26 ± 0.04	**0.00**
Main Ear Harvest Index	0.81 ± 0.02	0.83 ± 0.02	0.08	0.82 ± 0.02	0.82 ± 0.02	0.55	0.81 ± 0.02	0.84 ± 0.02	**0.00**
Main Ear TKW (g)	35.52 ± 4.66	43.82 ± 5.61	**0.00**	37.97 ± 4.37	45.29 ± 6.10	**0.01**	51.40 ± 3.74	48.76 ± 2.58	0.08
Main Ear Seed Area (mm^2)	14.44 ± 0.77	16.25 ± 1.27	**0.00**	13.93 ± 1.05	15.68 ± 1.48	**0.01**	18.35 ± 0.69	17.24 ± 0.50	**0.00**
Watersum (l)	2.82 ± 0.14	3.73 ± 0.43	**0.00**	2.92 ± 0.17	2.85 ± 0.21	0.43	3.31 ± 0.30	3.34 ± 0.38	0.86

A t-test with a significance level of $p < 0.05$ was used to detect significant differences between lines and has been highlighted here in bold.

environment of the HTP experiment. Compared to the field, plants in the HTP experiment were smaller and had a lower grain yield and lower values for other grain-yield related parameters across all genotypes and treatments such as TKW or HI (Table 5).

Significant differences between parents and NILs were found for several traits across the environments. For example, NIL-B-7A-5 was significantly larger than BarNir in all environments, as measured by culm length. NIL-U-2B-3 was significantly smaller in the HTP experiment and significantly larger in the field experiment. The increased grain yield and plant biomass for NIL-B-7A-5 was also significantly greater for all environments between 43 and 69%. For TKG, the difference between the first field/screenhouse experiment and the HTP experiment was equally significant. In both environments, NIL-U-2B-3 showed a number of spikes, but it was only significant under control for both environments.

Dynamic phenotyping revealed effect of wild emmer wheat QTLs on drought resilience

Effect of QTL on chromosome 7A for NIL-B-7A-2

Significant differences were found for EB between BarNir and NIL-B-7A-2 for the period from DAS 45–102 in the control treatment and DAS 33–102 in stress treatment (Figure 3; Supplementary materials 8, 9). Thus, differences were observed in both treatments, but they occurred earlier under drought. In both treatments, the NIL showed a higher EB. Furthermore, when testing whether the treatment had a significant effect on the EB of each genotype, NIL-B-7A-2 showed a six-day later response to drought stress treatment than BarNir (Supplementary materials 10).

Consistent with the observations at maturity, plants of NIL-B-7A-2 were significantly taller than those of the parent BarNir throughout the entire life cycle under both conditions (Figure 4; Supplementary materials 11–14). Similar to EB, the PH in the NIL showed a response to drought stress 7 days later than in BarNir (Supplementary material 14).

The QTL 7A affected the CVa. Until around DAS 60, the NIL in the BarNir background had a significantly slightly lower CVa in both treatments in the BarNir background. However, in the severe drought treatment during the late ripening phase, plants of the NIL had a significantly higher CVa from DAS 90 onwards, showing a slower ripening of the NIL (Figure 5; Supplementary material 15).

The differences between the treatments were significant from DAS 70 and 71 onwards for the NIL-B-7A-2 and BarNir, respectively (Supplementary materials 16–18).

Effect of QTL on chromosome 7A for NIL-Z-7A-5

NIL-Z-7A-5 produced less EB in both treatments compared to Zahir, with this effect being more pronounced in the control treatment than in the stress treatment. However, the difference between NIL and parent was significant only for a few DAS, such as DAS 10 to 13 in the plant establishment phase and during the mild stress phase from DAS 33 to 43 (Figure 6; Supplementary materials 8, 11). However, the standard deviation for EB under control was high for Zahir and NIL, which might have confounded a larger EB effect of the QTL (Supplementary material 9). Nevertheless, also in the stress treatment, the two genotypes had a very similar EB. Only in the late ripening phase, during DAS 90–96, the EB was significantly higher under drought in NIL-Z-7A-5, showing a positive effect of the 7A QTL (Supplementary material 8). Moreover, when testing if the treatment had a significant influence on EB for each genotype, NIL-Z-7A-5 showed a seven-days later reaction to the drought compared to Zahir, similar as seen in the BarNir background (Supplementary material 10).

In the Zahir background in both treatments, Zahir and NIL-Z-7A-5 did not differ in PH throughout the life cycle, which is in accordance with the absent difference for PH at maturity (Figure 7; Supplementary materials 11–14). The differences in PH between the treatments became significant for Zahir from DAS 62 onwards and for NIL-Z-7A-5 from DAS 57 on, so the QTL carrying NIL reduced PH 5 days earlier compared to the parental line (Supplementary material 17), which contrasts with the observed later response to drought of EB of NIL-Z-7A-5.

In Zahir background, the 7A QTL showed no effect on CVa until the ripening stage and the treatment effect was significant from DAS 69 onwards for Zahir and from DAS 72 for NIL-Z-7A-5 (Figure 8; Supplementary materials 16–18). However, NIL-Z-7A-5 had significantly higher CVa from DAS 98–121 in the control treatment and DAS 82 - DAS 92 in the stress treatment (Figure 9; Supplementary material 15), showing a slower ripening arising from the 7A QTL.

Effect of QTL on chromosome 2B for NIL-U-2B-3

Regarding the effect of the 2B-QTL in the genetic background of Uzan, NIL-U-2B-3 produced significantly more EB compared to Uzan in the stress treatment during DAS 33–79 (Figure 10; Supplementary materials 8, 9). In the control treatment, the NIL also showed more EB, especially at DAS 48–90, but this difference was not significant. A treatment effect, i.e., a later response to drought in the biomass differences between control and stress treatment, of the 2B-QTL was also visible for the 2B-QTL, but less pronounced than in the 7A-QTL. From DAS 33 to 38 and from DAS 46 to harvest, the EB of NIL-U-2B-3 3 differed significantly in the two treatments, while in Uzan a significant difference between control and stress EB was observed from DAS 37 onwards (Supplementary material 10).

In accordance with reduced PH at maturity (Table 4), the NIL-U-2B-3 remained smaller than its parent Uzan, especially in the period after heading (Figure 11; Supplementary materials 11–13). In the control treatment, the difference between the genotypes in PH was significant from DAS 58 onwards and in the stress treatment from DAS 53 on (Supplementary material 14). PH in Uzan differed significantly between control and stress treatment from DAS 40 onwards, while in the NIL this difference occurred

TABLE 5 Comparison of the absolute values (mean) of the NILs and the parents of common traits of the HTP experiment and field/screenhouse experiments.

Trait	Treament	HTP			FY1			FY2		
		BarNir	NIL-B-7A-2		BarNir	NIL-B-7A-2		BarNir	NIL-B-7A-2	
Culm Length (cm)	Control	37	64	***	60	75	***	59	70	***
	Stress	34	59	***	56	70	***	50	62	***
BBCH55	Control	47	47		64	66	***	63	67	***
	Stress	45	46	**	63	65	***	62	66	***
Grains per Ear	Control	32	33		57	55		54	48	
	Stress	35	35		59	63		44	46	
Grain Yield (g)	Control	7.60	10.50		24	28.00		18.00	16.10	
	Stress	4.00	570	***	11.80	18.80	*	7.30	11.80	*
Harvest Index	Control	0.51	0.51		0.57	0.56		0.52	0.56	
	Stress	0.50	0.49		0.52	0.56		0.55	0.53	
Osmotic Potential	Control	−1.53	−1.52		−1.32	−1.26		−1.19	−1.26	
(Mpa)	Stress	−1.86	−1.89		−1.76	−1.61		−1.33	−1.52	***
Spikes per Plant	Control	7	7		13	14		10	8	
	Stress	4	4		7	9		5	7	
TKW	Control	37	45	***	49	55	**	48	48	
	Stress	33	39	***	41	47	**	48	50	
Plant Biomass (g)	Control	12.51	16.94	*	42.20	50.90		34.70	33.30	
	Stress	542	8.09	***	22.50	34.10	*	13.20	22.10	*
		Zahir	NIL-Z-7A-5		Zahir	NIL-Z-7A-5		Zahir	NIL-Z-7A-5	
Culm Length (cm)	Control	62	65		74	83	**	68	76	**
	Stress	60	58		69	75	*	63	67	*
BBCH55	Control	56	54		64	71	***	61	67	***
	Stress	53	53		62	71	***	59	67	***
Grains per Ear	Control	46	40		63	66		66	62	
	Stress	45	38		61	69		52	49	
Grain Yield (g)	Control	8.70	7.50		21.00	29.80	**	15.80	21.10	*
	Stress	4.00	4.00		12.90	17.00		8.10	11.00	
Harvest Index	Control	0.46	0.45		0.56	0.55		0.53	0.51	
	Stress	0.41	0.41		0.54	0.51		0.57	0.53	
Osmotic Potential	Control	−1.34	−1.38		−1.17	−1.18		−1.12	−1,15	
(Mpa)	Stress	−1.73	−1.72		−1.46	−1.54		−1.27	−1,22	
Spikes per Plant	Control	4	4		8	10		6	8	*
	Stress	3	2		5	7	*	4	5	*
TKW	Control	47	48		55	55		52	56	
	Stress	38	44		49	50		55	55	
Plant Biomass (g)	Control	13.27	11.76		39.80	54.60	**	29.50	41.20	*
	Stress	4.97	5.12		23.70	33.30		14.10	20.50	
		Uzan	NIL-U-2B-3		Uzan	NIL-U-2B-3		Uzan	NIL-U-2B-3	
Culm Length (cm)	Control	57	50	***				65	72	*
	Stress	52	44	***				54	60	*
BBCH55	Control	50	50					67	68	
	Stress	48	48					65	67	
Grains per Ear	Control	28	27					55	46	
	Stress	28	24	*				40	45	
Grain Yield (g)	Control	6.90	7.40					13.30	19.70	*
	Stress	3.90	4.40					4.30	11.00	*
Harvest Index	Control	0.44	0.46					0.52	0.49	
	Stress	0.42	0.46	*				0.45	0.52	

(Continued)

TABLE 5 (Continued)

Trait	Treament	HTP			FY1	FY2		
Osmotic Potential	Control	−154	−1.58			−1.18	−1.20	
(Mpa)	Stress	−1.82	−1.89			−1.40	−1.40	
Spikes per Plant	Control	5	6	*		5	8	***
	Stress	3	4	***		3	5	
TKW	Control	50	48			62	68	*
	Stress	47	47			60	66	**
Plant Biomass (g)	Control	11.69	12.51			25.60	40.00	*
	Stress	5.66	6.43			9.60	21.50	

The values for the field/screenhouse are taken from Merchuk-Ovnat et al. (2016a, Table 3, Supplementary Tables S4, S5). HTP, high-throughput phenotyping experiment; FY, field/screenhouse experiment year 1 and 2; BBCH55, heading. Significance data is from the original tables of Merchuk-Ovnat et al. (2016a) and Tables 3, 4. Mean comparisons by Student's t-test between each line and its recurrent parent (*, **, ***) under control and drought stress treatments at $p < 0.05$, 0.01, 0.001, respectively.

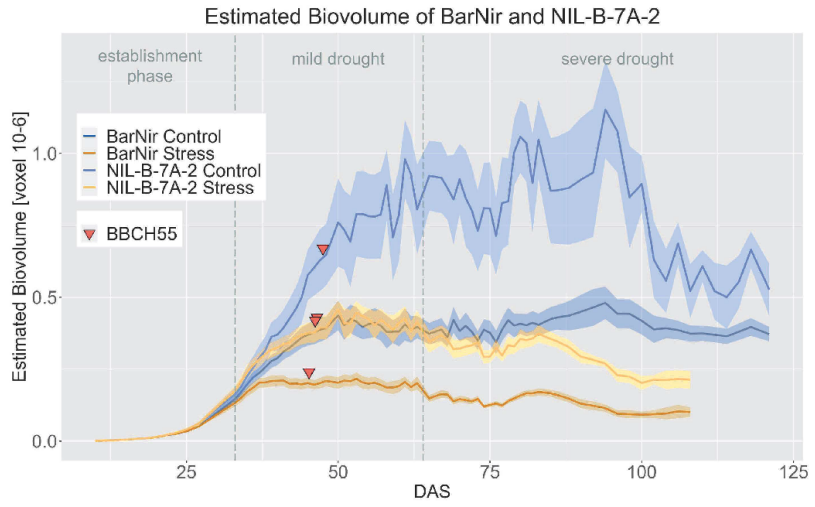

FIGURE 3
A Estimated biovolume of BarNir and NIL-B-7A-2 based on the calculated BLUEs values. DAS, days after sowing; BBCH55, heading day. The last DAS for each genotype was chosen for the DAS where the last time 60% of the plants were imaged (as mature plants were taken off subsequently). The shadows describe the confidence interval; as long as the shadows of the individual lines (parent and corresponding NIL) do not overlap, the significance level of a=0.05 is not reached and therefore a significant difference exists.

4 days later from DAS 44 onwards (Supplementary material 14), so the NIL responded later to drought concerning PH.

The 2B QTL showed a minor effect on the CVa. Uzan had a higher CVa during the mild drought phase than NIL-U-2B-3 (Figure 9; Supplementary materials 15, 16, 18). In the control treatment this difference was significant until DAS 90 and in stress treatment until DAS 76 (Supplementary material 15). The effect between the control and the stress treatment is for both Uzan and NIL-U-2B-3 significant from DAS 68 onwards (Supplementary material 17).

Discussion

In the present study, the detailed effects of two QTLs introduced from wild emmer wheat for higher productivity with respect to spike and total dry matter under drought (chromosome 7A) or productivity with respect to grain yield across drought and control environments (chromosome 2B) were examined under well-watered and drought stress conditions using non-destructive HTP, for the first time throughout the whole plant life cycle. Our daily phenotyping results confirm advantageous effects of yield or yield parameters of the QTLs which were identified under field/screenhouse conditions in Israel and enabled us to determine the QTL effects on growth and their timing.

Suitability of HTP phenotyping for evaluation of yield characteristics

The phenotyping platform used in this study has been used previously and has proven useful for estimating plant biomass up to

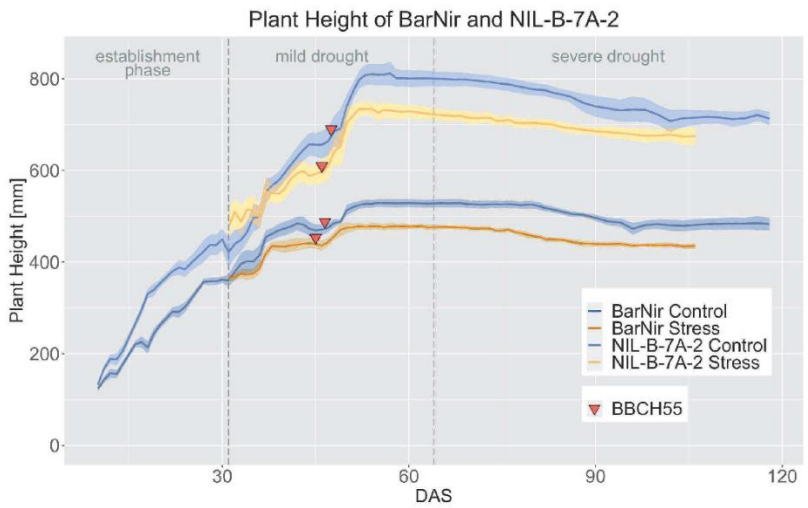

FIGURE 4
Plant height of BarNir and NIL-B-7A-2 based on the calculated BLUEs values. DAS, days after sowing; BBCH55, heading day. The last DAS for each genotype was chosen for the DAS where the last time 60% of the plants were imaged (as mature plants were taken off subsequently). The shadows describe the confidence interval; as long as the shadows of the individual lines do not overlap, the significance level of a=0.05 is not reached and therefore a significant difference exists.

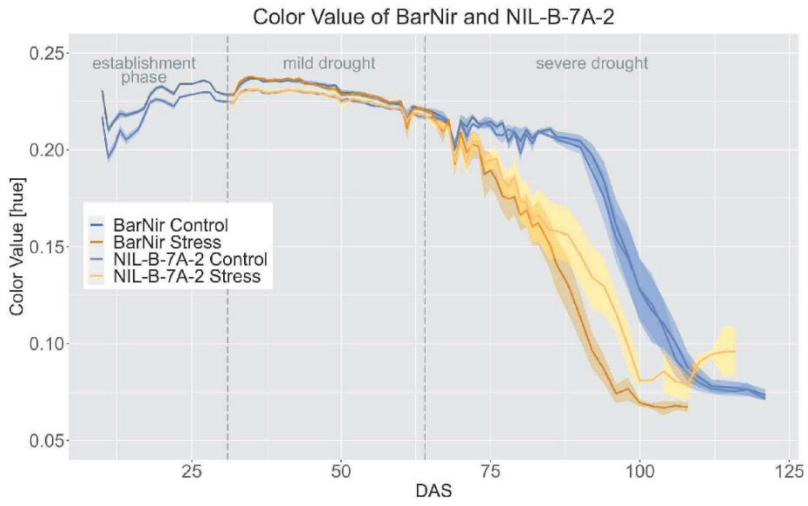

FIGURE 5
Color value of BarNir and NIL-B-7A-2 based on the calculated BLUEs values. DAS, days after sowing; BBCH55, heading day. The last DAS for each genotype was chosen for the DAS where the last time 60% of the plants were imaged (as mature plants were taken off subsequently). The shadows describe the confidence interval; as long as the shadows of the individual lines do not overlap, the significance level of a=0.05 is not reached and therefore a significant difference exists.

the flowering stage under well-watered and drought stress conditions in barley (Neumann et al., 2015). As the plant material was from Israel, the chosen setup and greenhouse conditions aimed at mimicking the field situation in Israel, with a rising temperature gradient corresponding to the seasonal pattern and a slowly progressing drought reaching severe stress during grain filling.

With the application of an established standardized phenotyping protocol, high repeatability was achieved for EB and PH for each day throughout the life cycle under both, well-watered and drought stress conditions. Except for a few days, the data quality of the CVa was also high. The results of this study are in line with the high data quality throughout the vegetative

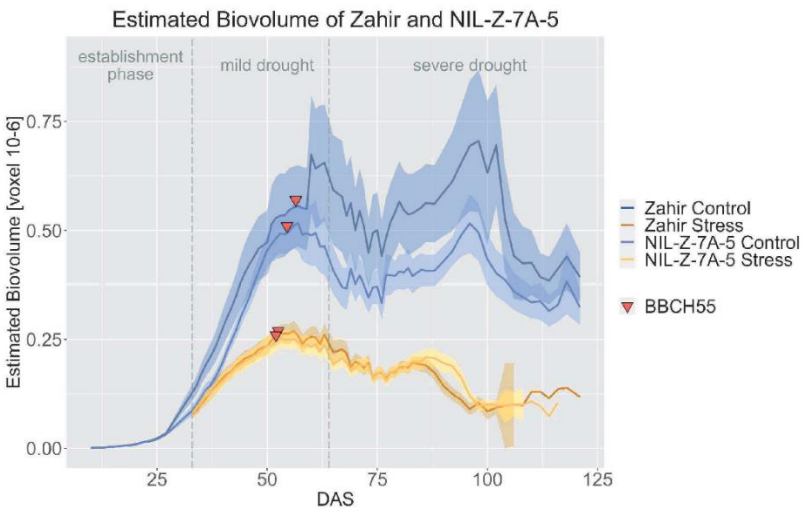

FIGURE 6
Estimated biovolume of Zahir and NIL-Z-7A-5 based on the calculated BLUEs values. DAS, days after sowing; BBCH55, heading day. The last DAS for each genotype was chosen for the DAS where the last time 60% of the plants were imaged (as mature plants were taken off subsequently). The shadows describe the confidence interval; as long as the shadows of the individual lines do not overlap, the significance level of a=0.05 is not reached and therefore a significant difference exists.

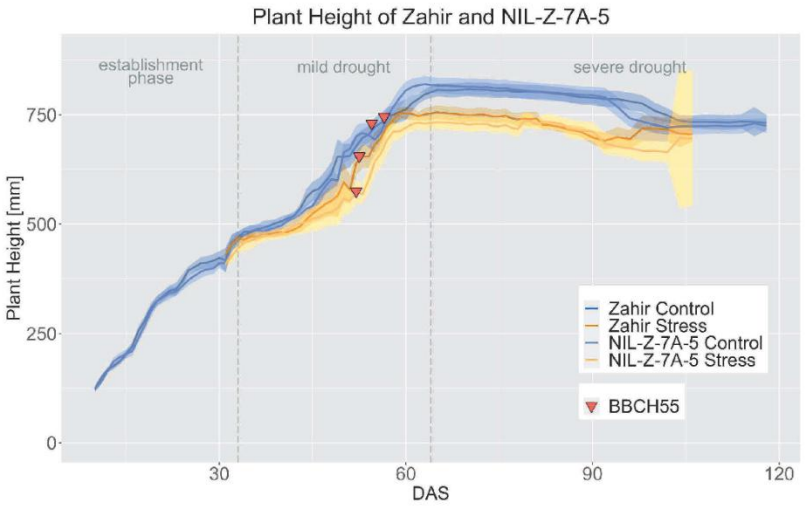

FIGURE 7
Plant height of Zahir and NIL-Z-7A-5 based on the calculated BLUEs values. DAS, days after sowing; BBCH55, heading day. The last DAS for each genotype was chosen for the DAS where the last time 60% of the plants were imaged (as mature plants were taken off subsequently). The shadows describe the confidence interval; as long as the shadows of the individual lines do not overlap, the significance level of a=0.05 is not reached and therefore a significant difference exists.

growth period in well-watered and drought stress conditions on the same HTP system (Neumann et al. 2017; Dhanagond et al., 2019). The suitability of EB as a true proxy of biomass was also evident, in agreement with previous studies that were restricted to vegetative growth stages, though (Munns et al., 2010; Golzarian et al., 2011; Dhanagond et al., 2019; Shorinola et al., 2019). The results demonstrate the usefulness of this proxy over the entire plant life cycle. Based on the high-quality data set, statistical analyses to reveal the QTL effects throughout the life cycle could be performed.

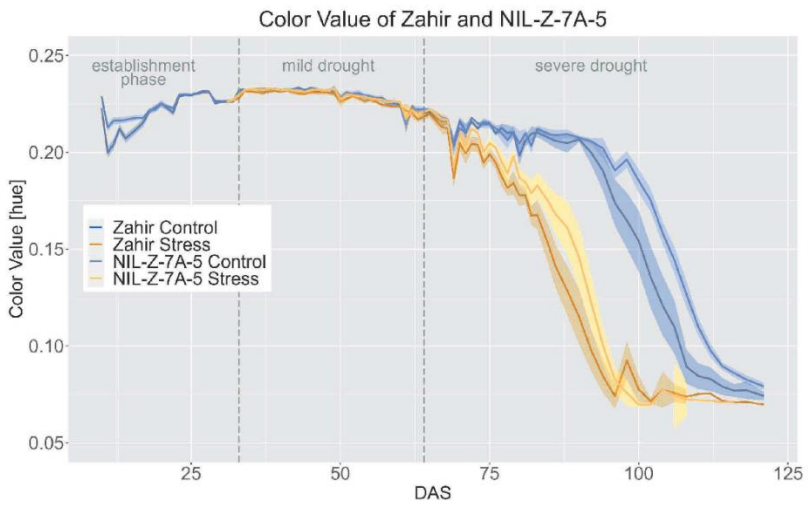

FIGURE 8
Color value of Zahir and NIL-Z-7A-5 based on the calculated BLUEs values. DAS, days after sowing; BBCH55, heading day. The last DAS for each genotype was chosen for the DAS where the last time 60% of the plants were imaged (as mature plants were taken off subsequently). The shadows describe the confidence interval; as long as the shadows of the individual lines do not overlap, the significance level of a=0.05 is not reached and therefore a significant difference exists.

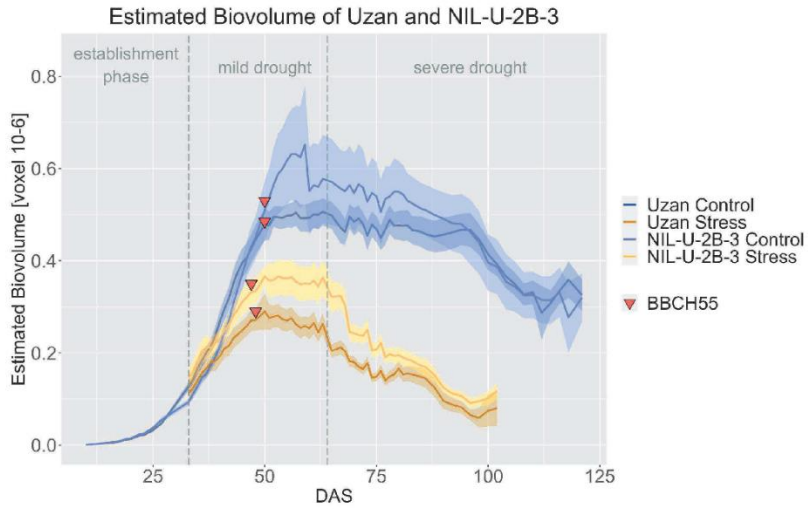

FIGURE 9
Color value of Uzan and NIL-U-2B-3 based on calculated BLUEs values.DAS, days after sowing; BBCH55, heading day. The last DAS for each genotype was chosen for the DAS where the last time 60% of the plants were imaged (as mature plants were taken off subsequently). The shadows describe the confidence interval; as long as the shadows of the individual lines do not overlap, the significance level of a=0.05 is not reached and therefore a significant difference exists.

Further, the data set allows to make statements about which imaging traits provide relevant information during or until which cereal developmental stage for HTP experiments. The EB increased dynamically until the milk ripening stage, while final PH was reached already shortly after flowering. After that, PH remained constant, while EB decreased with the ripening process due to the increase in mature plant parts, as these contain less water and thus the visible area is smaller. The CVa can be used to visualize and quantify the process of senescence of the plant by the changing plant color from green to yellow (Mikołajczak et al.,

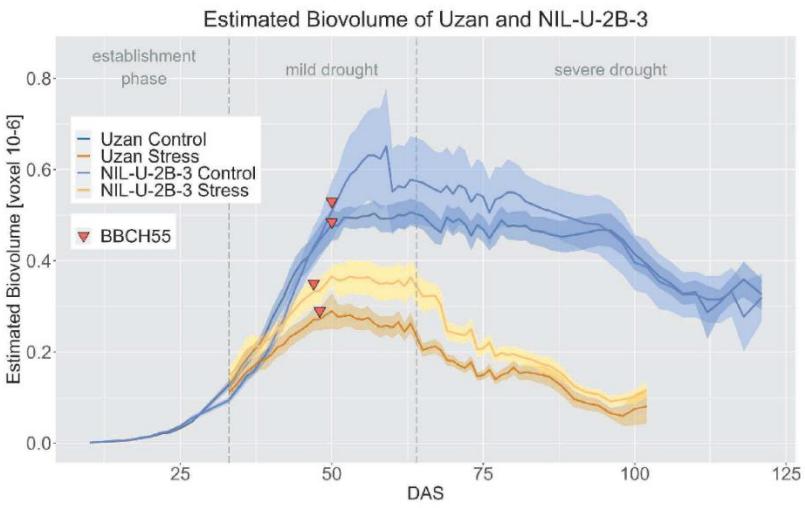

FIGURE 10
Estimated biovolume of Uzan and NIL-U-2B-3 based on the calculated BLUEs values. DAS, days after sowing; BBCH55, heading day. The last DAS for each genotype was chosen for the DAS where the last time 60% of the plants were images (as mature plants were taken off subsequently). The shadows describe the confidence interval; as long as the shadows of the individual lines do not overlap, the significance level of a=0.05 is not reached and therefore a significant difference exists.

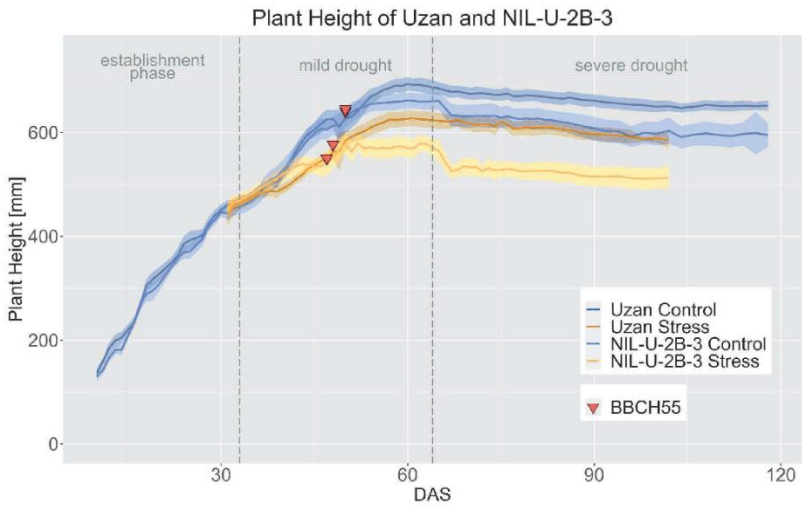

FIGURE 11
Plant height of Uzan and NIL-U-2B-3 based on calculated BLUEs values. DAS, days after sowing; BBCH55, heading day. The last DAS for each genotype was chosen for the DAS where the last time 60% of the plants were imaged (as mature plants were taken off subsequently). The shadows describe the confidence interval; as long as the shadows of the individual lines do not overlap, the significance level of a=0.05 is not reached and therefore a significant difference exists.

2020). If there is sufficient water available, the color of a plant is green and only changes with progressing senescence. However, drought stress can cause severe effects on plant pigments and changed the color of the plant when leaves were wilting during vegetative growth (Neumann et al., 2015). In the chosen setup of the current study of a slowly intensifying drought until maturity, the drought stressed plants started ripening earlier compared to the well-watered plants but showed no color changes during the vegetative phase with mild drought stress. The individual ripening curves reflected by the CVa of single plants are so clear

that they represent a promising resource for the application of mathematic models. Curve modeling can add valuable insights into growth dynamics and allows the estimation of further traits. By growth curve modelling of vegetative biomass formation in barley, time points of maximal growth or start of wilting under drought could be estimated and resulted in the detection of corresponding QTL (Chen et al., 2014; Neumann et al. 2017; Dhanagond et al., 2019). By modeling the ripening curve based on CVa, it may be possible to quantify the ripening speed, which differed between genotypes and treatments and will shed more light into this phenology phase.

General effects of drought stress during HTP experiment

The timing of drought significantly affects plant development. If drought stress occurs during the tillering stage, biomass, and the number of tillers per plant are reduced (Dhanagond et al., 2019). PH is affected when drought occurs during stem elongation (Ihsan et al., 2016) and the seed set is negatively affected by drought stress at the flowering stage (Sehgal et al., 2018). When drought stress occurs in the grain filling phase, TKW is reduced (V et al., 2019). As drought in our study started at the tillering stage and lasted until maturity, all these components were affected by progressing drought stress. Similar observations were made in a recent study in spring wheat (Fadoul et al., 2021).

In this HTP experiment, the plants of control and stress treatment started to show significant differences for EB and PH 7 days after the onset of drought. This is in accordance with previous observations in barley on the same HTP system, where biomass in control and drought treatment differed after 5 to 7 days (Neumann et al., 2015). The slower growth was accompanied by a decrease in tillering. Notably, the 10% loss in PH measured on DAS 47 was less than the 20–30% loss in tillering. Thus, the reduced EB may be mainly explained by reduced tillering rather than smaller plants. Similar losses caused by drought were also described in comparable HTP experiments (Honsdorf et al., 2014; Dhanagond et al., 2019; Pham et al., 2019). For the first time, a drought HTP experiment was conducted until maturity to simulate a natural progressing and intensifying drought. The long-term drought caused reductions of all yield components such as number of seeds, TKW and number of tillers and lead to faster maturity of stressed plants. Further, image capturing allowed to determine the heading date of each plant. Heading time is known to be affected by drought. Depending on the timing of the stress and its intensity, it can cause a delay in flowering (Chen et al., 2020; Gol et al., 2020) or lead to earlier flowering as a possible stress escape mechanism (Shavrukov et al., 2017). In the current study, there was only a small effect on heading time. This could be attributed to the fact that only mild drought was applied until flowering. However, a significant delay in the maturation date was observed in the NILs of 7A QTL, indicating that these plants are more resilient to drought. In addition, the Israeli plant material is already adapted to terminal drought and hardly changes their flowering time (Nevo et al., 2012).

Comparison of HTP experiment with the field/screenhouse experiment

Heading time occurred much earlier in the greenhouse compared to the field. A significantly earlier flowering of up to 15 days in controlled environments compared to the field has recently been described in wheat (Sales et al., 2022). Still, the small but significant increasing effect of the 7A QTL in the BarNir background on heading time was detected also in the HTP experiment. The observed general lower yield parameters for single plants in pots compared to plants grown in plant stands in the field/screenhouse were to be expected. However, when averaging the two field years and comparing across all genotypes and both treatments, we reach between 62% (spikes per plant) and 87% (TKW) of the average trait values in the field for the yield parameters and 80% for culm length.

Besides the obvious differences of single plant growth in pots to growth in plant stands in a field soil, the growing conditions in terms of temperature, light quantity and quality, humidity and water availability are not the same. Though the HTP study incorporated a temperature gradient over the growing period, temperatures during day and night are stable in the climate-controlled greenhouse and do not show fluctuations as in the field and also the maxima in temperature reached in the two field years are technically not possible to reach in our greenhouse. Water availability is also difficult to compare between pot and field, due to the different ways of measuring in liters per pot in HTP and mm of precipitation in the field, which are two entirely different systems. According to Merchuk-Ovnat et al. (2016a), the applied water in the control treatment was 690–710 mm and in the water-limited 290-320 mm, which is about 42% lower precipitation in drought stress. In this HTP study, an average of 9 liters was watered to control plants and 3.2 liters to the drought stressed plants, corresponding to one third of the well-watered amount.

Strikingly, NIL-U2-B-3 in the Uzan background had an increasing effect on plant height, while having a decreasing effect in the HTP study in contrast. In general, the plant density in a pot experiment is much lower than in a field experiment. Poorter et al. (2016) analyzed in a meta-analysis of 100 trials how plant height is affected by the different plant densities in the different environments of pot and field. Genotypes planted in different environments showed no consistent trend in their height with respect to environment (Poorter et al., 2016). Thus, the difference in the 2B-QTL effect on plant height could attributed to the genotype and environment interaction. While the NIL-B-7A-2 was significantly taller than the parent BarNir in both HTP and field study, the effect was more pronounced in the HTP study. Similarly, the other observed differences in QTL effect occurrence and size can be interpreted as genotype x environment interaction effects.

Dissection of wild emmer wheat QTL effects on shoot growth

In general, we could successfully reproduce the positive effects of the wild emmer wheat QTLs as had been observed in the previous field experiments. This demonstrates the suitability of the system and the applied setup to study complex traits such as drought resilience. The increased flag leaf area, photosynthesis and WUE of NIL-B-7A-2 in the HTP experiment have already been observed under stress and control treatments in the greenhouse and under control conditions in the field/screenhouse (Merchuk-Ovnat et al., 2016b). Furthermore, photosynthesis was measured both *via* gas exchange and with a portable device *via* photochemical quenching during sprouting and grain filling, and inferences were also made about WUE *via* carbon isotopes. In addition, the higher grain yield, TKW, and total dry matter of NIL-B-7A-2 (Merchuk-Ovnat et al., 2016a) were confirmed in the present experiment. However, the higher grain yield of NIL-Z-7A-2 in the control treatment in the field/screenhouse experiment (Merchuk-Ovnat et al., 2016a) was not observed in the HTP experiment, where TKW was increased under drought stress conditions.

The effect of the wild emmer wheat QTL on chromosome 7A revealed a mixed pattern in BarNir and Zahir backgrounds. For some traits it differed in both cultivars, while for others similar effects were observed. Thus, in both backgrounds a higher TKW was detected under drought stress conditions. In addition, a significant delay in the timing of senescence was observed in both based on CVa. This effect, known as 'stay-green' is advantageous under drought stress as it extends the photosynthetic activity, thus providing more assimilates for grain filling (Kamal et al., 2019). While 'stay-green' had a positive effect on TKW and yield in wheat mutants (Spano et al., 2003), a negative correlation of the late onset of senescence with yield was observed by Kipp et al. (2014). Non-invasive imaging methods such as those applied here, can visualize the 'stay-green' effect. In the field, the Normalized Difference Vegetation Index (NDVI) turned out to be suitable for its detection and could be modeled by a logistic model (Christopher et al., 2014). In a drought stress study it was possible to establish a clear relationship between higher yield and delayed senescence in wheat (Christopher et al., 2016; Rebetzke et al. 2016). The 'stay-green' effect was recently investigated in a GWAS study with sorghum based on several years of experiments with field-based drought stress in ten environments (Faye et al., 2021). It was detected that orthologs of the flowering genes in maize underlie the effect and thus cause an increased grain weight. HTP experiments until plant maturity offer the chance to investigate this effect in conjunction with other important traits to gain a holistic understanding of potential trade-offs.

The effect of the 7A-QTL may bear on the production and distribution of hormones at the time of grain filling. In the study of the 'stay green' phenotype in wheat, an association with altered cytokinin metabolism and the hormone ABA has already been established (Wang et al., 2016). In a previous transcriptome study of drought effect in drought resilient vs. susceptible wild emmer wheat accessions, the involvement of plant hormones, mainly ABA, GA, IAA, and prolonged metabolic activity were associated with drought resilience (Krugman et al., 2010, 2011).

In the background of BarNir the 7A QTL also resulted in significantly greater EB in both treatments from the seedling stage on, which was connected with larger plants, higher photosynthetic rate, and an improved WUE. The slightly lower CVa observed during a phase when all other plants appeared normally green could be related to epicuticle growth. A link between leaf color and wax content has been demonstrated in oilseed rape by overexpressing the lipid transfer protein gene *BraLTP1* and in Spanish juniper (*Juniperus thurifera*) by measuring the leaf reflectance of green and glaucous leaves with a spectroradiometer (Esteban et al., 2014; Liu et al., 2014). Several studies have identified a relationship between epicuticular waxes and reduced transpiration and higher photosynthesis under drought stress (Guo et al., 2016; Bi et al., 2017). Future studies should evaluate epicuticular waxes on the leaf surface in more detail in addition to plant hormones in BarNir and NIL-B-7A-2.

Since these effects in the BarNir background were not found in the Zahir background, the origin of the QTL was scrutinized. The QTLs were selected from a RIL population originating from a cross between wild emmer wheat and the durum wheat cultivar Langdon. The selection of flanking markers for the QTLs was based on a DArT map (Peleg et al. 2008; Merchuk-Ovnat et al., 2016a). In 2020, another genetic map was created based on 15 K SNP array for the RIL 12 and NIL-B-7A-2 (Deblieck et al., 2020; Fatiukha et al., 2021). Based on this new map, that included 4,015 SNPs, it was found that genetic material from Langdon is also present in the selected QTL region.

Therefore, there is the potential that the differences of the QTL effects in NIL-B-7A-2 compared to NIL-Z-7A-5 arise from the Langdon fragment. Different effects of introgressed QTLs in different genetic backgrounds are not only caused by genotype-environment interactions, but are also due to the different backgrounds (Muellner et al., 2020; Ollier et al., 2020).

The 2B QTL showed a positive effect on the development of EB from flowering to maturity in stress treatment. In principle, there is a clear correlation between a higher number of tillers and a higher yield (Naruoka et al., 2011). However, under stress conditions, increased tillering can be a disadvantage for the plants because not all shoots form fertile ears (Wang Z. et al., 2016; Fábián et al., 2019). Nevertheless, NIL-U-2B-3, also showed a higher number of spikes in both treatments and a higher number of fertile spikes under drought. Higher grain weight, as observed in the field/screenhouse, could not be confirmed here, which may be due to genotype-environment interactions (Merchuk-Ovnat 2016a). Although the plant grain weight was not higher under any treatment in NIL-U-2B-3 in the HTP experiment, the WUE and the HI were increased under drought. The higher tillering and WUE may be related to abscisic acid (ABA; Wang et al., 2018; Itam et al., 2020). The plant hormone ABA is involved in many metabolic pathways. It is an important regulator of water use because it directly regulates stomatal aperture, thereby affecting transpiration (Dunn et al., 2019; Mega et al., 2019). CIPK genes play an important role as they mediate between the ABA signaling pathway and drought stress responses (Cui et al., 2018). Sensitivity for ABA should be tested in the future.

The fact that a higher grain weight was not achieved despite the increased number of fertile ears may be explained by the source-sink relationship. Although more EB or leaf area is available as a source and more fertile ears as sinks, the process of filling the grains was nevertheless interrupted by drought stress or earlier onset of senescence, which interrupts photosynthesis.

Presumably, many resources were invested in tillering, which is far higher for single plants than for plants in field stands, leaving fewer resources in the form of water-soluble carbohydrates available for grain filling (Abdelrahman et al., 2020).

Conclusion

This study demonstrates that non-invasive imaging under controlled conditions and a well-chosen setup can shed light on complex traits such as yield formation under drought even with the drawbacks of a pot experiment. For the first time, an HTP experiment was conducted over the whole plant life cycle in wheat and was able to not only confirm the effect of improved yield and dry matter of two wild emmer wheat QTLs introgressed into Israeli wheat cultivars but also resulted in further insights of their effects during plant development and their temporal dynamics. Thus, it is clear that HTP and field experiments can be combined to complement elucidation of intogressed QTLs in NILs, as in this study, and serve to further decipher mechanisms. Lessons from this experiment can also be drawn with respect to the useful phenotyping period for traits such as PH and EB. Maximum PH and EB were reached about a week after heading, so experiments that only aim at exploring these traits can be stopped at that time. To obtain information on different onset and progress of senescence, the evaluation period should be extended, accordingly. Here, the CVa curves represented best the ongoing senescence of plants. This process can be subjected to modelling of growth curves to obtain parameters for the rate of maturation as the curves of CVa of individual plants are very clear at that time.

The effects of beneficial QTLs of wild emmer wheat in drought and also in control conditions demonstrate the importance of using wild alleles for crop improvement. The differences in the effect of the 7A QTL in the two genetic backgrounds need to be further evaluated in the future. Since the effect of wild emmer wheat QTLs was confirmed in field/screenhouse and pot trials, the NILs were recently crossed with elite German cultivars for future research.

Data availability statement

The raw data supporting the conclusions of this article will be made available by the authors, without undue reservation.

Author contributions

YS and KN designed the study. KN conducted the experiment. ML analyzed the precision phenotyping data and was together with KN the major contributor in writing the manuscript. YS supported in statistical analysis of the phenotypic data. CK supported in image analysis and developed an update of the image analysis software IAP. YS and TK developed the material and together with AG, MD, DP, and FO supported in interpretation of the results about QTL effects. All authors contributed to the article and approved the submitted version.

Funding

This study was supported by the Israel Ministry of Agriculture and Rural Development, Chief Scientist Foundation (Grants 837-0079-10, 837-0162-14) and the German Federal Ministry of Food and Agriculture (FKZ: 2813IL03). YS is the incumbent of the Haim Gvati Chair in Agriculture. This work was conducted as part of the STARGATE project funded by the European Union's Horizon 2020 Research and Innovation Program under grant agreement number 952339.

Acknowledgments

The authors thank Ingo Mücke, Ute Krajewski, Katrin Trnka, and the gardener team of Kathrin Gramel-Koch for support with experimental work. Special thanks to Yusheng Zhao and Dennis Psaroudakis for the support with the statistical analysis.

Conflict of interest

CK was employed by company BASF SE.

The remaining authors declare that the research was conducted in the absence of any commercial or financial relationships that could be construed as a potential conflict of interest.

Publisher's note

Supplementary material

The Supplementary material for this article can be found online at: https://www.frontiersin.org/articles/10.3389/fpls.2022.965287/full#supplementary-material

References

Abdelrahman, M., Burritt, D. J., Gupta, A., Tsujimoto, H., Tran, L. S. P., and Foyer, C. (2020). Heat stress effects on source-sink relationships and metabolome dynamics in wheat. *J. Exp. Bot.* 71, 543–554. doi: 10.1093/jxb/erz296

Anscombe, F. J., and Tukey, J. W. (1963). The examination and analysis of residuals. *Technometrics* 5, 141–160. doi: 10.1080/00401706.1963.10490071

Asseng, S., Ewert, F., Martre, P., Rötter, R. P., Lobell, D. B., Cammarano, D., et al. (2015). Rising temperatures reduce global wheat production. *Nat. Clim. Chang.* 5, 143–147. doi: 10.1038/nclimate2470

Barzana, G., Rios, J. J., Lopez-Zaplana, A., Nicolas-Espinosa, J., Yepes-Molina, L., Garcia-Ibañez, P., et al. (2020). Interrelations of nutrient and water transporters in plants under abiotic stress. *Physiol. Plant.* 171, 595–619. doi: 10.1111/ppl.13206

Bi, H., Kovalchuk, N., Langridge, P., Tricker, P. J., Lopato, S., and Borisjuk, N. (2017). The impact of drought on wheat leaf cuticle properties. *BMC Plant Biol.* 17, 85–13. doi: 10.1186/s12870-017-1033-3

Blum, A. (2017). Osmotic adjustment is a prime drought stress adaptive engine in support of plant production. *Plant Cell Environ.* 40, 4–10. doi: 10.1111/pce.12800

Buckley, T. N., and Mott, K. A. (2013). Modelling stomatal conductance in response to environmental factors. *Plant Cell Environ.* 36, 1691–1699. doi: 10.1111/pce.12140

Chen, D., Neumann, K., Friedel, S., Kilian, B., Chen, M., Altmann, T., et al. (2014). Dissecting the phenotypic components of crop plant growth and drought responses based on high-throughput image analysis. *Plant Cell* 26, 4636–4655. doi: 10.1105/tpc.114.129601

Chen, C., Wang, B., Feng, P., Xing, H., Fletcher, A. L., and Lawes, R. A. (2020). The shifting influence of future water and temperature stress on the optimal flowering period for wheat in Western Australia. *Sci. Total Environ.* 737:139707. doi: 10.1016/j.scitotenv.2020.139707

Christopher, J. T., Christopher, M. J., Borrell, A. K., Fletcher, S., and Chenu, K. (2016). Stay-green traits to improve wheat adaptation in well-watered and water-limited environments. *J. Exp. Bot.* 67, 5159–5172. doi: 10.1093/jxb/erw276

Christopher, J. T., Veyradier, M., Borrell, A. K., Harvey, G., Fletcher, S., and Chenu, K. (2014). Phenotyping novel stay-green traits to capture genetic variation in senescence dynamics. *Funct. Plant Biol.* 41, 1035–1048. doi: 10.1071/FP14052

Cui, X. Y., Du, Y. T., Fu, J., Dong, Y. U. T. F., Wang, C. T., Chen, M., et al. (2018). Wheat CBL-interacting protein kinase 23 positively regulates drought stress and ABA responses. *BMC Plant Biol.* 18, 93–13. doi: 10.1186/s12870-018-1306-5

Deblieck, M., Fatiukha, A., Grundman, N., Merchuk-Ovnat, L., Saranga, Y., Krugman, T., et al. (2020). GenoTypeMapper: graphical genotyping on genetic and sequence-based maps. *Plant Methods* 16, 123–111. doi: 10.1186/s13007-020-00665-7

Dhanagond, S., Liu, G., Zhao, Y., Chen, D., Grieco, M., Reif, J., et al. (2019). Non-invasive phenotyping reveals genomic regions involved in pre-anthesis drought tolerance and recovery in spring barley. *Front. Plant Sci.* 10, 1–21. doi: 10.3389/fpls.2019.01307

Dunn, J., Hunt, L., Afsharinafar, M., Al Meselmani, M., Mitchell, A., Howells, R., et al. (2019). Reduced stomatal density in bread wheat leads to increased water-use efficiency. *J. Exp. Bot.* 70, 4737–4748. doi: 10.1093/jxb/erz248

Esteban, R., Fernández-Marín, B., Olano, J. M., Becerril, J., and García-Plazaola, J. I. (2014). Does plant colour matter? Wax accumulation as an indicator of decline in *Juniperus thurifera*. *Tree Physiol.* 34, 267–274. doi: 10.1093/treephys/tpu006

Fábián, A., Sáfrán, E., Szabó-Eitel, G., Barnabás, B., and Jäger, K. (2019). Stigma functionality and fertility are reduced by heat and drought co-stress in wheat. *Front. Plant Sci.* 10, 1–18. doi: 10.3389/fpls.2019.00244

Fadoul, H. E., Martínez Rivas, F. J., Neumann, K., Balazadeh, S., Fernie, A. R., and Alseekh, S. (2021). Comparative molecular and metabolic profiling of two contrasting wheat cultivars under drought stress. *Int. J. Mol. Sci.* 22:13287. doi: 10.3390/ijms222413287

FAOSTAT (2020). FAOSTAT Database. Rome: FAO.

Fatiukha, A., Deblieck, M., Klymiuk, V., Merchuk-Ovnat, L., Peleg, Z., Ordon, F., et al. (2021). Genomic architecture of phenotypic plasticity in response to water stress in tetraploid wheat. *Int. J. Mol. Sci.* 22:1723. doi: 10.3390/ijms22041723

Faye, J. M., Akata, E. A., Sine, B., Diatta, C., Cisse, N., Fonceka, D., et al. (2021). Quantitative and population genomics suggest a broad role of staygreen loci in the drought adaptation of sorghum. *Bio Rxiv, June*, 15.09.447769. doi: 10.1002/tpg2.20176

Gol, L., Haraldsson, E. B., and von Korff, M. (2020). Ppd-H1 integrates drought stress signals to control spike development and flowering time in barley. *J. Exp. Bot.* 72, 122–136. doi: 10.1093/jxb/eraa261

Golzarian, M. R., Frick, R. A., Rajendran, K., Berger, B., Roy, S., Tester, M., et al. (2011). Accurate inference of shoot biomass from high-throughput images of cereal plants. *Plant Methods* 7, 1–11. doi: 10.1186/1746-4811-7-2

Grieco, M., Roustan, V., Dermendjiev, G., Rantala, S., Jain, A., Leonardelli, M., et al. (2020). Adjustment of photosynthetic activity to drought and fluctuating light in wheat. *Plant Cell Environ.* 43, 1484–1500. doi: 10.1111/pce.13756

Guo, J., Xu, W., Yu, X., Shen, H., Li, H., Cheng, D., et al. (2016). Cuticular wax accumulation is associated with drought tolerance in wheat near-isogenic lines. *Front. Plant Sci.* 7, 1–10. doi: 10.3389/fpls.2016.01809

Honsdorf, N., March, T. J., Berger, B., Tester, M., and Pillen, K. (2014). High-throughput phenotyping to detect drought tolerance QTL in wild barley introgression lines. *PLoS One* 9:e97047. doi: 10.1371/journal.pone.0097047

Ihsan, M. Z., El-Nakhlawy, F. S., Ismail, S. M., Fahad, S., and Daur, I. (2016). Wheat phenological development and growth studies as affected by drought and late season high temperature stress under arid environment. *Front. Plant Sci.* 7:795. doi: 10.3389/fpls.2016.00795

Itam, M., Mega, R., Tadano, S., Abdelrahman, M., Matsunaga, S., Yamasaki, Y., et al. (2020). Metabolic and physiological responses to progressive drought stress in bread wheat. *Sci. Rep.* 10, 17189–17114. doi: 10.1038/s41598-020-74303-6

Kamal, N. M., Gorafi, Y. S. A., Abdelrahman, M., Abdellatef, E., and Tsujimoto, H. (2019). Stay-green trait: a prospective approach for yield potential, and drought and heat stress adaptation in globally important cereals. *Int. J. Mol. Sci.* 20. doi: 10.3390/ijms20235837

Kipp, S., Mistele, B., and Schmidhalter, U. (2014). Identification of stay-green and early senescence phenotypes in high-yielding winter wheat, and their relationship to grain yield and grain protein concentration using high-throughput phenotyping techniques. *Funct. Plant Biol.* 41, 227–235. doi: 10.1071/FP13221

Klukas, C., Chen, D., and Pape, J. M. (2014). Integrated analysis platform: an open-source information system for high-throughput plant phenotyping. *Plant Physiol.* 65, 506–518. doi: 10.1104/pp.113.233932

Krugman, T., Chagué, V., Peleg, Z., Balzergue, S., Just, J., Korol, A. B., et al. (2010). Multilevel regulation and signalling processes associated with adaptation to terminal drought in wild emmer wheat. *Funct. Integ. Gen.* 10, 167–186. doi: 10.1007/s10142-010-0166-3

Krugman, T., Nevo, E., Beharav, A., Sela, H., and Fahima, T. (2018). The institute of evolution wild cereal gene bank at the University of Haifa. *Isr. J. Plant Sci.* 65, 129–146. doi: 10.1163/22238980-00001065

Krugman, T., Peleg, Z., Quansah, L., Chagué, V., Korol, A. B., Nevo, E., et al. (2011). Alteration in expression of hormone-related genes in wild emmer wheat roots associated with drought adaptation mechanisms. *Funct. Integ. Gen.* 11, 565–583. doi: 10.1007/s10142-011-0231-6

Langridge, P., and Reynolds, M. (2021). Breeding for drought and heat tolerance in wheat. *Theor. Appl. Genet.* 134, 1753–1769. doi: 10.1007/s00122-021-03795-1

Langstroff, A., Heuermann, M. C., Stahl, A., and Junker, A. (2022). Opportunities and limits of controlled-environment plant phenotyping for climate response traits. *Theor. Appl. Genet.* 135, 1–16. doi: 10.1007/s00122-021-03892-1

Leng, G., and Hall, J. (2019). Crop yield sensitivity of global major agricultural countries to droughts and the projected changes in the future. *Sci. Total Envir.* 654, 811–821. doi: 10.1016/j.scitotenv.2018.10.434

Liu, F., Xiong, X., Wu, L., Fu, D., Hayward, A., Zeng, X., et al. (2014). Bra LTP1, a lipid transfer protein gene involved in epicuticular wax deposition, cell proliferation and flower development in *Brassica napus*. *PLoS One* 9:e110272. doi: 10.1371/journal.pone.0110272

Mascher, M., Schreiber, M., Scholz, U., Graner, A., Reif, J. C., and Stein, N. (2019). Genebank genomics bridges the gap between the conservation of crop diversity and plant breeding. *Nat. Genet.* 51, 1076–1081. doi: 10.1038/s41588-019-0443-6

Mega, R., Abe, F., Kim, J. S., Tsuboi, Y., Tanaka, K., Kobayashi, H., et al. (2019). Tuning water-use efficiency and drought tolerance in wheat using abscisic acid receptors. *Nat. Plants* 5, 153–159. doi: 10.1038/s41477-019-0361-8

Merchuk-Ovnat, L., Barak, V., Fahima, T., Ordon, F., Lidzbarsky, G. A., Krugman, T., et al. (2016a). Ancestral QTL alleles from wild emmer wheat improve drought resistance and productivity in modern wheat cultivars. *Front. Plant Sci.* 7, 1–14. doi: 10.3389/fpls.2016.00452

Merchuk-Ovnat, L., Fahima, T., Krugman, T., and Saranga, Y. (2016b). Ancestral QTL alleles from wild emmer wheat improve grain yield, biomass and photosynthesis across environments in modern wheat. *Plant Sci.* 251, 23–34. doi: 10.1016/j.plantsci.2016.05.003

Mikołajczak, K., Ogrodowicz, P., Ćwiek-Kupczyńska, H., Weigelt-Fischer, K., Mothukuri, S. R., Junker, A., et al. (2020). Image phenotyping of spring barley (*Hordeum vulgare* L.) RIL population under drought: selection of traits and biological interpretation. *Front. Plant Sci.* 11:743. doi: 10.3389/fpls.2020.00743

Muellner, A. E., Buerstmayr, M., Eshonkulov, B., Hole, D., Michel, S., Hagenguth, J. F., et al. (2020). Comparative mapping and validation of multiple

disease resistance QTL for simultaneously controlling common and dwarf bunt in bread wheat. *Theor. Appl. Genet.* 134, 489–503. doi: 10.1007/s00122-020-03708-8

Munns, R., James, R. A., Sirault, X. R. R., Furbank, R. T., and Jones, H. G. (2010). New phenotyping methods for screening wheat and barley for beneficial responses to water deficit. *J. Exp. Bot.* 61, 3499–3507. doi: 10.1093/jxb/erq199

Naruoka, Y., Talbert, L. E., Lanning, S. P., Blake, N. K., Martin, J. M., and Sherman, J. D. (2011). Identification of quantitative trait loci for productive tiller number and its relationship to agronomic traits in spring wheat. *Theor. Appl. Genet.* 123, 1043–1053. doi: 10.1007/s00122-011-1646-0

Neumann, K., Klukas, C., Friedel, S., Rischbeck, P., Chen, D., Entzian, A., et al. (2015). Dissecting spatiotemporal biomass accumulation in barley under different water regimes using high-throughput image analysis. *Plant Cell Environ.* 38, 1980–1996. doi: 10.1111/pce.12516

Neumann, K., Zhao, Y., Chu, J., Keilwagen, J., Reif, J. C., Kilian, B., et al. (2017). Genetic architecture and temporal patterns of biomass accumulation in spring barley revealed by image analysis. *BMC Plant Biol.* 17:137. doi: 10.1186/s12870-017-1085-4

Nevo, E., and Beiles, A. (1989). Genetic diversity of wild emmer wheat in Israel and Turkey-Structure, evolution, and application in breeding. *Theor. Appl. Genet.* 77, 421–455. doi: 10.1007/BF00305839

Nevo, E., Pu, Y. B., Pavlicek, T., Khalifa, S., Tavasi, M., and Beiles, A. (2012). Evolution of wild cereals during 28 years of global warming in Israel. *Proc. Natl. Acad. Sci. U. S. A.* 109, 3412–3415. doi: 10.1073/pnas.1121411109

Ollier, M., Talle, V., Brisset, A. L., Le Bihan, Z., Duerr, S., Lemmens, M., et al. (2020). QTL mapping and successful introgression of the spring wheat-derived QTL Fhb 1 for Fusarium head blight resistance in three European triticale populations. *Theor. Appl. Genet.* 133, 457–477. doi: 10.1007/s00122-019-03476-0

Peleg, Z., Fahima, T., Abbo, S., Krugman, T., Nevo, E., Yakir, D., et al. (2005). Genetic diversity for drought resistance in wild emmer wheat and its ecogeographical associations. *Plant Cell Environ.* 28, 176–191. doi: 10.1111/j.1365-3040.2005.01259.x

Peleg, Z., Fahima, T., Krugman, T., Abbo, S., Yakir, D., Korol, A. B., et al. (2009). Genomic dissection of drought resistance in durum wheat x wild emmer wheat recombinant inbreed line population. *Plant Cell Environ.* 32, 758–779. doi: 10.1111/j.1365-3040.2009.01956.x

Peleg, Z., Saranga, Y., Suprunova, T., Ronin, Y., Röder, M. S., Kilian, B., et al. (2008). High-density genetic map of durum wheat × wild emmer wheat based on SSR and DArT markers. *Theor. Appl. Genet.* 117, 103–115. doi: 10.1007/s00122-008-0756-9

Pham, A. T., Maurer, A., Pillen, K., Brien, C., Dowling, K., Berger, B., et al. (2019). Genome-wide association of barley plant growth under drought stress using a nested association mapping population. *BMC Plant Biol.* 19, 134–116. doi: 10.1186/s12870-019-1723-0

Poorter, H., Fiorani, F., Pieruschka, R., Wojciechowski, T., Putten, W. H., Kleyer, M., et al. (2016). Pampered inside, pestered outside? Differences and similarities between plants growing in controlled conditions and in the field. *New Phytol.* 212, 838–855. doi: 10.1111/nph.14243

Prathap, V., Ali, K., Singh, A., Vishwakarma, C., Krishnan, V., Chinnusamy, V., et al. (2019). Starch accumulation in rice grains subjected to drought during grain filling stage. *Plant Physiol. Biochem.* 142, 440–451. doi: 10.1016/j.plaphy.2019.07.027

Rebetzke, G. J., Jimenez-Berni, J. A., Bovill, W. D., Deery, D. M., and James, R. A. (2016). High-throughput phenotyping technologies allow accurate selection of stay-green. *J. Exp. Bot.* 67, 4919–4924. doi: 10.1093/jxb/erw301

Sales, C., Molero, G., Evans, J., Taylor, S., Joynson, R., Furbank, R., et al. (2022). Phenotypic variation in photosynthetic traits in wheat grown under field versus glasshouse conditions. *J. Exp. Bot.* 73, 3221–3237. doi: 10.1093/jxb/erac096

Saranga, Y., Peleg, Z., and Fahima, T. (2008). "Physiological-genetic dissection of drought resistance in wild emmer wheat" in *The 11th International Wheat Genetics Symposium Proceedings*. eds. R. Appels, R. Eastwood, E. Lagudah, P. Langridge, M. Mackay and L. McIntyreet al. (Sydney: Sydney University Press)

Sehgal, A., Sita, K., Siddique, K. H. M., Kumar, R., Bhogireddy, S., Varshney, R. K., et al. (2018). Drought or/and heat-stress effects on seed filling in food crops: impacts on functional biochemistry, seed yields, and nutritional quality. *Front. Plant Sci.* 9:1705. doi: 10.3389/fpls.2018.01705

Shavrukov, Y., Kurishbayev, A., Jatayev, S., Shvidchenko, V., Zotova, L., Koekemoer, F., et al. (2017). Early flowering as a drought escape mechanism in plants: how can it aid wheat production? *Front. Plant Sci.* 8, 1–8. doi: 10.3389/fpls.2017.01950

Shiferaw, B., Smale, M., Braun, H. J., Duveiller, E., Reynolds, M., and Muricho, G. (2013). Crops that feed the world 10. Past successes and future challenges to the role played by wheat in global food security. *Food Secur.* 5, 291–317. doi: 10.1007/s12571-013-0263-y

Shorinola, O., Kaye, R., Golan, G., Peleg, Z., Kepinski, S., and Uauy, C. (2019). Genetic screening for mutants with altered seminal root numbers in hexaploid wheat using a high-throughput root phenotyping platform. *G3* 9, 2799–2809. doi: 10.1534/g3.119.400537

Spano, G., Di Fonzo, N., Perrotta, C., Platani, C., Ronga, G., Lawlor, D. W., et al. (2003). Physiological characterization of 'stay green' mutants in durum wheat. *J. Exp. Bot.* 54, 1415–1420. doi: 10.1093/jxb/erg150

Toreti, A., Belward, A., Perez-Dominguez, I., Naumann, G., Luterbacher, J., Cronie, O., et al. (2019). The exceptional 2018 European water seesaw calls for action on adaptation. *Earth's Fut.* 7, 652–663. doi: 10.1029/2019EF001170

Tschiersch, H., Junker, A., Meyer, R. C., and Altmann, T. (2017). Establishment of integrated protocols for automated high throughput kinetic chlorophyll fluorescence analyses. *Plant Methods* 13:54. doi: 10.1186/s13007-017-0204-4

Wang, H., Chen, W., Eggert, K., Charnikhova, T., Bouwmeester, H., Schweizer, P., et al. (2018). Abscisic acid influences tillering by modulation of strigolactones in barley. *J. Exp. Bot.* 69, 3883–3898. doi: 10.1093/jxb/ery200

Wang, W., Hao, Q., Tian, F., Li, Q., and Wang, W. (2016). The stay-green phenotype of wheat mutant tasg1 is associated with altered cytokinin metabolism. *Plant Cell Rep.* 35, 585–599. doi: 10.1007/s00299-015-1905-7

Wang, Z., Liu, Y., Shi, H., Mo, H., Wu, F., Lin, Y., et al. (2016). Identification and validation of novel low-tiller number QTL in common wheat. *Theor. Appl. Genet.* 129, 603–612. doi: 10.1007/s00122-015-2652-4

Wang, J. Y., Turner, N. C., Liu, Y. X., Siddique, K. H. M., and Xiong, Y. C. (2017). Effects of drought stress on morphological, physiological and biochemical characteristics of wheat species differing in ploidy level. *Funct. Plant Biol.* 44, 219–234. doi: 10.1071/FP16082

Witzenberger, A., Hack, H., and van den Boom, T. (1989). Erläuterungen zum BBCH Dezimal-Code für die Entwicklungsstadien des Getreides – mit Abbildungen. *Gesunde Pflanzen* 41, 384–388.

2.2 HTP of chickpeas during drought stress

"Engaging Precision Phenotyping to Scrutinize Vegetative Drought Tolerance and Recovery in Chickpea Plant Genetic Resources"

by

Madita Lauterberg, Henning Tschiersch, Roberto Papa, Elena Bitocchi and Kerstin Neumann

Published in
Plants; 4. August 2023
https://www.mdpi.com/2223-7747/12/15/2866

plants

MDPI

Article

Engaging Precision Phenotyping to Scrutinize Vegetative Drought Tolerance and Recovery in Chickpea Plant Genetic Resources

Madita Lauterberg [1], Henning Tschiersch [1], Roberto Papa [2], Elena Bitocchi [2] and Kerstin Neumann [1,*]

[1] Leibniz Institute of Plant Genetics and Crop Plant Research (IPK), 06466 Gatersleben, Germany; lauterberg@ipk-gatersleben.de (M.L.)
[2] Department of Agricultural, Food and Environmental Sciences, Università Politecnica delle Marche, 60131 Ancona, Italy
* Correspondence: neumannk@ipk-gatersleben.de

Abstract: Precise and high-throughput phenotyping (HTP) of vegetative drought tolerance in chickpea plant genetic resources (PGR) would enable improved screening for genotypes with low relative loss of biomass formation and reliable physiological performance. It could also provide a basis to further decipher the quantitative trait drought tolerance and recovery and gain a better understanding of the underlying mechanisms. In the context of climate change and novel nutritional trends, legumes and chickpea in particular are becoming increasingly important because of their high protein content and adaptation to low-input conditions. The PGR of legumes represent a valuable source of genetic diversity that can be used for breeding. However, the limited use of germplasm is partly due to a lack of available characterization data. The development of HTP systems offers a perspective for the analysis of dynamic plant traits such as abiotic stress tolerance and can support the identification of suitable genetic resources with a potential breeding value. Sixty chickpea accessions were evaluated on an HTP system under contrasting water regimes to precisely evaluate growth, physiological traits, and recovery under optimal conditions in comparison to drought stress at the vegetative stage. In addition to traits such as Estimated Biovolume (EB), Plant Height (PH), and several color-related traits over more than forty days, photosynthesis was examined by chlorophyll fluorescence measurements on relevant days prior to, during, and after drought stress. With high data quality, a wide phenotypic diversity for adaptation, tolerance, and recovery to drought was recorded in the chickpea PGR panel. In addition to a loss of EB between 72% and 82% after 21 days of drought, photosynthetic capacity decreased by 16–28%. Color-related traits can be used as indicators of different drought stress stages, as they show the progression of stress.

Keywords: chickpea; image-derived traits; growth dynamics; plant genetic resources; drought stress; chlorophyll fluorescence

Citation: Lauterberg, M.; Tschiersch, H.; Papa, R.; Bitocchi, E.; Neumann, K. Engaging Precision Phenotyping to Scrutinize Vegetative Drought Tolerance and Recovery in Chickpea Plant Genetic Resources. *Plants* **2023**, *12*, 2866. https://doi.org/10.3390/plants12152866

Academic Editors: Barbara Pipan and Vladimir Meglič

Received: 1 June 2023
Revised: 24 July 2023
Accepted: 28 July 2023
Published: 4 August 2023

1. Introduction

In addition to the rising global population, the changing climate poses challenges for agriculture [1]. In Europe, droughts will be 11–28 times more frequent in different regions and will become much more severe in terms of their spatial and temporal spread [2]. However, there is already a high variability in the severity, timing, and intensity of droughts with severe consequences for Europe [3]. This is especially true for legumes, as they are summer crops, which are more yield-instable than winter crops [4–6]. Many studies among several crop species have employed plant genetic resources (PGR) to detect quantitative trait loci (QTL) that can harbor beneficial alleles at loci for relevant phenotypic traits under challenging environments [7–10]. In chickpea, valuable QTLs from landraces against abiotic and biotic stress factors and improved root growths have been introgressed by marker-assisted backcrossing into cultivars [11,12]. Other methods for the introgression

of regions of interest or more specific genes include CRISPR [13,14]. However, besides drought tolerance per se, it is also essential to further investigate the ability to recover from drought, as precipitation is becoming more extreme and unpredictable [15]. Hence, it is necessary to evaluate PGR not only for drought tolerance but also for drought recovery and to analyze drought stress in the vegetative stage in addition to the drought stress at the end of the season [16]. So far, it is not sufficiently understood how plants respond to drought stress at different growth stages and during recovery to contribute to a more resilient agricultural system.

Chickpea (*Cicer arietinum* L.) is one of the legumes of the future [17–19]. Global production was 15 million tons, with cultivation being carried out primarily in India and Turkey, followed by Pakistan, Myanmar, and Ethiopia; an increasing production can be observed in Europe [20,21] (FAO, 2021). With their high protein content and important nutrients, they are not only in line with the dietary trend towards less meat consumption but because they form symbiotic nodulation with bacteria, they require less fertilizer and thus fit into an agriculture in which the use of fertilizers is viewed critically [22–24]. There are two different types of chickpea: *desi* and *kabuli*. The rough grains of *desi* are different in color and smaller than the beige and softer-coated *kabuli*. In addition, there are differences in biomass formation, in the metabolomic response to drought stress, and in anthocyanin synthesis [25–27]. To increase chickpea production in Europe, studying drought stress during the vegetative stage is crucial, as is the development of genotypes that are less sensitive to cold and more tolerant of *Ascochyta blight* [28–31]. The response of chickpea to drought stress depends on its duration and intensity, as well as the growth stage of the plants [18]. Terminal drought stress, which occurs from the early pod set, reduces biomass, reproductive growth, the harvest index, and final seed yield [32]. A higher abscisic acid content was also found in the seeds, which presumably leads to pod abortion. Reduced grain yield could be explained by a reduced growth rate, the leaf area index during the pod-filling stage, and reduced biomass during the reproductive growth stage [33]. Field studies have shown that chickpeas develop a deeper and denser root system to absorb water from deeper soil regions and that they tend to deposit lignin in the root xylem when exposed to drought stress [34–36]. Furthermore, drought stress has a negative impact on nodulation, which has a negative impact on yield [37]. Animoacids, especially asparagine, and organic acids such as malate accumulate in the nodules and lead to inhibition of respiration, nitrogen accumulation, an imbalance in the cell redox status in the nodules, and reduced nitrogenase activity [38].

Until now, little has been known about drought tolerance during the vegetative stage, because most studies have focused on terminal drought stress, which is prevailing in the major production areas and to which chickpea is adapted. In addition to the rooting ability, a low relative loss of above-ground biomass is an important criterion to assess drought tolerance. Losses in biomass production due to drought stress are primarily due to the inhibition of photosynthesis since it is the basic process for maintaining plant growth [16,32]. To evaluate photosynthesis, the pigments, chlorophyll, and carotenoids, which play a role in light trapping and photoprotection of the photosynthetic apparatus, were considered [39]. Recently, chlorophyll fluorescence traits were studied and provided insights into photosynthetic activity, especially under stress conditions [40–42]. To keep up with the progress of other technologies, the measurement of chlorophyll fluorescence was implemented in high-throughput phenotyping (HTP) [43].

The field of genotyping has developed tremendously in recent years with decreasing costs and increasing precision, but the acquisition of phenotype expression is often even more complex, objective, and costly [44,45]. HTP is a way to evaluate genotypes in detail, particularly under controlled greenhouse conditions [46]. Traits such as plant height, color-related traits, or most importantly, the Estimated Biovolume (EB) are assessed [47]. So far, in chickpea, HTP has only been employed to evaluate salinity tolerance and to detect genetic loci for growth rate, water use efficiency (WUE), and the number of seeds under

salinity and control conditions, among others [48,49]. No study on chickpea for drought stress tolerance employing HTP has been conducted yet.

Numerous HTP studies with high data quality on cold, heat, or drought stress, for example in pea (*Pisum sativum*), *Arabidopsis thaliana*, barley (*Hordeum vulgare*), and maize (*Zea mays*), were conducted to search for tolerance traits or combined with genetic data in a genome-wide association study (GWAS) to decipher relevant QTL with spatial and temporal precision [50–53]. HTP has the strength to assess the temporal dynamics of agriculturally important traits such as biomass or plant height and reveal traits related to plant physiology such as WUE and the efficiency of photosynthesis [50,54]. Furthermore, color-related information was used to study the progress of drought stress and senescence in barley (*H. vulgare*), rice (*Oryza sativa*), maize (*Z. mays*), and wheat (*Triticum aestivum*, *T. durum*) [47,53–55].

The study is aimed at the investigation of vegetative drought tolerance and recovery in a panel of PGR of chickpea by employing HTP. The panel is balanced for the two types of chickpea, *desi* and *kabuli*, and was selected to maximize the genetic diversity of the species on the basis of passport data. The study will reveal (1) how drought during the vegetative stage affects chickpea growth performance and physiology, (2) how chickpea is able to recover from this type of drought, and (3) how to identify superior genotypes for further studies within the panel of PGR.

2. Results

2.1. Data Quality and HTP Experiment

The data quality, represented here as heritability, was high for the EB throughout the whole experiment (Figure 1). Heritability for the stress treatment was higher than that of the control treatment, averaging 0.80 compared to 0.55 in the control.

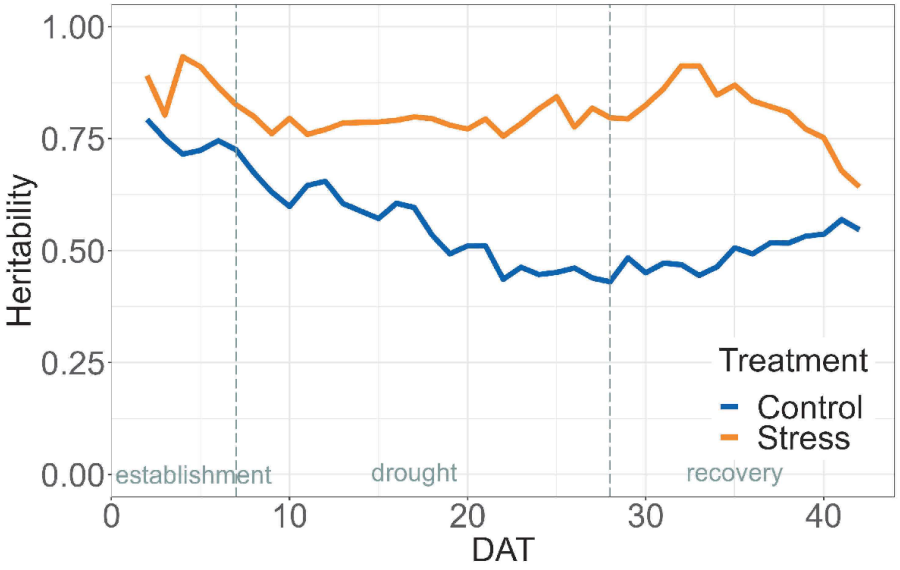

Figure 1. Heritability of Estimated Biovolume (EB).

The heritability of the manually determined plant weights was in line with EB results (Figure S1). The data quality of the PH was very high with a heritability of over 0.75 throughout all days (Figure S2). Similarly, the heritability for the MCV was approximately 0.7, except for some initial days and the last days during the recovery phase in the drought stress treatment. Furthermore, the heritability for r2g was very high with over 0.75 for the control treatment, but generally lower in the drought stress treatment. In contrast, heritability for y2g was higher in the drought stress treatment, primarily towards the end.

For the traits obtained from chlorophyll fluorescence imaging, the heritability was also high, with averages of 0.76 and 0.65 in control and stress treatments, respectively (Figure S3).

The EB of the last imaging day DAT 43 has been correlated with the manually measured plant weights; high coefficients of correlation (r = 0.96 and 0.97) were revealed for plant dry weight and fresh weight, respectively (Figure 2; Figure S4).

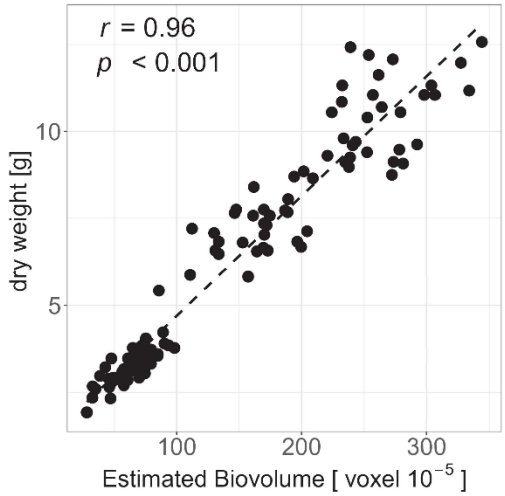

Figure 2. Correlation of Estimated Biovolume (EB) from DAT42 and dry weight from DAT43. Based on BLUEs across both experiments of all 60 genotypes. p indicates the level of significance and r is the coefficient of correlation.

In conclusion, all investigated traits have sufficient data quality for almost all days and can be used to gain further insights into drought effects and trait relations.

In the first experiment, no nodulation was observed in a single plant. Since the second experiment was a repeat of the first experiment with the same conditions, it was assumed that no nodulation occurred here either.

2.2. *Impact of Drought*

When looking at the EB and the manually recorded plant weights in both treatments, it is clear that lowering the PAW had a significant influence on the formation of EB (Tables S1–S3). Thus, a negative RGR for drought stress was observed at DAT 22 (Figure S5 and Table S4). This was followed by another week of very low RGR until it finally increased, with the onset of re-watering for the recovery (Table S4).

Thus, plants in the two treatments differed significantly in EB after seven days of drought from DAT 14 onwards (Figure 3). EB was 18.5 $\times$ 10^{-5} voxels for the drought stress treatment at DAT 28, the last day of drought, and 85.1 $\times$ 10^{-5} voxels in the control treatment. Therefore, the drought period resulted in an average of 78% loss of EB (Table S2).

The CV for EB was similar for both treatments up to DAT 12, but in the further course, the CV for the control treatment was 30% higher than that for the drought stress treatment, which was only approximately 20% (Figure S6).

Drought stress also had a significant effect on PH, MCV, r2g, and y2g (Figure 4 and Table S2). For PH, stressed plants were significantly smaller than unstressed plants from DAT 16 onwards. At the end of the drought period, the stressed plants were 32% smaller than those in the control treatment. A significant treatment difference in MCV was observed between DAT 16 and DAT 36. Initially, the MCV in stress increased but then the loss remained relatively constant at −6.4 to −5.79% during the last days of drought stress from DAT 24–28. With the onset of re-watering, the MCV in stress decreased again until there was no significant difference to control from DAT 36 onwards. The r2g ratio was significantly higher in stress treatment from DAT 17 until the end. It was 0.005 for the

control and 0.013 for the stress treatment on the last day of drought, representing a loss of −160% and indicating an increase compared to the control. As the recovery progressed, the r2g of stressed plants decreased again, so that the r2g on DAT42 was 0.004 for stressed plants and 0.006 for non-stressed plants. A very similar pattern was observed for the y2g. For y2g, on DAT 28, the control was 0.029 and the drought stress treatment was 0.069, showing a loss of −138%.

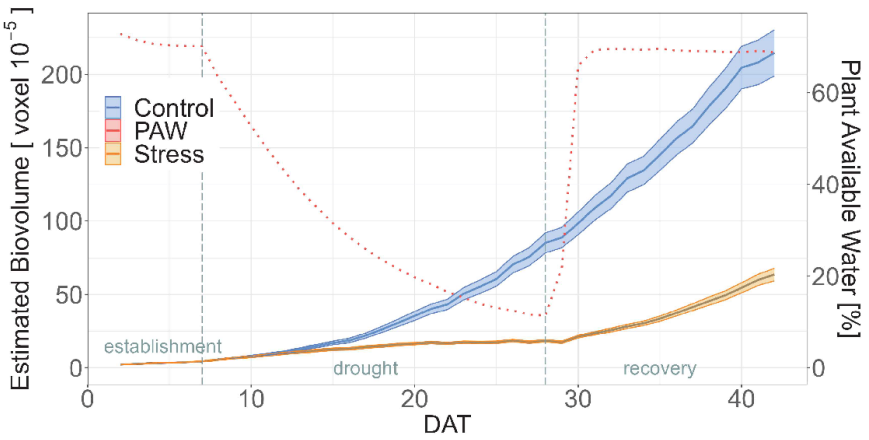

Figure 3. Estimated Biovolume (EB) in drought stress and control treatments. The dotted line indicates the plant available water (PAW) to which the secondary axis refers to The shadows describe the 95% confidence interval; as long as the shadows of the individual lines do not overlap, the significance level of $\alpha = 0.05$ was reached and therefore a significant difference exists. Based on means of BLUEs across both experiments of all 60 genotypes.

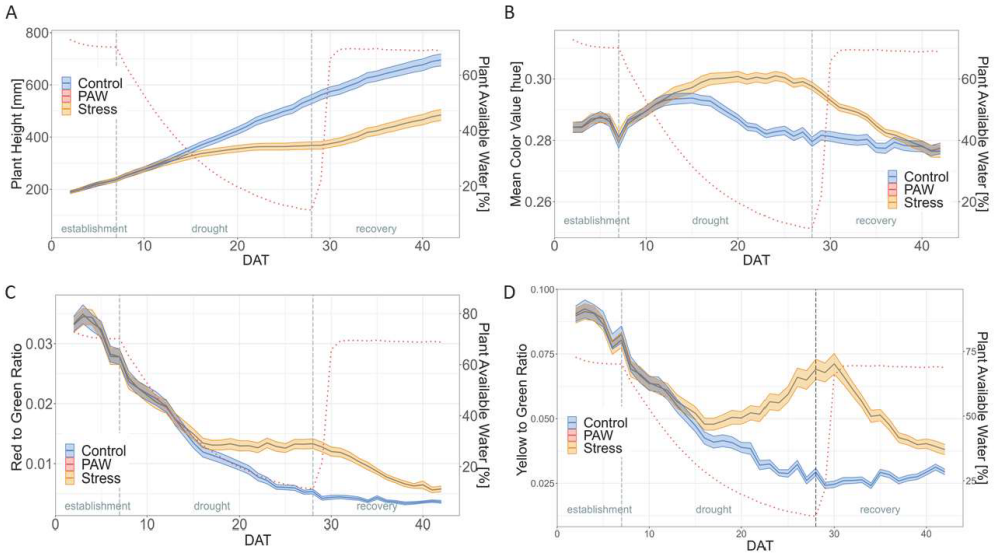

Figure 4. Further image-based traits under drought stress and control treatments. (**A**) Plant Height (PH); (**B**) Mean Color Value (MCV); (**C**) red to green ratio (r2g); (**D**) yellow to green ratio (y2g). The dotted line indicates the plant available water (PAW) to which the secondary axis refers to. The shadows describe the 95% confidence interval; as long as the shadows of the individual lines do not overlap, the significance level of $\alpha = 0.05$ was reached and therefore a significant difference exists. Based on means of BLUEs across both experiments of all 60 genotypes.

The CV for PH was relatively constant throughout the whole experiment in the control treatment but increased continuously from DAT 16 onwards in stress up to 18% at DAT 42 (Figure S6). For the MCV, the CV was higher for the drought stress treatment compared to the control treatment for DAT 12–22 and 41 and 42, but for the remaining days, from DAT 22–40, the opposite was true. Overall, the CV for MCV was the lowest of all considered traits, ranging between 1.5 and 2.5%. The CV for the r2g increased in both treatments from 13% on DAT 2 to 25% on DAT 15. For the following DATs, it was higher for the control treatment by up to 7% until, finally, for the last DAT 40–42, the CV was higher in the drought stress treatment. The CV pattern for y2g was similar to that of r2g, but continuously higher in the drought stress treatment from DAT 22 onwards.

The WUE in the three different drought phases was evaluated (Figure 5, Tables S5 and S6). The mean during DA was 0.038 voxel/mL for the control and 0.039 voxel/mL for drought stress (Tables S5 and S6). During DR, the WUE was lower in drought (0.026 voxel/mL) compared to the control treatment (0.04 voxel/mL). In DT, WUE was significantly higher in drought stress (9.63 voxels/mL) than in the control treatment (0.033 voxels/mL).

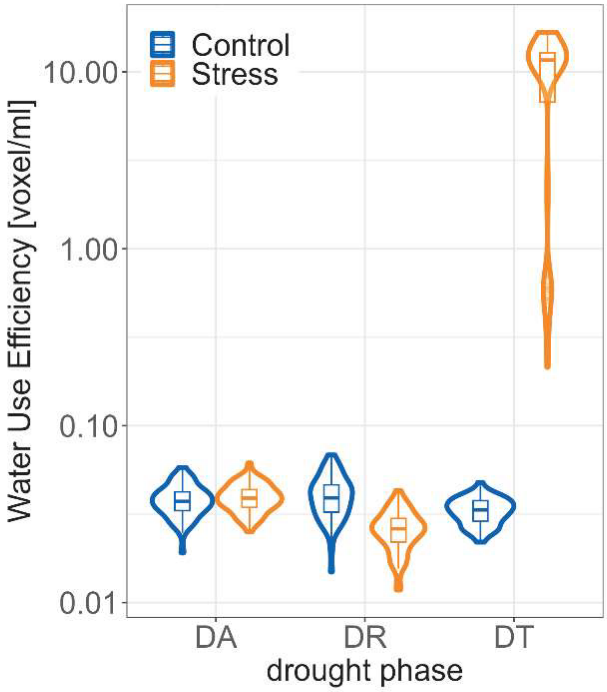

Figure 5. Water Use Efficiency (WUE) in different drought phases for drought stress and control treatments. Estimated Biovolume (EB) was based on BLUEs across both experiments of all 60 genotypes. The shape around the boxplot is a violin plot and describes the continuous distribution of the data at different values. DA = drought adaptability DAT 8–42; DR = drought recovery DAT 29–42; DT = drought tolerance DAT 8–28.

The ΦPSII imaging results showed differences between the two treatments, some of which were significant (Figure 6, Tables S7 and S8). ΦPSIIh decreased with continued drought stress and increased again with re-watering. At DAT 20 and 27, after 13 and 19 days of drought stress, respectively, the control treatment and the drought stress treatment differed significantly. The loss in the stressed plants was 7% on DAT 20 and 20% on DAT 27 of the ΦPSIIh in the control treatment (Table S7).

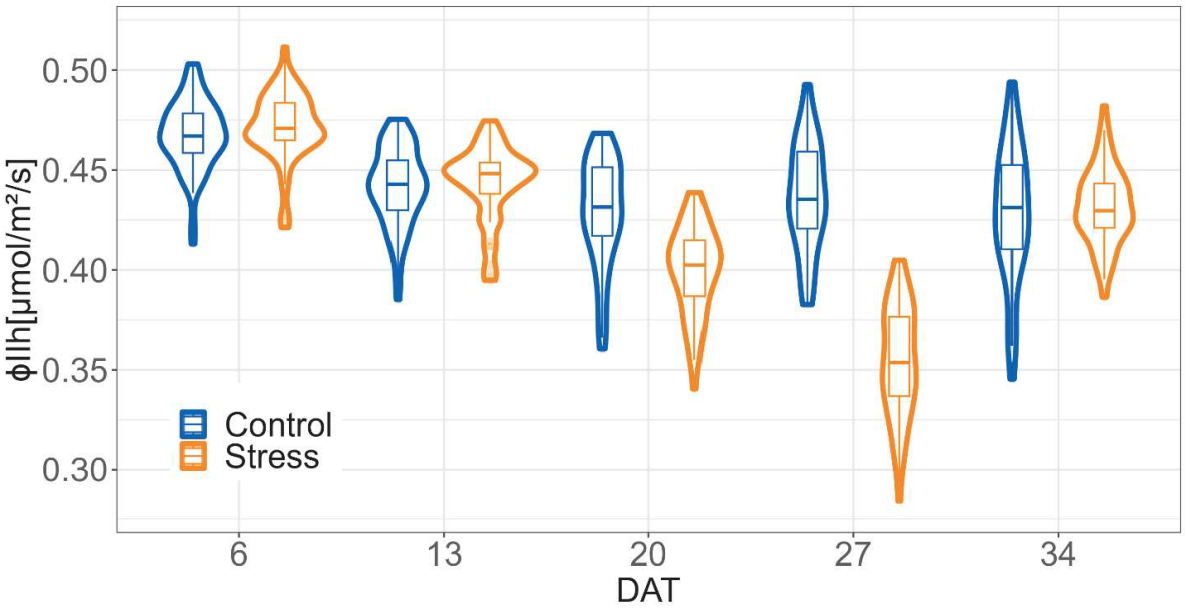

Figure 6. ϕPSIIh for drought stress and control treatments on several DATs. Based on BLUEs across both experiments of all 60 genotypes. The shape around the boxplot is a violin plot and describes the continuous distribution of the data at different values; 1 day before drought = DAT 6, 7 days of drought = DAT13, 13 days of drought = DAT20, 19 days of drought = DAT 27, 6 days of recovery = DAT34. ϕPSIIh = operating efficiency of photosystem II under high-light conditions.

For the ΦPSIIr and ΦPSIIh, comparable results and significances were found (Tables S7 and S8 and Figure S7).

2.3. *Correlations between Traits*

Correlation coefficients *r* between EB and PH, r2g, and y2g traits over each phase of DA, DT, and DR have been calculated (Table S9). For PH and EB, *r* ranged from 0.56 to 0.87 in all phases and both treatments. In contrast, there was a negative correlation between the MCV and EB in both treatments, for DA and DR. In DT, there was a significant difference between the treatments. For the control treatment, *r* was −0.54, but for DT in the drought stress treatment, it was 0.53. Considering the EB and r2g traits, *r* was strongly negative (approximately −0.7 for all combinations of treatment and phase); only for the DR phase in the control treatment did *r* result in −0.54. All *r* values for all the pairs of traits for each phase and treatment yielded significant results, with the only exception being *r* between EB and y2g for the DR phase and control treatment ($r = 0.005$; $p = 0.88$). In contrast, for DR in drought stress, there was a strong negative correlation between y2g and EB ($r = -0.74$; $p < 0.0001$); for the DT, *r* between y2g and EB was −0.75 for the control treatment but only −0.33 in the drought stress treatment, even if both were significant.

The coefficient of correlation *r* between ΦPSIIh and ΦPSIIl was 0.5, while *r* between ΦPSIIr and ΦPSIIh was significantly higher, equal to −0.94 (Figure S8).

Furthermore, some correlations between ΦPSIIh and image-based traits were significant with persistent drought stress (Table S10). On DAT 27, after 19 days of drought stress, the correlations of ΦPSIIh to EB and PH were significantly positive ($r = 0.69$ and $r = 0.55$), and to the color-related traits, MCV, r2g, and y2g were significantly negative ($r = -0.62$; $r = -0.7$ and $r = -0.68$; Figure S9). In addition, on DAT 27, a strong positive correlation between the color-related traits and between EB and PH was visible as well (Figure S10).

2.4. PGR under Drought Stress

The set of 60 genotypes could be grouped on the basis of biological status and *desi* and *kabuli* types. In particular, the differences in *kabuli* and *desi* in terms of their tolerance to vegetative stage drought stress were of interest and were evaluated based on the drought stress period DAT 8–28 (Figure S11). In the control treatment, principal component (PC) 1 explained 75%. The EB and PH traits were approximately opposite to y2g and r2g, respectively. For PC2, which explained 15.3% in the control treatment, the genotypes are subdivided primarily for MCV. A clear separation of the two chickpea types or even a tendency to be different was not detected. PC1 explained 57% of the drought stress treatment, which was less than the control treatment. Furthermore, PC1 separates genotypes based on EB and PH versus r2g and y2g. PC2 explained 19.5% of the variation and was influenced by MCV. In the PCA for drought stress, there was a slight differentiation of *desi* and *kabuli* genotypes, with *desi* mostly present in the positive range of PC1 (high EB and PH, low r2g and y2g). There were no significant differences in biological status between cultivars, domesticated material, landraces, and breeding material (Figure S12).

To evaluate whether *desi* or *kabuli* were more tolerant to drought stress, the percentage loss caused by drought was investigated (Table S2 and Figure S13) There were no significant differences in losses for EB, r2g, and y2g between both types. Loss of PH was lower for *desi* from DAT 16–19, but on DAT 28, a similar loss was detected for *desi* (31%) and *kabuli* (34%) types (Table S2). Similarly, loss for MCV was significantly different from DAT 24–31 for the two types. For DAT 28, the loss between drought stress and control treatment was lower for *desi* (−5.8%) compared to *kabuli* (−7.2%).

Considering the biological status, the loss ratio of drought stress and control treatment was calculated to verify if breeding materials, cultivars and landraces, or domesticated materials are different in terms of their drought tolerance (Figure S14). However, no significant differences were detected. In addition, the genotypes of the domesticated material group were very heterogeneous.

In addition, we investigated for each individual the deviation from the mean value of the BLUEs of the entire set of materials for both treatments in relation to their EB (Figure 7). At DAT28, the last day of stress, mostly *desi* genotypes had significantly higher mean values of both drought stress and control treatment. Thus, these genotypes behave significantly better than the *kabuli* genotypes. A similar result was obtained for the last day of the experiment (DAT 42), that is, after drought stress and recovery. *Desi* was significantly better than *kabuli* over the mean of all 60 genotypes.

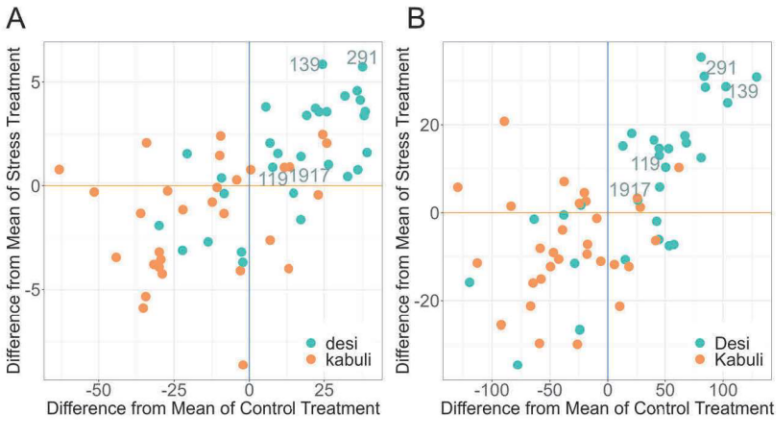

Figure 7. Deviation of the individual genotypes with their affiliation to *desi* and *kabuli*, from the mean value of Estimated Biovolume (EB) of all 60 genotypes. The superior genotypes were labeled with the INCCP plant material number and the labels touch the designated places. Based on BLUEs across both experiments and all 60 genotypes. (**A**) DAT 28; (**B**) DAT42.

In contrast, no significant differences in terms of deviation from the mean values of BLUEs for EB in both treatment conditions were detected considering the different biological statuses of the genotypes (Figure S15).

Comparing the WUE for the *desi* and *kabuli* types, a significantly higher WUE was detected for desi genotypes (11.5 voxel/mL) compared to *kabuli* ones (7.76 voxel/mL) in the drought stress treatment during the DT phase (Figures 8 and S16, Tables S5 and S6). No significant differences in the biological status of the genotypes were detected for WUE.

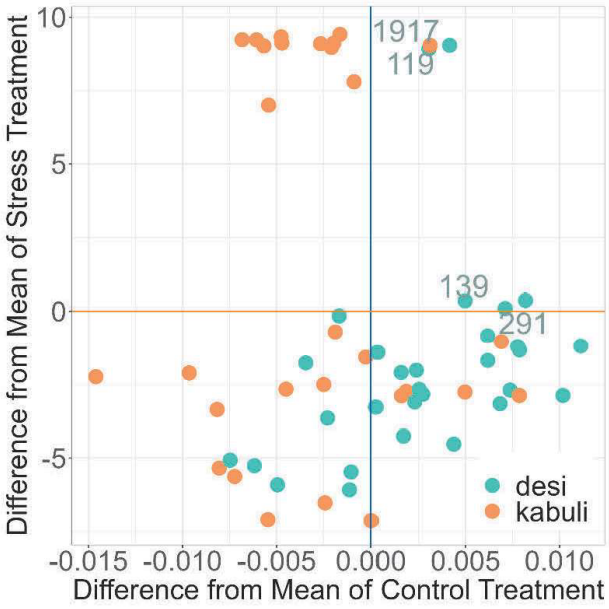

Figure 8. Deviation of the individual genotypes with their affiliation to *desi* and *kabuli*, from the mean value during DT of Water Use Efficiency (WUE) of all 60 genotypes. Estimated Biovolume (EB) based on BLUEs across both experiments and all 60 genotypes. The superior genotypes were labeled with the INCCP plant material number and the labels touch the designated places. DT = drought tolerance DAT 8–28.

When looking at the image-derived traits r2g, y2g, and MCV for the deviation from the mean values of the entire panel, the *kabuli* genotypes showed a significantly higher r2g than *desi* ones, but no significant difference was detected for MCV (Figure S17).

Concerning photosynthesis traits, the two chickpea types showed a significant difference only on DAT 34 (Tables S7 and S8): The mean ΦPSIIh was higher for *desi* (0.438) than for *kabuli* (0.425) types. When the deviation from the mean of ΦPSIIh was calculated for the *desi* and *kabuli* groups and biological status, no significant differences or trends were visible (Figure S18).

There were 32 genotypes that have better EB and WUE in the different phases of DT, DR, and DA and at DAT 28 and DAT 42 than the panel mean of 60 genotypes (Table S11). These 32 genotypes include 10 Kabuli and 22 Desi genotypes. INCCP_00119 (*desi*, Turkey, landrace), INCCP_00139 (*desi*, Tajikistan, landrace), INCCP_00291 (*desi*, Mexico, cultivar), and INCCP_01917 (*kabuli*, Portugal, landrace) were better for WUE and EB than the mean of the panel for both treatments on the significant days DAT 28 and 42 and in all phases, DA, DT, and DR.

3. Discussion

HTP is considered an important tool that allows the rapid and precise testing of genotype environmental interactions [56]. In the present study, the effects of drought stress during the vegetative growth period under well-watered and drought stress conditions

using non-destructive HTP was investigated for the first time in chickpea using a diverse panel of PGR. The high data quality results of the daily phenotyping showed the varying tolerance of PGR and allowed us to draw conclusions about the suitability of PGR for pre-breeding.

3.1. Suitability of HTP

The HTP system used in this study has already proven useful for studies to test the biomass development and color change of wheat Near Isogenic Lines throughout the life cycle in phases of varying drought stress and also the biomass development of barley PGR under drought stress in the vegetative stage [47,55]. The greenhouse conditions met the temperature requirements for chickpea and were combined with an irrigation system that simulates drought stress followed by recovery during vegetative development.

The heritability of EB in the drought stress and control treatment was comparable to results from a chickpea HTP experiment for salinity tolerance [48]. Furthermore, the heritability was also high for PH, MCV, and r2g in the control treatment. On some days, especially at the beginning and towards the end of the experiment, the heritability for the y2g, MCV, and r2g was lower in the drought stress treatment. This could be partly attributed to the non-uniform development and maturation of the PGR and the associated physiological changes in pigment composition during these days. In addition, the heritability for the chlorophyll fluorescence imaging traits was satisfactory. In general, heritability was comparable to that of previous experiments in barley on this HTP system and is suitable for future genome-wide association studies [52,55]. The high correlation of EB to measured plant weight demonstrates the suitability of EB as a proxy for biomass. Based on the high-quality dataset, statistical analyses could be carried out to evaluate the PGR in terms of their tolerance to drought stress and ability to recover after drought.

The CV was used to determine the degree of phenotypic variation over time [53]. The change in the CV reflected the variation in PGR, confirming the method and utility of this dataset for further analysis. Thus, the CV for this PGR under drought stress was highest for the r2g and y2g color ratios and also high for EB, resultant WUE, PH, and ΦPSIIh.

3.2. General Effect of Drought Stress during HTP Experiments

Drought stress significantly impairs plant development for several traits and yield components, making the breeding of tolerant varieties a complex task. This study highlights the importance of HTP for the screening of vegetative drought stress tolerance to identify superior genotypes within the PGR panel.

According to the timeline of the irrigation regime, statements can be made about the relevance of traits at certain DATs, e.g., at the maximum sustained drought stress on DAT 28, or in certain phases such as the DT, DR, and DA [53]. The difference between treatments became significant for each trait within a few days, but the difference in EB occurred first. EB showed a significant difference on DAT 14, i.e., 7 days after the onset of drought stress, 2–3 days before the other traits. This is slightly later compared to results in barley PGR [55]. As there is a correlation between biomass and seed yield in chickpea, the reduced EB formation in drought and low biomass of genotypes would likely result in lower seed yield [48,49].

Drought stress altered the image-based traits that differed even after re-watering. MCV was the only trait of the image-based traits for which the values of the two treatments converged again in the recovery phase, so from DAT38 onwards, there was no longer any significant difference between the treatments. To describe differences between genotypes based on percentage losses and coefficients of variation, r2g, EB, and y2g were most informative [53,54].

The effect of drought stress and the optimal choice of the timing of re-watering was shown in the RGR. As RGR became negative with continued drought stress, the objective of the study to evaluate the drought tolerance and recovery of chickpea was realized with

the scheduling of irrigation. If irrigation had been delayed, some genotypes would not have shown recovery.

WUE based on EB and water use was another informative trait. It is considered for breeding plants more tolerant to drought and involves optimizing biomass accumulation and transpiration [57]. It is advisable to supplement the WUE with data on transpiration, stomatal density conductivity, or vapor pressure deficit [58]. In a field study with one chickpea variety, optimum WUE was achieved with early sowing and increased irrigation [59]. Furthermore, in chickpea, better adaptation to water deficit was associated with higher relative water content, longer chlorophyll retention, and higher osmotic adjustment [60]. The significant differences and variations in WUE during DT can be used to select suitable PGR genotypes.

PH is an important trait that correlates with shoot biomass and thus also with seed yield [49]. Drought reduced PH in our study, and the PGR panel showed substantial phenotypic variation in PH and losses in PH.

Color-related traits have been used previously to represent physiological responses to challenging environmental conditions in HTP in wheat (*T. aestivum*; *T. durum*), barley (*H. vulgare*), and maize (*Z. mays*), as well as rice (*O. sativa*) and lettuce (*Lactuca sativa*) [47,54,55,61,62].

Under drought, both color ratios, y2g and r2g, increased, indicating pigment changes such as chlorophyll, carotenoids, and anthocyanins, which play a role in plants' reactions to stress and starting senescence symptoms [63]. Carotenoids, for example, stabilize the lipid membrane, are important for photosynthetic light collection, and protect photosystems from oxidative damage caused by light radiation [63]. Similarly, anthocyanins, which are of red to blue color, reduce the photoinhibition and photobleaching of chlorophyll and occur in response to environmental extremes [64,65]. In addition to anthocyanin, in chickpea, lower chlorophyll and carotenoid content was observed under drought stress conditions in the field, which could explain the changes in r2g and y2g [66,67].

The MCV first increased under drought stress, indicating a deeper green color of the leaves, then remained constant from DAT 24–28 during advanced drought stress, and finally fell back to the value of the control treatment with the resumption of normal watering. In principle, there is a high correlation between hue value and chlorophyll concentration, which has been observed in a wide range of species, including tobacco (*Nicotiana*), grapevine (*Vitis labrusca*), or *Arabidopsis thaliana* [65,68,69]. The initially darker green shade of the leaves could be explained by the fact that under drought stress, the water content in the cells decreased and therefore the chlorophyll content increased in relative terms [67]. Another reason could be the short-term overcompensation of chlorophyll, which has already been observed in soybean (*Glycin max*) under drought stress [70]. The constant hue value of DAT 24–28 could be due to anthocyanin accumulation, which correlates negatively with hue [65].

Many studies in greenhouse and field conditions demonstrated a negative effect of drought stress on photosynthesis, e.g., in soybean (*G. max*), lettuce (*L. sativa*), and wheat (*T. durum*) [16,62,71]. In this study, the lower ΦPSIIh, which represents a lower light quantum yield, showed a reduced photosynthetic capacity. However, in our study, when plants recovered from drought, photosynthetic capacity had not been permanently damaged and ΦPSIIh returned to well-watered levels, similar to a field study with soybean (*G. max*) and drought stress [16]. Similarly, [47] ΦPSIIr was higher under drought stress.

In line with the study for salinity tolerance in chickpea, EB and PH were always positively correlated in control and drought stress [49]. While correlations between EB and the other imaging traits were quite constant, correlation to MCV showed a different pattern. The delayed change from a positive to a negative correlation with the onset of re-watering suggested that MCV might be important for the selection of PGR for drought stress tolerance and was found for the DT phase. Y2g and r2g showed a more durable correlation with EB and y2g appeared to be more informative for DR, with a defined shift in correlation between control and drought stress. The color traits had a high heritability,

which is in accordance with studies in barley and maize and therefore could be used in evaluating the wilting process [55,72].

Precision phenotyping thus allows one to select the most suitable traits, but moreover, also determines the critical moment for their evaluation [73].

In addition, the use of chlorophyll fluorescence imaging enabled a complex analysis of chickpeas under drought stress and highlights the importance of studying with complementary methods [43,50,54,62]. A high correlation between plant area and chlorophyll fluorescence imaging has been noted previously, which is comparable to the EB and PH traits, which have a high correlation to ΦPSIIh [54].

3.3. PGR for Drought Stress Tolerance during Vegetative Phase

The diverse PGR panel showed high phenotypic diversity throughout the whole experiment. Grouping according to geographical area and biological status revealed no differences in performance under well-watered or drought stress conditions, which could be due to the sample size.

However, significant differences are known for the two types of chickpea, *desi* and *kabuli*. *Desi* has been reported to be more tolerant to drought stress than *kabuli* [25,74]. A higher dry weight in the seedling stage, specific leaf area, and reduced growth for the *desi* type were observed in pot and climate-chamber experiments [25,74]. In our panel, no significant difference was found between *desi* and *kabuli* in the image-derived traits for the entire course of the experiments. When evaluating the performance in comparison to the deviation from the panel mean values on specific DAT, *desi* genotypes behaved significantly better for EB on DAT 28 and 42 and WUE during DT. This was in agreement with earlier studies that identified a higher WUE and transpiration efficiency in *desi* and could be in part attributed to the anatomy of the xylem vessels and cortical layers of roots, which have less resistance to water [25,74].

In general, the differences between the two types, *desi* and *kabuli*, have been intensively discussed in the literature. Re-sequencing of 29 varieties revealed that only 2% of the genomes are different regions and these are likely signatures of selection during improvement [75]. Interestingly, markers for proanthocyanin were found to be significantly different for *desi* and *kabuli*, with *kabuli* showing a reduced function for blocking transcription factors for anthocyanin biosynthesis [26]. In this study, *kabuli* showed a significantly higher deviation from the mean of the panel for the r2g value than *desi* at DAT 28 under drought stress. This higher r2g value could be due to a higher anthocyanin content. However, there was no significant difference for MCV at DAT 28 under drought stress compared to the mean of the panel between *desi* and *kabuli*, although the hue value is correlated to anthocyanin content [65].

In contrast to [74], our study did not reveal a significantly better photosynthetic performance of *desi* types under drought stress. This could be due to the different genotypes, type of stress timing, and severity or measurement of photosynthesis. *Desi* tended to perform better photosynthetically during the late drought stress phase and during recovery in the context of our study.

Based on a pre-screening, we were able to gain insights into the suitability of PGR for drought stress and recovery. For the relevant trait EB, there were 22 *desi* and 10 *kabuli* genotypes that were better than the mean of the panel at key DAT 28 and 42 and for the different phases DR, DA, and DT. Four superior genotypes are identified that can be used for future improvement of vegetative drought tolerance. The four genotypes INCCP_00119 (*desi*, Turkey, landrace), INCCP_00139 (*desi*, Tajikistan, landrace), INCCP_00291 (*desi*, Mexico, cultivar), and INCCP_01917 (*kabuli*, Portugal, landrace) showed superior WUE and EB and are valuable genotypes for further studies.

4. Material and Methods

4.1. Plant Material

The set of materials used in the present study consisted of 60 chickpea accessions (Supplementary Material). Each accession is represented by single seed descent (SSD) material derived by at least two cycles of selfing from 12 accessions from the IPK Gatersleben genebank and 48 accessions from the Western Regional Plant Introduction Station (USDA-ARS, Washington State University, Pullman, WA, USA) [20,21]. These materials represent a subset of a larger collection (Training CORE, T-CORE) developed within the INCREASE (Intelligent Collection of Food Legumes Genetic Resources for European Agro-food Systems) [21,76] and EMCAP (European and Mediterranean Chickpea Association Panel) projects [20]; and is being tested in field experiments in collaboration with partners in Italy, too. The 60 genotypes were selected to maximize the genetic diversity of the T-CORE using passport data; in particular, the genotypes originated from 39 countries and 16 regions worldwide. Moreover, the set of materials is balanced for being *desi* (30 genotypes) and *kabuli* (30 genotypes). Considering the biological status, the set is composed of 3 breeding materials, 13 cultivars, and 42 landraces; for the remaining two genotypes, the biological status is domesticated material (Table S12).

4.2. HTP Experiments

The HTP system (LemnaTec-Scanalyzer 3D) used in the present study is installed in an environmentally controlled greenhouse at IPK Gatersleben (51°49′23″ N, 11°17′13″ E, altitude 112 m). In this system, each plant was transported by conveyor belts to the imaging chambers equipped with top and side view RGB (Red, Green, Blue) and fluorescence cameras, where a lifter allows imaging from different angles in side view. The balance-watering station enables controlled watering and thereby defined drought setups.

Plant material was tested in two experiments with two biological replicates per genotype and treatment. The first experiment was conducted from 24 March 2021 to 19 May 2021 and the second from 10 June 2021 to 5 August 2021. Two experiments were planned to obtain a total of four biological replicates per genotype and treatment. For both experiments, two seeds were sown directly into the pots and thinned out to one seedling per pot after emergence. Each pot (18.5 cm height × 14.9 cm diameter) was filled with Klasman substrate No. 2 described in [47]. After 14 days of pre-cultivation in a regular greenhouse chamber outside the HTP system at 24 °C during the day and 20 °C during the night, with a relative humidity of 67% during the day and 76% during the night, a daylight period of greenhouse lights of 15 h (from 6 am to 9 pm), and manual watering, the plants were transferred to the greenhouse with the HTP system with the same growing conditions. To each pot, 7 g of fertilizer with a composition of 19% total nitrogen, 9% P_2O_5, and 10% K_2O was added, and no inoculation was carried out to promote nodulation. Nevertheless, each plant in the first experiment was examined for nodulation after the experiment was completed. A plant support was placed on each pot and each pot was placed into a tray so that any water added could be absorbed by the plant. During the experiment, LemnaTec software was used to randomize the arrangement of the plants twice a week resulting in a fully randomized design. After an establishment phase to bring all plants to the same level of plant-available water (PAW) of 70%, the irrigation level was lowered to 10% from day 8 after transferring (DAT) for plants in the drought stress treatment (Table 1; SM S2). The watering regime and simulation of drought stress were developed on this HTP system and have already been published [52]. The plants of the control treatment were maintained at 70% PAW from DAT 1 until the end at DAT 42 (SM S2).

Table 1. Timeline of both experiments. DAS = Days after sowing; DAT = Days after transferring; PAW = Plant-available water.

DAS	DAT	Action
0		Sowing and pre-cultivation in greenhouse
14	0	Transferring to HTP system and set watering to 70% PAW
15	1	First image
20	6	Chlorophyll fluorescence measurement
22	8	Initiation drought stress: 10% PAW
27	13	Chlorophyll fluorescence measurement
34	20	Chlorophyll fluorescence measurement
41	27	Chlorophyll fluorescence measurement
43	29	First step of recovery: + 300 mL
44	30	Second step of recovery: 70% PAW
48	34	Chlorophyll fluorescence measurement
55	41	Last imaging on HTP system
56	42	Harvest

On DAT 29, gradual re-watering was planned for both experiments with 300 mL initially, followed by irrigation to 70% on DAT 30. The irrigation was performed in two steps to allow the plants to slowly absorb the water. Information on daily watering based on weight before and after watering can be extracted with the system software. At the experiment's end, fresh and dry weights of the above-ground shoot part were determined. Furthermore, due to technical difficulties, only an incomplete set of images could be recorded on DAT 1 for experiment 1 and on DAT 14 for experiment 2. These two days were excluded from the analysis.

4.3. Image-Derived Plant Traits

The images were analyzed using the IAP version 2.3.0 (Integrated Analysis Platform (IAP)) [77]. The traits used here include Estimated Biovolume (EB, [voxel 10^{-5}]), Plant Height (PH; [mm]), Mean Color Value (MCV; [hue]), the red to green ratio (r2g; [%]), and the yellow to green ratio (y2g; [%]) [55,77]. The MCV refers to the HSV color space. A 20-bin histogram was calculated, which provides information about the composition of the detected plant color [77]. Based on this model, a mean hue of 0.23 corresponds to an image of a green plant. The values y2g and r2g indicate the percentage of yellow and red pixels in the image, respectively. The EB was calculated from the images from the top view camera and the images of three side views:

$$Estimated\ Biovolume\ [voxel] = \sqrt{average\ pixel\ side\ area^2 * top\ area}$$

The PH results from pictures of the side view and the y2g, r2g and MCV result from pictures of the top view.

To determine the PAW, the pot weight before watering was taken into account, as was described in [52].

To draw conclusions about the tolerance of, for example, the two chickpea types or biological status, the loss was calculated as the ratio of drought stress to control for the imaging traits.

$$Loss\ of\ Trait\ [\%] = \left(1 - \frac{trait_{drought\ stress}}{trait_{control}}\right) \times 100$$

Based on the mean of the BLUE values in the two experiments for the 60 genotypes, the relative growth rate (RGR) was calculated. The missing values at DAT1 and 14 were linearly interpolated to calculate the RGR.

$$Relative\ Growth\ Rate\ \left[\frac{voxel}{DAT}\right] = \frac{\ln(EB_i) - \ln(EB_{i-1})}{DAT_i - DAT_{i-1}}$$

For further analysis, the DATs were divided into phases. DAT 2 to 7 refers to the establishment phase, DAT 8–28 to the drought tolerance phase (DT), DAT 29–42 to the drought recovery phase (DR), and the period from DAT 8–42 was considered the drought adaptability phase (DA).

The WUE was calculated as EB per milliliter of water during each of the phases of DA, DT, and DR. If the irrigation was at zero milliliters, the amount of irrigation for the entire phase has been set to 1 milliliter to proceed with further analysis. Outliers which were detected for EB were removed from the irrigation data, and the mean for each genotype and each DAT was calculated. For each drought phase, the difference in the BLUEs of EB between the first and last DAT was calculated and divided by the sum of the irrigation to calculate the WUE.

4.4. Chlorophyll Fluorescence Imaging and Image Analysis

The system was supplemented with a chlorophyll fluorescence camera (FluorCam; version 7) from Photon Systems Instruments (PSI; Brno, Czech Republic) to measure photosynthetic performance from the top view. The FluorCam data were analyzed using the manufacturer's software Plant Data Analyzer (version 3).

These measurements took place at DAT 6 (2 days before drought stress); DAT 13 (five days of drought stress); DAT 20 (twelve days of drought stress); DAT 27 (19 days of stress); and DAT 34 (five days after re-watering) (Table 1). During these days, normal imaging was advanced to 00:01 am instead of 7 am to allow FluorCam measurements at 8 am (duration 12 h).

Chlorophyll fluorescence measurements were taken approximately once per week using FluorCam similar to [43]. For the measurement, the plants were first adapted to a light intensity of 800 µmol/m^2/s in an adaptation tunnel. This light intensity is higher than that in the greenhouse (during the growth). After the adaptation of five minutes, the plants were moved to the measuring chamber and illuminated once more for 10 s with a light intensity of 800 µmol/m^2/s. At the end of this phase, a first saturating light flash of 4000 µmol/m^2/s was applied to measure the operating efficiency under high light intensity (ΦPSIIh; µmol/m^2/s). This was followed by ten seconds of 80 µmol/m^2/s to allow the plants to adapt to low light conditions, and then a second light flash of 4000 µmol/m^2/s was used to measure the operating efficiency under low light conditions (ΦPSIIl; µmol/m^2/s).

The ΦPSIIl to ΦPSIIh ratio was calculated in order to measure the plasticity of photosystem II to fluctuating light (ΦPSIIr).

4.5. Statistics

The EB was divided by a factor of 10^{-5}. For further statistical analysis, R studio version 4.1.2 was used with the packages "tidyr", "dplyr", "stringr", "data.table", "multtest", "agricolae", and "lattice". Figures were created with the packages "ggplot2", "ggpubr", and "ggrepel". The package "ASReml" was used to calculate the outlier, the heritability, and the best linear unbiased estimators (BLUEs). Across the two experiments, outliers have been detected separately for each treatment. In the mixed model, the genotypes are fixed effects and the experiment and the genotype and experiment interaction were random factors. For every DAT, outliers were calculated separately.

To calculate the broad-sense heritability H^2, each DAT is a fixed effect, and the experiment, the genotype and experiment, and genotype interactions have been taken as random effects.

V_G, V_e, and V_{GxE} are the variance components of the genotype, the genotype × experiment interaction, and the residual, respectively. *numExp* is the number of experiments for the respective DAT, and *numRep* is the number of biological replicates.

$$H^2 = \frac{V_G}{V_G + \left(\frac{V_{G\times E}}{numExp}\right) + \left(\frac{V_e}{(numRep \times numExp)}\right)}$$

To calculate the BLUEs across the two experiments from the cleaned dataset, genotypes were used as fixed factors, similar to the outliers, and the experiment and the genotype–experiment interaction are random factors. The BLUEs across the experiments were used for all further analyses.

Pearson correlations with the coefficient of correlation r were estimated. The coefficient of variation (CV) has been calculated by the ratio of σ to μ. For the chlorophyll fluorescence values, an ANOVA followed by Tukey's test was performed to calculate the significance levels. Significant differences were highlighted by calculating the 95% confidence intervals using the package "Rmisc". The confidence intervals are shown as shadows in the figures. Principal component analysis (PCA) was performed using the package "factoextra".

5. Conclusions

Considering the differences observed between genotypes with respect to drought stress during the vegetative stage and recovery, HTP proved to be a useful method to study these complex quantitative traits in chickpea PGR. Genotypes with superior drought tolerance could be identified from the traits of growth performance and physiology derived from the images, suggesting that further studies are needed to elucidate the underlying processes.

For practical crop improvement, this method is valuable. PGR can be assessed in an HTP experiment; by linking genotypic data, root-related data, yield-related data, and, for example, metabolomic data, QTLs can be mapped by genome-wide association studies to unravel the underlying genetic architecture for drought tolerance and recovery in chickpea. In addition, these results can then be verified through field studies.

Once potentially valuable genotypes are identified, they can be incorporated into breeding programs and introduced into elite material, for example, via CRIPSR/Cas, backcrossing with marker-assisted selection, or other breeding methods, to breed chickpea varieties that are more tolerant to drought stress in the vegetative stage and recover quickly.

Supplementary Materials: The following supporting information can be downloaded at: https://www.mdpi.com/article/10.3390/plants12152866/s1, Figure S1: Heritability of dry and fresh weight from DAT 43. Figure S2: Heritability of image-derived traits. Figure S3: Heritability of Chlorophyll Fluorescence traits. Figure S4: Correlation of EB from DAT 42 and fresh weight from DAT 43. Figure S5: Relative growth rate of drought stress treatment. Figure S6: Coefficient of variation of image-derived traits. Figure S7: Chlorophyll Fluorescence traits for drought phases. Figure S8: Correlation among chlorophyll fluorescence traits. Figure S9: Correlation of ΦPSIIh and image-derived traits for DAT 27. Figure S10: Correlation matrix of Chlorophyll Fluorescence and image-derived traits. Figure S11: PCA for *desi* and *kabuli* for DT. Figure S12: PCA for DT for biological status. Figure S13: Loss of drought stress compared to control treatment of *desi* and *kabuli*. Figure S14: Loss of drought stress compared to control treatment of biological status. Figure S15: Deviation of the individual genotypes with their affiliation to the biological status, from the mean value of EB of all 60 genotypes. Figure S16: WUE of desi and kabuli during drought phases. Figure S17: Deviation of the individual genotypes with their affiliation to desi and kabuli, from the mean value of all 60 genotypes. Figure S18: Deviation of the individual genotypes from the mean value of ϕ PS IIh of all 60 genotypes; Table S1: PAW for experiment 1 and 2 and both experiments. Table S2: Descriptive statistics of image-derived traits for all genotypes and desi and kabuli. Table S3: Descriptive statistics of fresh and dry weight. Table S4: Descriptive statistics of RGR. Table S5: Descriptive statistics of WUE for drought phases and chickpea types. Table S6: Tukey's test of WUE in different drought phases and for desi and kabuli under drought phase. Table S7: Descriptive statistics of Chlorophyll Fluorescence traits. Table S8: Tukey's test for chlorophyll fluorescence traits. Table S9: Correlations of EB with further image-derived traits during the period of DA, DR and DT. Table S10: Correlation between ΦPSIIh and image-derived traits. Table S11: Superior genotypes for EB and WUE as measured by the difference from the mean of the panel under drought stress compared to the control treatment. Table S12: Description of Plant Material.

Author Contributions: M.L. and K.N. conceived and designed the research; E.B. managed the seeds of chickpea genetic resources; M.L. and K.N. carried out the phenotyping experiment; H.T. managed the Chlorophyll Fluorescence measurements, M.L. and H.T. carried out data analysis; M.L. wrote the manuscript; K.N., H.T., E.B. and R.P. contributed to the drafting and writing of the manuscript. All authors have read and agreed to the published version of the manuscript.

Funding: This work was conducted as part of the STARGATE project funded by the European Union's Horizon 2020 research and innovation program under grant agreement No. 952339 and as part of the INCREASE project funded by the European Union's Horizon 2020 research and innovation program under grant agreement No. 862862. Costs for open access publishing were partially funded by the Deutsche Forschungsgemeinschaft (DFG, German Research Foundation, grant 491250510).

Acknowledgments: The authors would like to thank the Western Regional Plant Introduction Station (USDA-ARS, Washington State University, USA) and Università Politecnica delle Marche (Ancona, Italy; UNIVPM) for providing seeds of accessions used in the present study. In addition, the authors would like to thank Yusheng Zhao for advice on statistical matters; Lorenzo Rocchetti, Markus Oppermann, Dennis Psaroudakis, Marcel Berkner, Dominic Knoch, Rhonda Meyer, Marc Heuermann, and Ana Patricia Goncalves for scientific advice; Ingo Mücke, Ute Krajewski, Heiko Kriegel, Annett Berge, Kathrin Gramel-Koch, and their entire team for their technical support; and Tara Crawford for linguistic revision of the manuscript.

Conflicts of Interest: The authors declare no conflict of interest.

References

1. Beillouin, D.; Schauberger, B.; Bastos, A.; Ciais, P.; Makowski, D. Impact of extreme weather conditions on european crop production in 2018. *Philos. Trans. R Soc. Lond. B Biol. Sci.* **2020**, *375*, 20190510. [CrossRef] [PubMed]
2. Grillakis, M.G. Increase in severe and extreme soil moisture droughts for europe under climate change. *Sci. Total Environ.* **2019**, *660*, 1245–1255. [CrossRef] [PubMed]
3. IPCC. Climate Change 2022: Impacts, Adaptation and Vulnerability. Ph.D. Thesis, Cambridge University Press, Cambridge, UK; New York, NY, USA, 2022; pp. 3–33.
4. Peltonen-Sainio, P.; Jauhiainen, L.; Trnka, M.; Olesen, J.E.; Calanca, P.; Eckersten, H.; Eitzinger, J.; Gobin, A.; Kersebaum, K.C.; Kozyra, J.; et al. Coincidence of variation in yield and climate in europe. *Agric. Ecosyst. Environ.* **2010**, *139*, 483–489. [CrossRef]
5. Cernay, C.; Ben-Ari, T.; Pelzer, E.; Meynard, J.M.; Makowski, D. Estimating variability in grain legume yields across europe and the americas. *Sci. Rep.* **2015**, *5*, 11171. [CrossRef]
6. Reckling, M.; Doring, T.F.; Bergkvist, G.; Stoddard, F.L.; Watson, C.A.; Seddig, S.; Chmielewski, F.M.; Bachinger, J. Grain legume yields are as stable as other spring crops in long-term experiments across northern europe. *Agron. Sustain. Dev.* **2018**, *38*, 63. [CrossRef]
7. Krishnamurthy, L.; Kashiwagi, J.; Gaur, P.M.; Upadhyaya, H.D.; Vadez, V. Sources of tolerance to terminal drought in the chickpea (*Cicer arietinum* L.) minicore germplasm. *Field Crops Res.* **2010**, *119*, 322–330. [CrossRef]
8. Merchuk-Ovnat, L.; Barak, V.; Fahima, T.; Ordon, F.; Lidzbarsky, G.A.; Krugman, T.; Saranga, Y. Ancestral qtl alleles from wild emmer wheat improve drought resistance and productivity in modern wheat cultivars. *Front. Plant Sci.* **2016**, *7*, 452. [CrossRef] [PubMed]
9. Pham, A.T.; Maurer, A.; Pillen, K.; Brien, C.; Dowling, K.; Berger, B.; Eglinton, J.K.; March, T.J. Genome-wide association of barley plant growth under drought stress using a nested association mapping population. *BMC Plant Biol.* **2019**, *19*, 134. [CrossRef]
10. Berger, J.; Pushpavalli, R.; Ludwig, C.; Parsons, S.; Basdemir, F.; Whisson, K. Wild and domestic differences in plant development and responses to water deficit in cicer. *Front. Genet.* **2020**, *11*, 607819. [CrossRef]
11. Varshney, R.K.; Gaur, P.M.; Chamarthi, S.K.; Krishnamurthy, L.; Tripathi, S.; Kashiwagi, J.; Samineni, S.; Singh, V.K.; Thudi, M.; Jaganathan, D. Fast-track introgression of "qtl-hotspot"for root traits and other drought tolerance traits in jg 11, an elite and leading variety of chickpea. *Plant Genome* **2013**, *9*, 1–9. [CrossRef]
12. Varshney, R.K.; Mohan, S.M.; Gaur, P.M.; Chamarthi, S.K.; Singh, V.K.; Srinivasan, S.; Swapna, N.; Sharma, M.; Pande, S.; Singh, S.; et al. Marker-assisted backcrossing to introgress resistance to fusarium wilt race 1 and ascochyta blight in c 214, an elite cultivar of chickpea. *Plant Genome* **2014**, *7*. [CrossRef]
13. Singh, C.; Kumar, R.; Sehgal, H.; Bhati, S.; Singhal, T.; Gayacharan; Nimmy, M.S.; Yadav, R.; Gupta, S.K.; Abdallah, N.A.; et al. Unclasping potentials of genomics and gene editing in chickpea to fight climate change and global hunger threat. *Front. Plant Sci.* **2023**, *14*, 1085024. [CrossRef] [PubMed]
14. Badhan, S.; Bali, A.S.; Mantri, N. First report of crispr/cas9 mediated DNA-free editing of 4cl and rve7 genes in chickpea protoplasts. *Int. J. Mol. Sci.* **2021**, *22*, 396. [CrossRef] [PubMed]
15. Hari, V.; Rakovec, O.; Markonis, Y.; Hanel, M.; Kumar, R. Increased future occurrences of the exceptional 2018–2019 central european drought under global warming. *Sci. Rep.* **2020**, *10*, 12207. [CrossRef] [PubMed]

16. Elsalahy, H.H.; Reckling, M. Soybean resilience to drought is supported by partial recovery of photosynthetic traits. *Front. Plant Sci.* **2022**, *13*, 971893. [CrossRef] [PubMed]
17. Foyer, C.H.; Lam, H.M.; Nguyen, H.T.; Siddique, K.H.; Varshney, R.K.; Colmer, T.D.; Cowling, W.; Bramley, H.; Mori, T.A.; Hodgson, J.M.; et al. Neglecting legumes has compromised human health and sustainable food production. *Nat. Plants* **2016**, *2*, 16112. [CrossRef]
18. Rani, A.; Devi, P.; Jha, U.C.; Sharma, K.D.; Siddique, K.H.M.; Nayyar, H. Developing climate-resilient chickpea involving physiological and molecular approaches with a focus on temperature and drought stresses. *Front. Plant Sci.* **2019**, *10*, 1759. [CrossRef]
19. Karges, K.; Bellingrath-Kimura, S.D.; Watson, C.A.; Stoddard, F.L.; Halwani, M.; Reckling, M. Agro-economic prospects for expanding soybean production beyond its current northerly limit in europe. *Eur. J. Agron.* **2022**, *133*, 126415. [CrossRef]
20. Rocchetti, L.; Bellucci, E.; Cortinovis, G.; Di Vittori, V.; Lanzavecchia, G.; Frascarelli, G.; Nanni, L.; Del Gatto, A.; Pieri, S.; Mangoni, L.; et al. The development of a european and mediterranean chickpea association panel (emcap). *Agronomy* **2020**, *10*, 1417. [CrossRef]
21. Bellucci, E.; Mario Aguilar, O.; Alseekh, S.; Bett, K.; Brezeanu, C.; Cook, D.; De la Rosa, L.; Delledonne, M.; Dostatny, D.F.; Ferreira, J.J.; et al. The increase project: Intelligent collections of food-legume genetic resources for european agrofood systems. *Plant J.* **2021**, *108*, 646–660. [CrossRef]
22. Esfahani, M.N.; Sulieman, S.; Schulze, J.; Yamaguchi-Shinozaki, K.; Shinozaki, K.; Tran, L.S. Approaches for enhancement of n(2) fixation efficiency of chickpea (*Cicer arietinum* L.) under limiting nitrogen conditions. *Plant Biotechnol. J.* **2014**, *12*, 387–397. [CrossRef]
23. Hughes, J.; Pearson, E.; Grafenauer, S. Legumes-a comprehensive exploration of global food-based dietary guidelines and consumption. *Nutrients* **2022**, *14*, 3080. [CrossRef]
24. Wallace, T.C.; Murray, R.; Zelman, K.M. The nutritional value and health benefits of chickpeas and hummus. *Nutrients* **2016**, *8*, 766. [CrossRef] [PubMed]
25. Purushothaman, R.; Upadhyaya, H.D.; Gaur, P.M.; Gowda, C.L.L.; Krishnamurthy, L. Kabuli and desi chickpeas differ in their requirement for reproductive duration. *Field Crops Res.* **2014**, *163*, 24–31. [CrossRef]
26. Varma Penmetsa, R.; Carrasquilla-Garcia, N.; Bergmann, E.M.; Vance, L.; Castro, B.; Kassa, M.T.; Sarma, B.K.; Datta, S.; Farmer, A.D.; Baek, J.M.; et al. Multiple post-domestication origins of kabuli chickpea through allelic variation in a diversification-associated transcription factor. *New Phytol.* **2016**, *211*, 1440–1451. [CrossRef] [PubMed]
27. Nisa, Z.U.; Arif, A.; Waheed, M.Q.; Shah, T.M.; Iqbal, A.; Siddiqui, A.J.; Choudhary, M.I.; El-Seedi, H.R.; Musharraf, S.G. A comparative metabolomic study on desi and kabuli chickpea (*Cicer arietinum* L.) genotypes under rainfed and irrigated field conditions. *Sci. Rep.* **2020**, *10*, 13919. [CrossRef]
28. Neugschwandtner, R.W.; Wichmann, S.; Gimplinger, D.M.; Wagentristl, H.; Kaul, H.-P. Chickpea performance compared to peam barley and oat in central europe: Growth analysis and yield. *Turk. J. Field Crops* **2013**, *18*, 179–184.
29. Reckling, M.; Bergkvist, G.; Watson, C.A.; Stoddard, F.L.; Zander, P.M.; Walker, R.L.; Pristeri, A.; Toncea, I.; Bachinger, J. Trade-offs between economic and environmental impacts of introducing legumes into cropping systems. *Front. Plant Sci.* **2016**, *7*, 669. [CrossRef]
30. Rubiales, D.; Annicchiarico, P.; Vaz Patto, M.C.; Julier, B. Legume breeding for the agroecological transition of global agri-food systems: A european perspective. *Front. Plant Sci.* **2021**, *12*, 782574. [CrossRef]
31. Fanning, J.; Brand, J.; Munoz Santa, I.; McDonald, L.; Taylor, J.; Hollaway, G. Management of chickpea ascochyta blight using fungicides and cultivar resistance improves grain yield, quality, and grower profitability. *Front. Plant Sci.* **2022**, *13*, 942220. [CrossRef]
32. Pang, J.; Turner, N.C.; Khan, T.; Du, Y.L.; Xiong, J.L.; Colmer, T.D.; Devilla, R.; Stefanova, K.; Siddique, K.H.M. Response of chickpea (*Cicer arietinum* L.) to terminal drought: Leaf stomatal conductance, pod abscisic acid concentration, and seed set. *J. Exp. Bot.* **2017**, *68*, 1973–1985. [PubMed]
33. Ramamoorthy, P.; Lakshmanan, K.; Upadhyaya, H.D.; Vadez, V.; Varshney, R.K. Shoot traits and their relevance in terminal drought tolerance of chickpea (*Cicer arietinum* L.). *Field Crops Res.* **2016**, *197*, 10–27. [CrossRef] [PubMed]
34. Sharma, N.K.; Gupta, S.K.; Dwivedi, V.; Chattopadhyay, D. Lignin deposition in chickpea root xylem under drought. *Plant Signal. Behav.* **2020**, *15*, 1754621. [CrossRef]
35. Purushothaman, R.; Krishnamurthy, L.; Upadhyaya, H.D.; Vadez, V.; Varshney, R.K. Genotypic variation in soil water use and root distribution and their implications for drought tolerance in chickpea. *Funct. Plant Biol.* **2017**, *44*, 235–252. [CrossRef] [PubMed]
36. Rurushothaman, R.; Krishnamurthy, L.; Upadhyaya, H.D.; Vadez, V.; Varshney, R.K. Root traits confer grain yield advantages under terminal drought inchickpea (*Cicer arietinum* L.). *Field Crops Res.* **2017**, *201*, 146–161.
37. Istanbuli, T.; Assar, A.A.; Twakaz, S.; Kumar, T.; Alsamman, A.M.; Hamwieh, A. The interaction between drought stress and nodule formation under multiple environments in chickpea. *PLoS ONE* **2022**, *17*, e0276732. [CrossRef]
38. Esfahani, M.N.; Sulieman, S.; Schulze, J.; Yama-Shinozaki, K.; Shinozaki, K.; Tran, L.-S.P. Mechanisms of physiological adjustment of n2 fixation in *Cicer arietinum* L. (chickpea) during early stages of water deficit: Single or multi-factor controls. *Plant J.* **2014**, *79*, 964–980. [CrossRef]
39. Mirkovic, T.; Ostroumov, E.E.; Anna, J.M.; van Grondelle, R.; Govindjee; Scholes, G.D. Light absoR.P.tion and energy transfer in the antenna complexes of photosynthetic organisms. *Chem. Rev.* **2017**, *117*, 249–293. [CrossRef]

40. Baker, N.R.; Rosenqvist, E. Applications of chlorophyll fluorescence can improve crop production strategies: An examination of future possibilities. *J. Exp. Bot.* **2004**, *55*, 1607–1621. [CrossRef]
41. Macar, T.K.; Ekmekci, Y. Psii photochemistry and antioxidant response of a chickpea variety exposed to drought. *Z. Für Naturforschung—Sect. C J. Biosci.* **2008**, *63*, 583–594. [CrossRef]
42. Saglam, A.; Terzi, R.; Demiralay, M. Effect of polyethylene glycol induced drought stress on photosynthesis in two chickpea genotypes with different drought tolerance. *Acta Biol. Hung.* **2014**, *65*, 178–188. [CrossRef] [PubMed]
43. Tschiersch, H.; Junker, A.; Meyer, R.C.; Altmann, T. Establishment of integrated protocols for automated high throughput kinetic chlorophyll fluorescence analyses. *Plant Methods* **2017**, *13*, 54. [CrossRef] [PubMed]
44. Furbank, R.T.; Tester, M. Phenomics—Technologies to relieve the phenotyping bottleneck. *Trends Plant Sci.* **2011**, *16*, 635–645. [CrossRef] [PubMed]
45. Tardieu, F.; Cabrera-Bosquet, L.; Pridmore, T.; Bennett, M. Plant phenomics, from sensors to knowledge. *Curr. Biol.* **2017**, *27*, R770–R783. [CrossRef]
46. Yang, W.; Feng, H.; Zhang, X.; Zhang, J.; Doonan, J.H.; Batchelor, W.D.; Xiong, L.; Yan, J. Crop phenomics and high-throughput phenotyping: Past decades, current challenges, and future perspectives. *Mol. Plant* **2020**, *13*, 187–214. [CrossRef]
47. Lauterberg, M.; Saranga, Y.; Deblieck, M.; Klukas, C.; Krugman, T.; Perovic, D.; Ordon, F.; Graner, A.; Neumann, K. Precision phenotyping across the life cycle to validate and decipher drought-adaptive qtls of wild emmer wheat (*Triticum turgidum* ssp. Dicoccoides) introduced into elite wheat varieties. *Front. Plant Sci.* **2022**, *13*, 965287.
48. Atieno, J.; Colmer, T.D.; Taylor, J.; Li, Y.; Quealy, J.; Kotula, L.; Nicol, D.; Nguyen, D.T.; Brien, C.; Langridge, P.; et al. Novel salinity tolerance loci in chickpea identified in glasshouse and field environments. *Front. Plant Sci.* **2021**, *12*, 667910. [CrossRef]
49. Atieno, J.; Li, Y.; Langridge, P.; Dowling, K.; Brien, C.; Berger, B.; Varshney, R.K.; Sutton, T. Exploring genetic variation for salinity tolerance in chickpea using image-based phenotyping. *Sci. Rep.* **2017**, *7*, 1300. [CrossRef]
50. Humplik, J.F.; Lazar, D.; Furst, T.; Husickova, A.; Hybl, M.; Spichal, L. Automated integrative high-throughput phenotyping of plant shoots: A case study of the cold-tolerance of pea (*Pisum sativum* L.). *Plant Methods* **2015**, *11*, 20. [CrossRef]
51. Awlia, M.; Nigro, A.; Fajkus, J.; Schmoeckel, S.M.; Negrao, S.; Santelia, D.; Trtilek, M.; Tester, M.; Julkowska, M.M.; Panzarova, K. High-throughput non-destructive phenotyping of traits that contribute to salinity tolerance in arabidopsis thaliana. *Front. Plant Sci.* **2016**, *7*, 1414. [CrossRef]
52. Dhanagond, S.; Liu, G.; Zhao, Y.; Chen, D.; Grieco, M.; Reif, J.; Kilian, B.; Graner, A.; Neumann, K. Non-invasive phenotyping reveals genomic regions involved in pre-anthesis drought tolerance and recovery in spring barley. *Front. Plant Sci.* **2019**, *10*, 1307. [CrossRef] [PubMed]
53. Dodig, D.; Bozinovic, S.; Nikolic, A.; Zoric, M.; Vancetovic, J.; Ignjatovic-Micic, D.; Delic, N.; Weigelt-Fischer, K.; Altmann, T.; Junker, A. Dynamics of maize vegetative growth and drought adaptability using image-based phenotyping under controlled conditions. *Front. Plant Sci.* **2021**, *12*, 652116. [CrossRef] [PubMed]
54. Kim, S.L.; Kim, N.; Lee, H.; Lee, E.; Cheon, K.S.; Kim, M.; Baek, J.; Choi, I.; Ji, H.; Yoon, I.S.; et al. High-throughput phenotyping platform for analyzing drought tolerance in rice. *Planta* **2020**, *252*, 38. [CrossRef]
55. Neumann, K.; Klukas, C.; Friedel, S.; Rischbeck, P.; Chen, D.; Entzian, A.; Stein, N.; Graner, A.; Kilian, B. Dissecting spatiotemporal biomass accumulation in barley under different water regimes using high-throughput image analysis. *Plant Cell Environ.* **2015**, *38*, 1980–1996. [CrossRef] [PubMed]
56. Zhao, C.; Zhang, Y.; Du, J.; Guo, X.; Wen, W.; Gu, S.; Wang, J.; Fan, J. Crop phenomics: Current status and perspectives. *Front. Plant Sci.* **2019**, *10*, 714. [CrossRef]
57. Condon, A.G.; Richards, R.A.; Rebetzke, G.J.; Farquhar, G.D. Breeding for high water-use efficiency. *J. Exp. Bot.* **2004**, *55*, 2447–2460. [CrossRef]
58. Burridge, J.D.; Grondin, A.; Vadez, V. Optimizing crop water use for drought and climate change adaptation requires a multi-scale approach. *Front. Plant Sci.* **2022**, *13*, 824720. [CrossRef]
59. Oweis, T.; Hachum, A.; Pala, M. Water use efficiency of winter-sown chickpea under supplemental irrigation in a mediterranean environment. *Agric. Water Manag.* **2004**, *66*, 163–179. [CrossRef]
60. Das, A.; Basu, P.S.; Kumar, M.; Ansari, J.; Shukla, A.; Thakur, S.; Singh, P.; Datta, S.; Chaturvedi, S.K.; Sheshshayee, M.S.; et al. Transgenic chickpea (*Cicer arietinum* L.) harbouring atdreb1a are physiologically better adapted to water deficit. *BMC Plant Biol.* **2021**, *21*, 39. [CrossRef]
61. Mikołajczak, K.; Ogrodowicz, P.; Cwiek-Kupczynska, H.; Weigelt-Fischer, K.; Mothukuri, S.R.; Junker, A.; Altmann, T.; Krystkowiak, K.; Adamski, T.; Surma, M.; et al. Image phenotyping of spring barley (*Hordeum vulgare* L.) ril population under drought: Selection of traits and biological inteR.P.retation. *Front. Plant Sci.* **2022**, *11*, 1–18. [CrossRef]
62. Amitrano, C.; Junker, A.; D'Agostino, N.; De Pascale, S.; De Micco, V. Integration of high-throughput phenotyping with anatomical traits of leaves to help understanding lettuce acclimation to a changing environment. *Planta* **2022**, *256*, 68. [CrossRef]
63. Simkin, A.J.; Kapoor, L.; Doss, C.G.P.; Hofmann, T.A.; Lawson, T.; Ramamoorthy, S. The role of photosynthesis related pigments in light harvesting, photoprotection and enhancement of photosynthetic yield in planta. *Photosynth. Res.* **2022**, *152*, 23–42. [CrossRef] [PubMed]
64. Steyn, W.J.; Wand, S.J.E.; Holcroft, D.M.; Jacobs, G. Anthocyanins in vegetative tissues: A proposed unified function in photoprotection. *New Phytol.* **2002**, *155*, 349–361. [CrossRef] [PubMed]

65. Farago, D.; Sass, L.; Valkai, I.; Andrasi, N.; Szabados, L. Plantsize offers an affordable, non-destructive method to measure plant size and color in vitro. *Front. Plant Sci.* **2018**, *9*, 219. [CrossRef]
66. Mafakheri, A.; Siosemardeh, A.; Bahramnejad, B.; Struik, P.C.; Sohrabi, Y. Effect of drought stress on yield, proline and chlorophyll contents in three chickpea cultivars. *Aust. J. Crop Sci.* **2010**, *4*, 580–585.
67. Talebi, R.; Ensafi, M.H.; Baghebani, N.; Karami, E.; Mohammadi, K. Physiological responses of chickpea (cicer arietinum) genotypes to drought stress. *Environ. Exp. Biol.* **2013**, *11*, 9–15.
68. Majer, P.; Sass, L.; Horvath, G.V.; Hideg, E. Leaf hue measurements offer a fast, high-throughput initial screening of photosynthesis in leaves. *J. Plant Physiol.* **2010**, *167*, 74–76. [CrossRef]
69. Liang, Y.; Urano, D.; Liao, K.L.; Hedrick, T.L.; Gao, Y.; Jones, A.M. A nondestructive method to estimate the chlorophyll content of arabidopsis seedlings. *Plant Methods* **2017**, *13*, 26. [CrossRef]
70. Dong, S.; Jiang, Y.; Dong, Y.; Wang, L.; Wang, W.; Ma, Z.; Yan, C.; Ma, C.; Liu, L. A study on soybean responses to drought stress and rehydration. *Saudi J. Biol. Sci.* **2019**, *26*, 2006–2017. [CrossRef]
71. Zendonadi Dos Santos, N.; Piepho, H.P.; Condorelli, G.E.; Licieri Groli, E.; Newcomb, M.; Ward, R.; Tuberosa, R.; Maccaferri, M.; Fiorani, F.; Rascher, U.; et al. High-throughput field phenotyping reveals genetic variation in photosynthetic traits in durum wheat under drought. *Plant Cell Environ.* **2021**, *44*, 2858–2878. [CrossRef]
72. Dodig, D.; Bozinovic, S.; Nikolic, A.; Zoric, M.; Vancetovic, J.; Ignjatovic-Micic, D.; Delic, N.; Weigelt-Fischer, K.; Junker, A.; Altmann, T. Image-derived traits related to mid-season growth performance of maize under nitrogen and water stress. *Front. Plant Sci.* **2019**, *10*, 814. [CrossRef] [PubMed]
73. Araus, J.L.; Cairns, J.E. Field high-throughput phenotyping: The new crop breeding frontier. *Trends Plant Sci.* **2014**, *19*, 52–61. [CrossRef] [PubMed]
74. Farooq, M.; Ullah, A.; Lee, D.-L.; Alghamdi, S.S.; Siddique, K.H.M. Desi chickpea genotypes tolerate drought stress better than kabuli types by modulating germination metabolism, trehalose accumulation, and carbon assimilation. *Plant Physiol. Biochem.* **2018**, *126*, 47–54. [CrossRef] [PubMed]
75. Thudi, M.; Chitikineni, A.; Liu, X.; He, W.; Roorkiwal, M.; Yang, W.; Jian, J.; Doddamani, D.; Gaur, P.M.; Rathore, A.; et al. Recent breeding programs enhanced genetic diversity in both desi and kabuli varieties of chickpea (*Cicer arietinum* L.). *Sci. Rep.* **2016**, *6*, 38636. [CrossRef]
76. Rocchetti, L.; Gioia, T.; Logozzo, G.; Brezeanu, C.; Pereira, L.G.; la Rosa, L.; Marzario, S.; Pieri, A.; Fernie, A.R.; Alseekh, S.; et al. Towards the development, maintenance and standardized phenotypic characterization of single-seed-descent genetic resources for chickpea. *Curr. Protoc.* **2022**, *2*, e371. [CrossRef]
77. Klukas, C.; Chen, D.; Pape, J.M. Integrated analysis platform: An open-source information system for high-throughput plant phenotyping. *Plant Physiol.* **2014**, *165*, 506–518. [CrossRef]

2.3 Theoretical non-photochemical quenching ($NPQ_{(T)}$)

"Implementation of theoretical non-photochemical quenching ($NPQ_{(T)}$) to investigate NPQ of chickpea under drought stress with High-throughput Phenotyping"

by

Madita Lauterberg, Henning Tschiersch,Yusheng Zhao, Markus Kuhlmann, Ingo Mücke, Roberto Papa, Elena Bitocchi & Kerstin Neumann

Published in
Scientific Reports; 17. June 2024
https://www.nature.com/articles/s41598-024-63372-6

www.nature.com/scientificreports

scientific reports

Check for updates

OPEN

Implementation of theoretical non-photochemical quenching ($NPQ_{(T)}$) to investigate NPQ of chickpea under drought stress with High-throughput Phenotyping

Madita Lauterberg[1], Henning Tschiersch[1], Yusheng Zhao[1], Markus Kuhlmann[1], Ingo Mücke[1], Roberto Papa[2], Elena Bitocchi[2] & Kerstin Neumann[1]✉

Non-photochemical quenching (NPQ) is a protective mechanism for dissipating excess energy generated during photosynthesis in the form of heat. The accelerated relaxation of the NPQ in fluctuating light can lead to an increase in the yield and dry matter productivity of crops. Since the measurement of NPQ is time-consuming and requires specific light conditions, theoretical NPQ ($NPQ_{(T)}$) was introduced for rapid estimation, which could be suitable for High-throughput Phenotyping. We investigated the potential of $NPQ_{(T)}$ to be used for testing plant genetic resources of chickpea under drought stress with non-invasive High-throughput Phenotyping complemented with yield traits. Besides a high correlation between the hundred-seed-weight and the Estimated Biovolume, significant differences were observed between the two types of chickpea *desi* and *kabuli* for Estimated Biovolume and $NPQ_{(T)}$. *Desi* was able to maintain the Estimated Biovolume significantly better under drought stress. One reason could be the effective dissipation of excess excitation energy in photosystem II, which can be efficiently measured as $NPQ_{(T)}$. Screening of plant genetic resources for photosynthetic performance could take pre-breeding to a higher level and can be implemented in a variety of studies, such as here with drought stress or under fluctuating light in a High-throughput Phenotyping manner using $NPQ_{(T)}$.

Keywords Chickpea, Chlorophyll fluorescence, Non-photochemical quenching, High-throughput Phenotyping, Drought stress

Chickpea (*Cicer arietinum* L.) is a protein-rich legume that is becoming increasingly popular due to its health benefits and as replacement for energy intensive production of animal-based protein. Drought stress is reported to reduce chickpea yields by about 40–50% worldwide[1,2]. This is of the utmost importance, as drought events will occur more frequently in Europe in the future[3]. A good strategy is to improve yield potential and stability in challenging conditions by incorporating plant genetic resources into pre-breeding and modern breeding programs and exploiting their diversity to improve drought tolerance in chickpea[4,5]. Cultivated chickpeas are grouped into two types, based on their origin and their use in agriculture: *desi* and *kabuli*[6]. While the multi-colored *desi* is mainly used and cultivated in Indian subcontinent, the lighter-colored *kabuli* is mainly grown in the Mediterranean Basin. In pot and field studies, *desi* has been described as more tolerant to drought stress than *kabuli*, thus *desi* plant genetic resources are expected to be more promising for the identification of drought tolerant genotypes[7–10]. The assessment of photosynthetic capacity might be an interesting trait to be introduced for selecting genotypes to be included in breeding programs aimed to develop more resilient and drought tolerant plants.

Over the last decade, High-throughput Phenotyping (HTP) has developed into a state-of-the-art method. Plant genetic resources of crops such as barley (*Hordeum vulgare* L.), maize (*Zea mays* L.), pea (*Pisum sativum* L.) and chickpea, have been analysed on several HTP systems and tested for drought or cold tolerance using estimated biovolume for shoot biomass as the main trait[11–14]. The combination of morphological and physiological traits, measured with different imaging systems such as red–green–blue (RGB) or chlorophyll fluorescence, can

[1]Leibniz Institute of Plant Genetics and Crop Plant Research (IPK), Seeland, Germany. [2]Marche Polytechnic University (UNIVPM), Ancona, Italy. ✉email: neumannk@ipk-gatersleben.de

be used to deeply characterize plant genetic resources and to investigate their genetic architecture in a spatio-temporal pattern.

When light energy is captured by chlorophyll, it is passed to photochemistry, non-photochemical quenching (NPQ) or fluorescence to avoid production of reactive oxygen species and photodamage[15]. The chlorophyll fluorescence of photosystem II accounts for 0.6 to 3% of the absorbed light and can be measured with pulse-amplitude modulation (PAM)[16]. The operating efficiency of photosystem II (ΦPSII, F_q'/F_m'), measured on fully light-adapted plants, and the maximum quantum yield (F_v/F_m), measured on fully dark-adapted plants, have been measured frequently with different growth conditions and for many species such as brassica, rice, maize or tobacco (*Nicotina tabacum*)[14,17,18]. The advantage of these two traits F_v/F_m and ΦPSII is that the measurement is fast and therefore feasible for HTP.

NPQ is a mechanism to protect plants from photodamage and is described by two main components: fast relaxation (qE) and slow relaxation (qI)[15]. Xanthophylls interconvert between zeaxanthin and violaxanthin in a pH dependent manner, which modulates the qE component of NPQ. A conformational change of the PS-II unit and the PsbS protein is achieved by the binding of protons and xanthophylls to specific sites of the antenna complexes. qE is rapidly reversible and qI is a measure of slowly relaxing quenching, the main mechanism of which is photoinhibition.

Under fluctuating light conditions, a rapid conformational change in the antenna complexes is beneficial, implying a dynamic NPQ. Modelling has shown that the losses of potential carbon gain are between approximately 13 and 30% and strongly depend on the dynamically relaxation kinetics of the NPQ[19]. Studying photosynthesis in fluctuating light simulates conditions that are as close as possible to the outside environment where light conditions are often not constant, so the photosynthesis has to adapt to maximize daily carbon gain[20]. In experiments with tobacco (*Nicotiana tabacum*) and soybean (*Glycine max* L.), it was discovered that the ability to adapt dynamically with NPQ when changing from high to low light led to a 33% increase in yield and a 15% increase in dry matter productivity[21,22].

NPQ is calculated from F_m and F_m' which means fully light- and fully dark-adaptation are required[23]. Full light adaptation takes a minimum of 30 min and a dark adaptation a minimum of 1 h[24], thus the measurement is very time consuming and therefore not feasible for HTP[25].

Tietz et al.[26] presented a protocol for measuring theoretical NPQ ($NPQ_{(T)}$) in *Arabidopsis thaliana* that was not only faster but also worked under light-adapted conditions. To measure $NPQ_{(T)}$, F_v/F_m was not measured but a fixed value was used, taking advantage of the fact, that F_v/F_m is a consistent value within a species[24]. After a measurement of F_q'/F_m', far-red light was applied. Far-red light ensures that photosystem II (PSII) is fully opened and that the first stable electron acceptor of PSII the plastoquinone A (Q_A) and the plastoquinone pool is oxidized[27]. This avoids the waiting time in which PSII is oxidized and the final F_0' determination can be carried out more quickly. $NPQ_{(T)}$ has already been implemented in carry-on measurement tools and tested for species such as maize and soybean[28–30]. $NPQ_{(T)}$ appears to be suitable for High-throughput Phenotyping and could help to exploit plant genetic resources for future photosynthesis improvement.

Objective

In the present study

(1) A protocol for quantification of $NPQ_{(T)}$ was implemented which serves as proxy for NPQ;
(2) The trait $NPQ_{(T)}$ was validated as suitable method for High-throughput Phenotyping (HTP);
(3) $NPQ_{(T)}$ was compared with other image-based traits and yield traits and used as an example for screening plant genetic resources of chickpea under control and drought stress conditions.

Results

The results of the HTP experiment with 60 chickpea genotypes and 2 replicates each in control and drought stress treatment, are described below. During the plant establishment phase with control treatment for all plants, the $NPQ_{(T)}$ method was validated. For this purpose, F_v/F_m, NPQ and $NPQ_{(T)}$ were measured. Then, the drought stress was initiated and the $NPQ_{(T)}$ method was implemented during the period of drought stress and in the following recovery phase, and finally, yield traits were determined at maturity.

Description of data: data availability, repeatability and capacity of measurements

For method-validation of $NPQ_{(T)}$, all 240 plants were measured for F_v/F_m in the control treatment on the night of day 4 to 5 after the transfer (DAT) of the pots with the plants from the pre-cultivation in the greenhouse to the HTP system. Furthermore, 23 plants corresponding to 20 different genotypes were measured for NPQ and $NPQ_{(T)}$ in control treatment during the night of DAT 5 to 6 (Table S1).

For the method-implementation $NPQ_{(T)}$ during the drought stress and recovery from DAT 8–37, the raw data of image-derived traits of daily HTP has been inspected. The missing rate for Estimated Biovolume and Mean Color Value for the five DAT 12, 18, 19, 24 and 35 was higher than 20% (Table S2). For the red to green color ratio and plant height, the three DAT 19, 24 and 35 had a missing rate higher than 20%. It should be noted that the incomplete DAT were not the key DAT on which chlorophyll fluorescence measurements were conducted or drought stress was maximal or recovery were induced. Moreover, the rate of missing raw data from individual replicates was not higher than 6.6% across all DAT (Table S3). The missing rate for ΦPSII and $NPQ_{(T)}$ was on average 12.9% across the four DATs (Table S4).

The repeatability, which is an indicator of the consistency of the repeated measurement and varies between 0 and 1, with 1 representing the highest possible consistency, was calculated. For the method-validation, a high repeatability of 0.8 has been observed for F_v/F_m. For NPQ the repeatability was 0.69 and for $NPQ_{(T)}$ it was 0.48.

For the method-implementation, a high repeatability of more than 0.8 was calculated for Estimated Biovolume for the control treatment and was marginally lower for the drought stress with 0.7 (Figure S1). Repeatabilities of 0.8 on average also result for plant height and Mean Color Value for the two treatments (Figure S2). For plant height, the repeatability for both treatments increased with increasing experiment duration. The repeatability was at an average value of 0.65 for red to green color ratio. Furthermore, red to green color ratio had more fluctuations in repeatability across the time course.

In the control treatment the repeatability for ΦPSII was on average 0.66 and for $NPQ_{(T)}$ 0.47. Furthermore, in the drought stress treatment, the repeatability for ΦPSII and $NPQ_{(T)}$ was on average 0.4 (Figure S3).

For the yield trait, the repeatability was highest for the weight of seeds with 0.66 for control and 0.57 for drought stress treatment and lowest for number of empty pods with 0.14 for control and 0.3 for drought stress treatment (Figure S4). For the hundred-seed-weight, the repeatability was 0.45 for control and 0.27 for drought stress treatment.

For the method-validation, in the night from DAT 5 to 6, 9.4 dark-adapted plants per hour have been measured for NPQ. The average capacity for $NPQ_{(T)}$ measurements for the method-implementation and across the four measurement DATs 38.8 fully light-adapted plants per hour with a maximum of 42 plants per hour. This numbers for the capacity included the rotation of the conveyer belts, which transport the carriers with each one plant to the imaging chamber.

Method-validation of $NPQ_{(T)}$ as proxy for NPQ

For all 60 genotypes, the F_v/F_m average was 0.856 ± 0.002 (Table S5). Among the 23 measurements of replicates for NPQ the average was 0.685 ± 0.084 and for $NPQ_{(T)}$ it was 1.826 ± 0.147 (Table S6).

The correlation between NPQ and $NPQ_{(T)}$ could be explained by a regression with a coefficient of correlation r of 0.9 (Fig. 1).

Impact of drought stress on HTP image-derived and chlorophyll fluorescence traits

Estimated Biovolume was used as proxy for the shoot biomass and reduced accumulation of biomass can be used as indication for the impact of drought stress.

From DAT 17 onwards, at an average plant available water content of 23%, the Estimated Biovolume of the chickpea plants of drought stress and control treatments differed significantly (Fig. 2, Table S7). On DAT 28, at the last day of drought stress, average of Estimated Biovolume for the control plants was 99.1 ± 35 [voxel 10^{-5}]

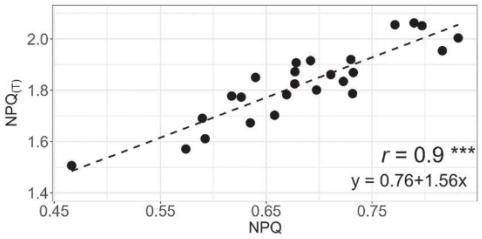

Figure 1. Correlation of NPQ and $NPQ_{(T)}$. r = coefficient of correlation. ***$p < 0.001$. Based on raw data of 20 genotypes and 23 replicates.

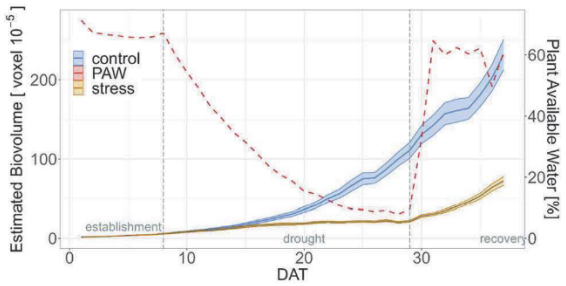

Figure 2. Estimated Biovolume in drought stress and control treatments. The red dashed line indicates the plant available water to which the secondary axis refers to. The two vertical grey dashed lines indicate the different phases of the experiment: establishment, drought and recovery. The shadows describe the 95% confidence interval; as long as the shadows of the individual lines do not overlap, the significance level of $\alpha = 0.05$ was reached. Based on average of BLUEs within the experiment of all 60 genotypes. Interpolated on DAT 12, 18, 19, 24, 35. DAT = days after transferring to the High-throughput Phenotyping system.

while for drought stress it was 20.3 ± 4.5 [voxel 10^{-5}] (Table S8). This was a reduction of 79.5% in drought stress compared to the control treatment. On DAT 37, after application of drought stress and a recovery phase, the average of Estimated Biovolume for the plants in control treatment was 231.5 ± 75.4 [voxel 10^{-5}] and for drought stress it was 72.5 ± 20.9 [voxel 10^{-5}], describing a difference of Estimated Biovolume for plants in drought stress of 68.7% compared to those in the control treatment.

A significant effect of drought stress on plant height, meaning smaller chickpea plants in drought stress, was observed on DAT 19 at a plant available water content of 18.7% (Figure S5, Tables S7, S8). On DAT 28, the difference of drought stress compared to the control treatment was 29% (control = 515 ± 72 [mm]; stress = 365 ± 57[mm]) and at the end of the experiment on DAT 37 the difference was 26.9% between the two treatments. From DAT 16 until DAT 36, starting at a plant available water content of 27%, the chickpeas of the drought stress and control treatments differed significantly for Mean Color Value. On DAT 28, the last day of drought stress, the average of Mean Color Value for the control replicates was 0.278 ± 0.004 [hue] and for drought stress it was 0.296 ± 0.005 [hue] (Table S8). This was a difference of −6.6% in drought stress compared to the control treatment and gave the impression of a darker green in drought stress treatment. In addition, the red to green color ratio was higher in drought stress treatment than in control treatment on DAT 28 (control = 0.125 ± 0.04; stress = 0.22 ± 0.06).

For ΦPSII the average across all phenotypes analyzed in control treatment ranged from 0.54 ± 0.02 to 0.56 ± 0.02 for the four measured DATs (Fig. 3, Tables S11, S12). In drought stress ΦPSII was between 0.56 ± 0.02 and 0.59 ± 0.01.

The two treatments drought stress and control differed significantly on DAT 16, 29 and 37 and on all three DATs the drought stressed chickpea plants had a slightly higher ΦPSII.

The average of $NPQ_{(T)}$ in the control treatment varied between 1.55 ± 0.15 and 1.61 ± 0.11 for the four DATs and there were no significant differences (Fig. 3, Tables S11, S12).

The plants in drought stress had a significantly different $NPQ_{(T)}$ between DAT 16 and 22 and between DAT 22 and 29 with the averages of 1.56 ± 0.11, 1.73 ± 0.18, 1.66 ± 0.09 and 1.62 ± 0.11 at the respective DATs.

On DAT 22, 29 and 37, the plants differed significantly from each other between the two treatments. At all three DATs, plants in drought stress had a higher value for $NPQ_{(T)}$, with the difference being highest at DAT 22.

There was a significant negative effect of drought stress on the yield traits (Figure S6, Tables S9, S10). The hundred-seed-weight showed a reduction of 58%, in drought stress compared to the control treatment with an average of 200.2 ± 100.2 g in control to 82.2 ± 73.4 in drought stress. For the other traits, the difference of drought

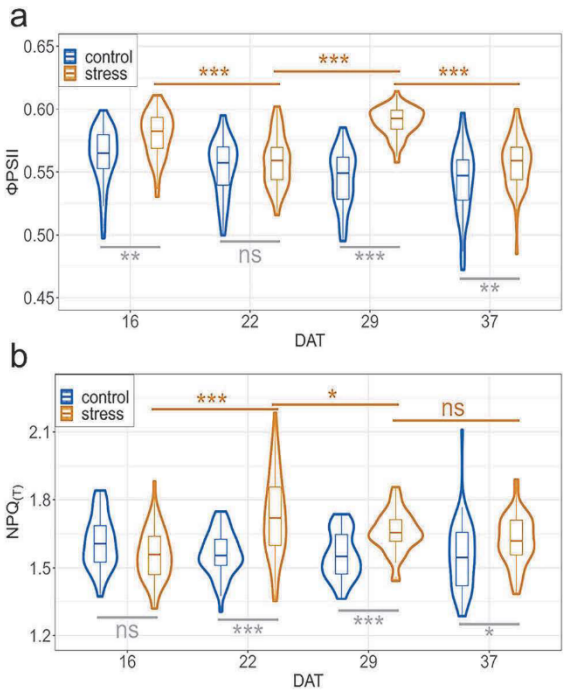

Figure 3. Chlorophyll fluorescence traits under drought stress and recovery. (**a**) ΦPSII; (**b**) $NPQ_{(T)}$. DAT 16 = 8 days of drought stress; DAT 22 = 14 days of drought stress; DAT 29 = first day of recovery; DAT 37 = 8 days of recovery. Based on BLUEs within the experiment. DAT = days after transferring to the High-throughput Phenotyping system. The brown lines above the plots refer to the significance between the adjacent DAT within the drought stress treatment. The gray lines below the plots refer to the significance between the two treatments on each DAT. All significances can be found in Table S12. ns = not significant; ***$p < 0.001$; **$p < 0.01$; *$p < 0.05$.

stress compared to the control treatment varied between 49.2% for number of empty pods and 77.5% for weight of seeds (Table S9). For all traits the difference was significant (Table S10).

Interaction of traits

When comparing $NPQ_{(T)}$ and ΦPSII under the control treatment, $NPQ_{(T)}$ had a higher coefficient of variation among all DATs and for both treatments (Figure S7). This was pronounced on DAT 22, when the coefficient of variation for drought stress was 10.5 for $NPQ_{(T)}$ and 3.6 for ΦPSII.

There were high correlations of $r = 0.61$ to 0.7 between Estimated Biovolume and hundred-seed-weight for DATs 16, 22, 29 and 37 for both treatments combined (Table S13). Similarly, there were correlations of $r = 0.42$ to 0.62 between Estimated Biovolume and weight of seeds for these DATs and both treatments combined. For both treatments combined, there was a significant negative correlation of $r = -0.19$ to -0.26 between $NPQ_{(T)}$ and hundred-seed-weight for DATs 22, 29 and 37. There was also a negative correlation of $r = -0.34$ to -0.45 between $NPQ_{(T)}$ and Estimated Biovolume for both treatments combined for DAT 22, 29, 37.

On DAT 22, after 14 days of drought stress, $NPQ_{(T)}$ and ΦPSII were significantly positively correlated in the control treatment ($r = 0.44$) and significantly negatively correlated in the drought stress treatment ($r = -0.58$) (Table S13).

The correlation between $NPQ_{(T)}$ and Estimated Biovolume was not significant on DAT 22 in control treatment (Fig. 5, Table S13). For drought stress, the correlation was significant and amounted to $r = 0.53$ and for the difference of drought stress compared to the control treatment, the significant correlation amounted to $r = -0.34$.

The plasticity for $NPQ_{(T)}$ can differentiate *desi* and *kabuli* chickpeas

On DAT 22, *desi* had significantly less Estimated Biovolume than *kabuli* under control treatment (*desi* = 43.57 ± 14.88; *kabuli* = 56.64 ± 19.91 (Fig. 5, Tables S14, S15). For drought stress, Estimated Biovolume was similar between both types of chickpea (*desi* = 20.1 ± 4.29; *kabuli* = 21.6 ± 4.97). Thus, *kabuli* had a significantly larger difference of Estimated Biovolume under drought stress compared to control treatment, than *desi*.

On DAT 22 the $NPQ_{(T)}$ of *desi* and *kabuli* differed in control treatment significantly (*desi* = 1.59 ± 0.08; *kabuli* = 1.53 ± 0.1), but not in drought stress treatment (*desi* = 1.7 ± 0.18; *kabuli* = 1.76 ± 0.18). Therefore, *desi* had a significantly lower difference of drought stress compared to the control treatment of $NPQ_{(T)}$ than *kabuli* (Fig. 4, Tables S14, S15).

An exemplary and representative genotype was highlighted for each type of chickpea. For the *desi* genotype INCCP_00508 (*desi*, breeding material, Middle East), the $NPQ_{(T)}$ was 1.62 in the control treatment and 1.55 in

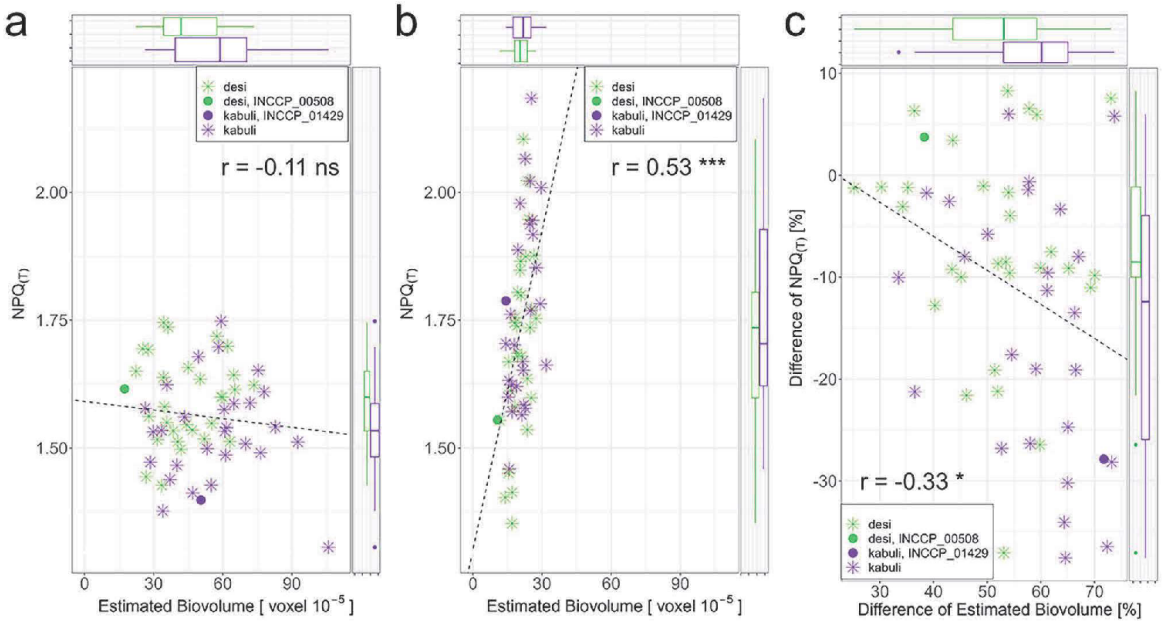

Figure 4. Correlations between Estimated Biovolume and $NPQ_{(T)}$ on DAT 22 for *desi* and *kabuli*. (**a**) for control treatment; (**b**) for drought stress treatment; (**c**) for the difference of drought stress compared to control treatment. Side-boxplots show the distribution of *desi* and *kabuli*, with the 25% and 75% quantiles and the median described by the boxes and for the corresponding axis. Based on Blues within experiment. Difference [%] = (1 − (drought stress/control)) * 100. r = coefficient of correlation; ns = not significant; *$p < 0.05$; ***$p < 0.001$. DAT 22 = days after transferring chickpeas to the High-throughput Phenotyping system with 14 days of drought stress. The two chickpea types, *desi* and *kabuli*, and one exemplary and representative genotype of each type were highlighted.

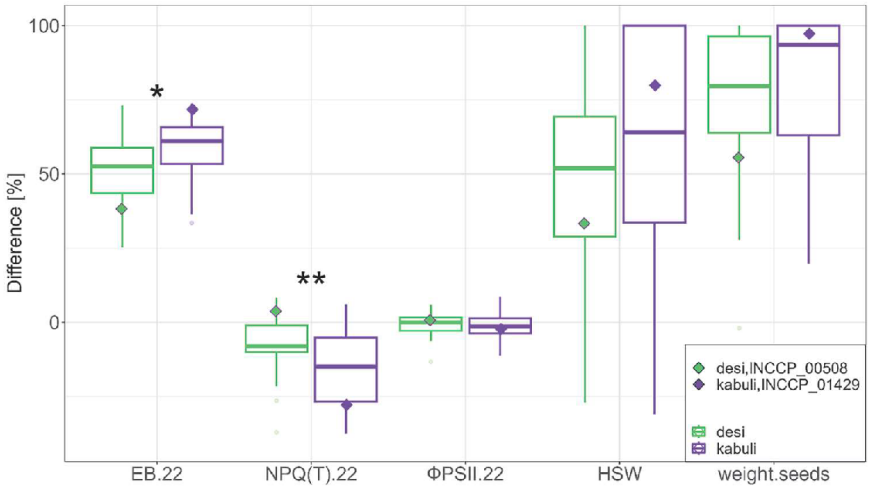

Figure 5. Difference of drought stress compared to control treatment of *desi* and *kabuli* for EB = Estimated Biovolume, $NPQ_{(T)}$, ΦPSII, HSW = hundred-seed-weight and weight of seeds at DAT 22. Difference [%] = (1 − (drought stress/control)) * 100. The two chickpea types *desi* and *kabuli* and one genotype of each type were highlighted. DAT 22 = days after transferring chickpeas to the High-throughput Phenotyping system with 14 days of drought stress. The two chickpea types, *desi* and *kabuli*, and one genotype of each type were highlighted. $*p < 0.05$; $**p < 0.01$. Comparisons between the two types that were not significant were not noted.

drought stress, with a small difference of drought stress compared to the control treatment for Estimated Biovolume of 38% (control = 17.35; drought stress = 10.71). For the *kabuli* genotype INCCP_01429 (*kabuli*, landrace, Middle East), $NPQ_{(T)}$ was 1.4 in the control treatment and significantly higher at 1.79 in drought stress, and there was a high difference of Estimated Biovolume of 71% (control = 50.49; drought stress = 14.27).

Furthermore, *kabuli* had a higher hundred-seed-weight in control treatment than *desi* (*desi* = 168.23 ± 81.7; *kabuli* = 232.25 ± 107.91), but under drought stress and for the difference of drought stress compared to the control treatment, both types did not differ significantly (Fig. 5, Tables S14, S15). For the weight of seeds, the results were similar to hundred-seed-weight. In addition, the two types did not differ in ΦPSII, r2g or Mean Color Value for any DAT or between the treatments.

Discussion

By using High-throughput Phenotyping (HTP), the interactions between genotype and environment can be precisely analyzed and specific traits can be dissected for plant breeding. In the present study, $NPQ_{(T)}$, a trait for NPQ for High-throughput Phenotyping, has been tested for its suitability. $NPQ_{(T)}$ could be applied to test plant genetic resources of chickpea under well-watered and drought stress conditions and be related to other traits such as EB. High repeatabilities were achieved in phenotyping using chlorophyll fluorescence and RGB imaging, which underlie the suitability of $NPQ_{(T)}$ in pre-breeding.

The HTP system used in this study has already proven successful in the investigation of chickpea plant genetic resources under drought stress and has provided the phenotypic data basis for other studies on bread and durum wheat (*Triticum aestivum* L., *T. durum* L.) and barley to decipher the genetic architecture of drought stress by GWAS[31,32].

For the method-validation of the experiment, the chlorophyll fluorescence measurements of F_v/F_m, NPQ and $NPQ_{(T)}$ were successfully performed and showed a satisfactory and solid repeatability. An exceptionally high correlation coefficient between NPQ and $NPQ_{(T)}$ of $r = 0.9$ illustrated that $NPQ_{(T)}$ could be used as a valid proxy for NPQ. In addition, this result, measured with chickpea on our HTP system, was consistent with the measurements obtained during the development of the protocol of $NPQ_{(T)}$ with *Arabidopsis*[26].

Chlorophyll fluorescence measurements for HTP must be precise and performed quickly in order to fit into the high-throughput process. For an NPQ measurement, a dark adaptation of at least 30 min is necessary, followed by a measurement of at least 15 min[23]. Including all technically necessary transport and circulation steps, we were able to measure at least 4.1 times more single plants on our HTP system during the day with the protocol for $NPQ_{(T)}$ than with the usual NPQ protocol during the night when all plants are dark-adapted. If NPQ is measured during the day and dark adaptation is necessary first, our $NPQ_{(T)}$ protocol is about 40 times faster. This makes $NPQ_{(T)}$ extremely suitable and advantageous for HTP.

For the method-implementation, during the drought stress, the repeatabilities for the image-derived traits were useful and comparable to the repeatabilities previously measured on this HTP system[32]. In a previous study, a high correlation of $r = 0.96$ was already calculated between Estimated Biovolume and dry weight of chickpea plants, so Estimated Biovolume can be used as a valid proxy for biomass[8].

The following applications under fully light adapted conditions of $NPQ_{(T)}$ and ΦPSII for the method-implementation during drought stress and recovery were comparable in terms of repeatability with previous studies on chickpea on ΦPSII[8]. Furthermore, the values of $NPQ_{(T)}$ were similar to experiments with maize under drought stress and soybean under cold stress[28,29,33]. In addition, $NPQ_{(T)}$was able to detect more variation within the plant genetic resources than other chlorophyll fluorescence measurements.

Drought stress has a significant negative impact on plant growth and development[34]. For the image derived traits Estimated Biovolume, plant height and Mean Color Value, there was a significant difference after 8 to 11 days of drought stress between the two treatments. This impact of drought stress was in line with previous results from chickpea and emphasized that the measurements of $NPQ_{(T)}$ and ΦPSII were made on drought-stressed chickpeas or in the recovery phase[8]. Besides the impact on Estimated Biovolume, plant height and Mean Color Value, drought stress significantly affected $NPQ_{(T)}$ and several yield traits such as hundred-seed-weight and seed weight.

Furthermore, the high correlation between hundred-seed-weight or seed weight and Estimated Biovolume throughout the study and especially on the last imaging day DAT 37 highlighted that Estimated Biovolume was a yield- relevant trait suitable to be implemented in pre-breeding. A comparable correlation was already observed in another HTP study with different chickpea genotypes[35].

In our study, Mean Color Value, which correlates with the chlorophyll content of various species such as *Arabidopsis*, tobacco and grapevine (*Vitis vinifera*), gave the impression of a darker green color of chickpeas under drought stress in line with our previous study and others[8,36–38]. The impression of green leaves under drought stress could be explained by a difference in the ratio of chlorophyll content and relative water, as has been investigated for chickpeas[39]. In addition, the color of the leaves could be explained by the formation of anthocyanin under stress conditions. Anthocyanins, which have a red to purple or blue color spectrum, are known to have protective properties under various stress conditions and are located between the and an increase in anthocyanin content has already been observed in a greenhouse experiment with drought stress in chickpeas[40,41].

In studies with lettuce (*Lactuca sativa* L.), rice (*Oryza sativa* L.) and chickpeas, ΦPSII decreased under drought stress[8,42,43]. In this experiment, ΦPSII did not decrease compared to the control treatment. ΦPSII is related to the light absorbed by the chlorophyll. When less light is absorbed by chlorophyll, ΦPSII is higher[44,45]. If anthocyanin has formed in drought stress, as indicated by the Mean Color Value and the red to green color ratio, anthocyanin increase the absorption and this may lead to a decrease the absorption by chlorophyll and thus the ΦPSII in this particular drought stress experiment did not decrease[46].

However, a tolerant chickpea cultivar was also found to maintain a stable ΦPSII under polyethylene glycol-induced drought stress, similar to our results[47].

This has already been documented in brassica, soybean and common bean (*Phaseolus vulgaris* L.), under abiotic stress[48–50]. Furthermore, the higher ΦPSII on the day of recovery of drought stress could be due to the reopening of the stomata which stimulates photosynthesis again as it has been observed in bread wheat[51].

Under drought stress, the average for $NPQ_{(T)}$ increased for the 60 genotypes. This was consistent with the results for NPQ from pot and field experiments with chickpea and mung bean (*Vigna radiata* L.) under drought stress[41,47,52].

$NPQ_{(T)}$ is a protective mechanism that releases excess energy in the form of heat to prevent photodamage[15]. Under these circumstances, the energy released by heat is no longer available for carbon assimilation. Comparing the difference of drought stress compared to the control treatment of Estimated Biovolume and $NPQ_{(T)}$ for the 60 genotypes, it was visible that genotypes with a low difference of Estimated Biovolume, i.e. more tolerant genotypes, show a small change for $NPQ_{(T)}$ under drought stress and a higher $NPQ_{(T)}$ in control treatment than drought-sensitive genotypes. In comparison, genotypes that were more sensitive to drought stress had lower $NPQ_{(T)}$ in control and tended to increase $NPQ_{(T)}$. When $NPQ_{(T)}$ was much higher in drought stress, the difference of drought stress compared to the control treatment for Estimated Biovolume was also higher, because the energy was not available for carbon assimilation. This was shown with the two types of chickpea. Similar results were documented in a pot experiment for chickpea based on two chickpea varieties[47]. The drought stress sensitive variety had a lower NPQ in the control than the drought stress tolerant variety, but a higher NPQ under drought stress than the tolerant variety.

In our study, we also found significant differences between the two types of chickpea *desi* and *kabuli*. Several studies in pot and field experiments showed that *desi* was more tolerant to drought stress than *kabuli*[7,9,53]. Proline is considered an osmoprotectant as it maintains the osmotic potential and thus the turgor of the leaves. In addition, free proline and sugar helps to stabilize macromolecules and prevents oxidative damage[7,53]. Higher levels of minerals in *desi* serve as cofactors in various osmoregulatory and antioxidant mechanisms and also contribute to drought stress tolerance[9].

In addition to a significant difference for Estimated Biovolume, we also found a significant difference for $NPQ_{(T)}$ between *desi* and *kabuli*. After recovery of drought stress, the two types no longer differed, but *desi* tended to have a lower difference of drought stress compared to the control treatment for hundred-seed-weight and seed weight than *kabuli*, although this difference was not significant. We have now shown that one reason for the better drought tolerance of *desi* could be the effective dissipation of excess excitation energy in the PSII efficiently measurable as $NPQ_{(T)}$.

Drought tolerance is a quantitative trait that affects yield from the time, duration, and severity of the plants in physiological and developmental processes up to yield. Similar to the work of Kromdijk et al.[22] in which the dynamic NPQ relaxation kinetics were measured in fluctuating light, the steady-state plasticity of $NPQ_{(T)}$ in drought stress was used here to investigate its relation with yield in challenging environments. In this context, NPQ is a protective mechanism of photosynthesis whose plasticity is reflected in carbon assimilation.

The advantage of $NPQ_{(T)}$ over NPQ is not only the measurement time. Environmental stresses can lead to an underestimation of F_m due to chloroplast movement or reflecting sustained qI[26]. In contrast, for $NPQ_{(T)}$ the F_m

is determined for unstressed plants and used for the calculation. Instead of NPQ, PSII maximum efficiency (F_v'/F_m') could be measured, since there is a non-linear coincidence[16]. However, this consistency can be inaccurate at higher NPQ values, as changes in F_v'/F_m' are indicative of the contribution of NPQ to F_q'/F_m'[16].

The present study of chickpea plant genetic resources showed how $NPQ_{(T)}$ can be successfully implemented for steady-state NPQ in High-throughput Phenotyping. We demonstrated this in a diverse plant genetic resources of chickpea, so the results are robust and valid for a wide range of genotypes. Significant differences in tolerance to drought stress could be identified between chickpeas, especially between the two types *desi* and *kabuli*, using $NPQ_{(T)}$ in combination with other image-derived and yield traits. As studies in tobacco and soybean have shown, the potential of accelerating recovery from photoprotection represents potential for enormous seed yield increases of 33% and dry matter productivity of 15%[21,22]. HTP studies with drought or other challenging environments could include $NPQ_{(T)}$ measurements to investigate the ability to restore the steady-state photoprotection of genotypes.

Material and methods

Plant material

Sixty selected genotypes of chickpea (*Cicer arietinum* L.) used in this study have been previously investigated in Lauterberg et al.[8] (Table S1). These 60 genotypes are selected from the T-CORE collection developed in INCREASE (Intelligent Collection of Food Legumes Genetic Resources for European Agrofood Systems)[54,55] and EMCAP (European and Mediterranean Chickpea Association Panel) projects[56]. Our set of analysed chickpea genotypes consisted of 30 *desi* and 30 *kabuli*.

High-throughput phenotyping (HTP) experiment

We employed the experimental setup of Lauterberg et al.[8] with modifications. The HTP system (LemnaTec-Scanalyzer 3D) used in the present study is installed in an environmentally controlled greenhouse at IPK Gatersleben (51°4902300 N, 11°1701300 E, altitude 112 m). In this HTP system, individual plants are analysed and transported in a carrier by conveyor belts to the imaging chambers. The imaging chambers are equipped with cameras for top and side view, respective for visual (Red, Green, Blue, RGB) and fluorescence imaging and a lifter which allows imaging from three different angles in side view. The balance-based watering station enabled controlled irrigation and thus defined drought stress settings.

The plant material was tested with two biological replicates per genotype and treatment. The sowing date of the experiment was the 7th of September and the last image was taken on the 28th of October 2022 on the HTP system (Table S17). Two seeds were sown in the pots and thinned out to one seedling per pot. Each pot (18.5 cm × 14.9 cm diameter) was filled with Substrate No.2 (Klasmann-Deilmann GmbH, Geeste, Germany). Plant establishment was performed for 14 days under greenhouse conditions at 24 °C day/20 °C night and a relative humidity of 67% day and 76% night. A daylight period of greenhouse lights of 15 h (from 6 am to 9 pm) and manual watering. The light intensity was 200 µmol photons m^{-2} s^{-}, and controlled with shading in the greenhouse or additional assimilation light. Fourteen days after sowing plants were transferred to the HTP system run at comparable growing conditions and treatment and imaging started on 15 days after sowing. During the transfer, 7 g of fertilizer with composition of 19% total nitrogen, 9% P_2O_5 and 10% K_2O was added and to each pot. In addition, a plant supporter was placed on each pot and each pot was placed into a tray so that the water was completely available for the plant. During the experiment, LemnaTec software was used to randomize the arrangement of the plants twice a week resulting in a fully randomized design. For the establishment phase of the first eight days plants were kept on a level of 65% plant available water. The plants for the control treatment were kept at this level throughout the experiment. For drought stress treatment, the irrigation level was successively lowered to 10% by withholding water (Tables S17, S7). From DAT 29 on, gradual re-watering took place, followed by irrigation to 65% plant available water content on DAT 30. Irrigation took place in two steps to allow plants to absorb all of the water. Information on daily watering based on weight before and after watering can be extracted with the HTP system software. The watering regime and simulation of drought stress were developed on this HTP system initially for barley and transferred to chickpea[8,31].

The imaging was on a daily basis and after the last imaging at DAT 37, the plants were moved from the HTP system to a regular greenhouse for the phase of maturation until harvest and to record yield traits. The number of pods, the number of empty pods and the number of seeds were scored manually for each pot with the individual plant. For quantification of weight of seeds and hundred-seed-weight MARViN, a machine for seed analysis (MARViNTECH, Wittenburg, Germany), was used. The difference of drought stress compared to the control treatment was calculated for the yield traits.

$$Difference\ of\ Trait[\%] = \left(1 - \frac{trait_{drought\ stress}}{trait_{control}}\right) \times 100 \quad (1)$$

Image-derived traits

The images were analysed using the IAP version 2.3.0 (IAP;[57]). The traits used in this study include Estimated Biovolume ([voxel]), plant height (PH; [mm]) and Mean Color Value ([hue]). The Estimated Biovolume was calculated from the images of the top view camera and the images of three side views:

$$Estimated\ Biovolume[voxel] = \sqrt{average\ pixel\ side\ area^2 * top\ area} \quad (2)$$

The plant height was based on side view imaging and the Mean Color Value on top view imaging. Mean Color Value referred to the HSV color space [hue] and provided insights in the composition of the detected color of the plant (Klukas et al., 2014). An Mean Color Value of 0.23 corresponded to a green plant, based on this model. The red to green color ratio indicated the proportion of red plant pixels divided by the number of green pixels in the HSV color space and was based on side view imaging[57]. The difference of drought stress compared to the control treatment was calculated using the above Eq. 1.

Chlorophyll fluorescence traits

As described in Lauterberg et al.[8], the HTP system was supplemented with a chlorophyll fluorescence camera (FluorCam; version 7) from Photon Systems Instruments (PSI; Brno, Czech Republic) to measure photosynthetic performance from the top view. The FluorCam data was analyzed using the manufacturer's software Plant Data Analyzer (version 3). When chlorophyll fluorescence measurements were performed, daily RGB imaging was performed before or after the chlorophyll fluorescence measurements.

A detailed timeline of the experiment is given in Table S17.

For the first part of the experiment, the method validation, the maximum quantum yield of photosystem II (F_v/F_m) was measured during the night from DAT 4 to 5 on plants that were adapted to darkness for at least 1 h (Table S17). Therefore, minimal fluorescence level (F_0) was determined by the application of a weak, pulsed measuring light (PAR ≤ 0.2 µmol s^{-1} m^{-2}), followed by a saturating light pulse (800 ms; PAR: 4000 µmol s^{-1} m^{-2}) to induce maximal fluorescence level (F_m), as described by Tschiersch et al.[14].

In the night from DAT 5 to 6, an experiment was carried out as a method-validation to demonstrate the correlation between NPQ and $NPQ_{(T)}$. NPQ was calculated based on the following equation:

$$NPQ = \left(\frac{F_m}{F'_m}\right) - 1 \tag{3}$$

$NPQ_{(T)}$ was calculated based on Tietz et al.[26]. In Tietz et al. (2017) the equation includes the assumption $F_v/F_m = 0.83$[24].

$$NPQ(T) = \left(\frac{\left(\frac{1}{\left(1-\left(\frac{Fv}{Fm}\right)\right)}\right) - 1}{\left(\frac{F'_m}{F'_0}\right) - 1}\right) - 1 = \left(\frac{4.88}{\left(\frac{F'_m}{F'_0}\right) - 1}\right) - 1 \tag{4}$$

In the calculation of $NPQ_{(T)}$, we have used $F_v/F_m = 0.856$, that was previously measured in this experiment.

To measure $NPQ_{(T)}$ a protocol with a duration of 5 min actinic illumination (PAR: 480 µmol s^{-1} m^{-2}) was used. At the beginning the F_m and F_0 level was measured as described above and at the end of the actinic light phase steady-state fluorescence yield, F_s, was recorded and the sample was exposed to a saturating light pulse to measure the maximal fluorescence yield under actinic illumination F_m'. After the subsequent exposure of far-red light for 5 s, F_0' was measured. Far-red light with a peak at 733 nm was applied to oxidize the plastoquinone A (Q_A) and the plastoquinone pool.

For the second part of the experiment, the method-implementation, $NPQ_{(T)}$ and the operating efficiency of photosystem II (ΦPSII)

$$\Phi\text{PSII} = \frac{(F'_m - F_s)}{F'_m} \tag{5}$$

were measured for all 60 genotypes and drought stress with subsequent recovery. The plants were light acclimated in the plant adaptation tunnel for at least 5 min according to Tschiersch et al.[14] followed by 60 s illumination (PAR 480 µmol photons m^{-2} s^{-1}) after moving into the chlorophyll fluorescence imaging chamber. Finally, maximum F_m' was measured during 800 ms exposure to a saturating light flash (PAR: 4000 µmol photons m^{-2} s^{-1}) and F_0' was recorded after a subsequent illumination with far-red light for 5 s.

These measurements of $NPQ_{(T)}$ and ΦPSII took place during the day with light-adapted plants on DAT 16 (8 days of drought stress), DAT 22 (14 days of drought stress), DAT 29 (first day of recovery) and DAT 37 (8 days of recovery). The difference of drought stress compared to the control treatment was calculated using the above formula.

Statistics

The Estimated Biovolume has been downscaled by a factor of 10^{-5} and values for red to green color ratio greater than 1.25 were removed. For statistical analysis, R studio version 4.1.2 was used. For the interpolation of the image-derived traits the package "zoo" and the spline interpolation were used. The package "ASRemL" was used to calculate the outlier within the experiment, the repeatability, and the best linear unbiased estimators (BLUEs) within the experiment. We use the following model to remove outliers and use the same model to estimate BLUEs across environments:

$$Trait \sim Genotype + Rep + residual, \tag{6}$$

while "*Genotype*" is the effect of genotype, "*Rep*" is the effect of biological replicates. For BLUE estimation and outlier detection, the genotype is set as a fixed effect, and the rest are all random effects. The outlier detection

test was performed following the method M4 as described by Bernal-Vasquez et al.[58], where the standardized residuals are used in combination with the Bonferroni-Holm test to identify an outlier.

Furthermore, the repeatability has been calculated use the same model but set genotype also as random:

$$Repeatability = \frac{\sigma_G^2}{\sigma_G^2 + \frac{\sigma_e^2}{N_{Rep}}} \quad (7)$$

With σ_G^2 is the genotypic variance, σ_e^2 is the error variance and N_{Rep}, number of biological replicates. All correlations were Pearson correlations and were calculated using the "rstatix" package with the associated *p*-values. The coefficient of variation has been calculated by the ratio of σ to μ. ANOVA followed by Tukey`s test was performed to calculate the significance levels for a series of measurements such as ΦPSII and $NPQ_{(T)}$.

Data availability

The datasets used and analysed during the current study available from the corresponding author on reasonable request.

Received: 5 February 2024; Accepted: 27 May 2024
Published online: 17 June 2024

References

1. Ahmad, F., Gaur, P. M. & Croser, J. S. Chickpea (*Cicer arietinum* L.). In *Genetic resources, chromosome engineering, and crop improvement—Grain legumes* vol. 1, 187–217 (Taylor & Francis Group, 2005).
2. Merga, B. & Haji, J. Economic importance of chickpea: Production, value, and world trade. *Cogent Food Agric.* **5**, 1–12 (2019).
3. Grillakis, M. G. Increase in severe and extreme soil moisture droughts for Europe under climate change. *Sci. Total Environ.* **660**, 1245–1255 (2019).
4. Gowda, C. L. L., Upadhyaya, H. D., Sharma, S., Varshney, R. K. & Dwivedi, S. L. Exploiting genomic resources for efficient conservation and use of chickpea, groundnut, and pigeonpea collections for crop improvement. *Plant Genome* **6**, 1–11 (2013).
5. Varshney, R. K. *et al.* Fast-track introgression of "QTL-hotspot" for root traits and other drought tolerance traits in JG 11, an Elite and leading variety of chickpea. *Plant Genome* **6**, 1–9 (2013).
6. van der Maesen, L. J. G. Origin, history and taxonomy of Chickpea. In *The chickpea* 11–34 (C.A.B. International, 1987).
7. Farooq, M. A., Ullah, A., Lee, D.-J. & Alghamdi, S. S. Desi chickpea genotypes tolerate drought stress better than kabuli types by modulating germination metabolism, trehalose accumulation, and carbon assimilation. *Plant Physiol. Biochem.* **126**, 47–54 (2018).
8. Lauterberg, M., Tschiersch, H., Papa, R., Bitocchi, E. & Neumann, K. Engaging precision phenotyping to scrutinize vegetative drought tolerance and recovery in chickpea plant genetic resources. *Plants* **12**, 2866 (2023).
9. Medeiros, J. S., Nunes Da Silva, M., Carvalho, S. M. P., Santos, C. S. & Vasconcelos, M. W. Low water supply differentially affects the growth, yield and mineral profile of kabuli and desi chickpeas (Cicer arietinum). *Ann. Appl. Biol.* https://doi.org/10.1111/aab.12835 (2023).
10. Purushothaman, R., Upadhyaya, H. D., Gaur, P. M., Gowda, C. L. L. & Krishnamurthy, L. Kabuli and desi chickpeas differ in their requirement for reproductive duration. *Field Crops Res.* **163**, 24–31 (2014).
11. Humplík, J. F. *et al.* Automated integrative high-throughput phenotyping of plant shoots: A case study of the cold-tolerance of pea (*Pisum sativum* L.). *Plant Methods* **11**, 1–11 (2015).
12. Neumann, K. *et al.* Genetic architecture and temporal patterns of biomass accumulation in spring barley revealed by image analysis. *BMC Plant Biol.* **17**, 1–12 (2017).
13. Shi, R., Seiler, C., Knoch, D., Junker, A. & Altmann, T. Integrated phenotyping of root and shoot growth dynamics in maize reveals specific interaction patterns in inbreds and hybrids and in response to drought. *Front. Plant Sci.* **14**, 1–16 (2023).
14. Tschiersch, H., Junker, A., Meyer, R. C. & Altmann, T. Establishment of integrated protocols for automated high throughput kinetic chlorophyll fluorescence analyses. *Plant Methods* **13**, 1–16 (2017).
15. Müller, P., Li, X.-P. & Niyogi, K. K. Non-photochemical quenching. A response to excess light energy. *Plant Physiol.* **125**, 1558–1566 (2001).
16. Murchie, E. H. & Lawson, T. Chlorophyll fluorescence analysis: A guide to good practice and understanding some new applications. *J. Exp. Bot.* **64**, 3983–3998 (2013).
17. Chen, W. *et al.* Purple stem Brassica napus exhibits higher photosynthetic efficiency, antioxidant potential and anthocyanin biosynthesis related genes expression against drought stress. *Front. Plant Sci.* **13**, 1–16 (2022).
18. Punchkhon, C. *et al.* Role of LOC_Os01g68450, containing DUF2358, in salt tolerance is mediated via adaptation of absorbed light energy dissipation. *Plants* **11**, 1–15 (2022).
19. Zhu, X., Ort, D. R., Whitmarsh, J. & Long, S. P. The slow reversibility of photosystem II thermal energy dissipation on transfer from high to low light may cause large losses in carbon gain by crop canopies: A theoretical analysis. *J. Exp. Bot.* **55**, 1167–1175 (2004).
20. Retkute, R. *et al.* Exploiting heterogeneous environments: Does photosynthetic acclimation optimize carbon gain in fluctuating light?. *J. Exp. Bot.* **66**, 2437–2447 (2015).
21. De Souza, A. P. *et al.* Soybean photosynthesis and crop yield are improved by accelerating recovery from photoprotection. *Science* **377**, 851–854 (2022).
22. Kromdijk, J. *et al.* Improving photosynthesis and crop productivity by accelerating recovery from photoprotection. *Science* **354**, 857–861 (2016).
23. Baker, N. R. Chlorophyll fluorescence: A probe of photosynthesis in vivo. *Annu. Rev. Plant Biol.* **59**, 89–113 (2008).
24. Björkmann, O. & Demming, B. Photon yield of 0 2 evolution and chlorophyll fluorescence characteristics at 77 K among vascular plants of diverse origins. *Planta* **170**, 489–504 (1987).
25. Long, S. P. *et al.* Into the shadows and back into sunlight: Photosynthesis in fluctuating light. *Annu. Rev. Plant Biol.* **73**, 617–648 (2022).
26. Tietz, S., Hall, C. C., Cruz, J. A. & Kramer, D. M. NPQ(T): A chlorophyll fluorescence parameter for rapid estimation and imaging of non-photochemical quenching of excitons in photosystem-II-associated antenna complexes: New, rapid probe of non-photochemical quenching. *Plant Cell Environ.* **40**, 1243–1255 (2017).
27. Diner, B. A. Dependence of the deactivation reactions of photosystem II on the redox state of plastoquinone pool a varied under anaerobic conditions. Equilibria on the acceptor side of photosystem II. *Biochim. Biophys. Acta BBA Bioenerg.* **460**, 247–258 (1977).
28. Epaku, G. T. *et al.* Stay green physiological capacity of drought tolerant maize inbred lines. *Afr. Crop Sci. J.* **29**, 309–323 (2021).

29. Hussain, M. A. *et al.* Comparative analysis of physiological variations and genetic architecture for cold stress response in soybean germplasm. *Front. Plant Sci.* **13**, 1–20 (2023).
30. Kuhlgert, S. *et al.* MultispeQ Beta: a tool for large-scale plant phenotyping connected to the open PhotosynQ network. *R. Soc. Open Sci.* **3**, 1–17 (2016).
31. Dhanagond, S. *et al.* Non-invasive phenotyping reveals genomic regions involved in pre-anthesis drought tolerance and recovery in spring barley. *Front. Plant Sci.* **10**, 1–21 (2019).
32. Lauterberg, M. *et al.* Precision phenotyping across the life cycle to validate and decipher drought-adaptive QTLs of wild emmer wheat (Triticum turgidum ssp. dicoccoides) introduced into elite wheat varieties. *Front. Plant Sci.* **13**, 965287 (2022).
33. Shamim, M. J., Kaga, A., Tanaka, Y., Yamatani, H. & Shiraiwa, T. Analysis of physiological variations and genetic architecture for photosynthetic capacity of Japanese Soybean Germplasm. *Front. Plant Sci.* **13**, 1–13 (2022).
34. Rani, A. *et al.* Developing climate-resilient chickpea involving physiological and molecular approaches with a focus on temperature and drought stresses. *Front. Plant Sci.* **10**, 1–29 (2020).
35. Atieno, J. *et al.* Exploring genetic variation for salinity tolerance in chickpea using image-based phenotyping. *Sci. Rep.* **7**, 1–11 (2017).
36. Faragó, D., Sass, L., Valkai, I., Andrási, N. & Szabados, L. PlantSize offers an affordable, non-destructive method to measure plant size and color in vitro. *Front. Plant Sci.* **9**, 1–12 (2018).
37. Liang, Y. *et al.* A nondestructive method to estimate the chlorophyll content of Arabidopsis seedlings. *Plant Methods* **13**, 26 (2017).
38. Majer, P., Sass, L., Horváth, G. V. & Hideg, É. Leaf hue measurements offer a fast, high-throughput initial screening of photosynthesis in leaves. *J. Plant Physiol.* **167**, 74–76 (2010).
39. Das, A. *et al.* Transgenic chickpea (*Cicer arietinum* L.) harbouring AtDREB1a are physiologically better adapted to water deficit. *BMC Plant Biol.* **21**, 1–17 (2021).
40. Gould, K. S. Nature's swiss army knife: The diverse protective roles of Anthocyanins in leaves. *J. Biomed. Biotechnol.* **2004**, 314–320 (2004).
41. Macar, K. T. & Ekmekçi, Y. PSII photochemistry and antioxidant responses of a chickpea variety exposed to drought. *Z. Für Naturforschung C* **63**, 583–594 (2008).
42. Amitrano, C., Junker, A., D'Agostino, N., De Pascale, S. & De Micco, V. Integration of high-throughput phenotyping with anatomical traits of leaves to help understanding lettuce acclimation to a changing environment. *Planta* **256**, 1–19 (2022).
43. Khan, F., Upreti, P., Singh, R., Shukla, P. K. & Shirke, P. A. Physiological performance of two contrasting rice varieties under water stress. *Physiol. Mol. Biol. Plants* **23**, 85–97 (2017).
44. Habash, D. Z., Genty, B. & Baker, N. R. The consequences of chlorophyll deficiency for photosynthetic light use efficiency in a single nuclear gene mutation of cowpea. *Photosynth. Res.* **42**, 17–25 (1994).
45. Harbinson, J., Genty, B. & Baker, N. R. Relationship between the quantum efficiencies of photosystems I and 11 in Pea leaves. *Plant Physiol.* **90**, 1029–1034 (1989).
46. Gould, K. S., Vogelmann, T. C., Han, T. & Clearwater, M. J. Profiles of photosynthesis within red and green leaves of Quintinia serrata. *Physiol. Plant.* **116**, 127–133 (2002).
47. Saglam, A., Terzi, R. & Demiralay, M. Effect of polyethylene glycol induced drought stress on photosynthesis in two chickpea genotypes with different drought tolerance. *Acta Biol. Hung.* **65**, 178–188 (2014).
48. Lizana, C. *et al.* Differential adaptation of two varieties of common bean to abiotic stress. *J. Exp. Bot.* **57**, 685–697 (2006).
49. Mushtaq, M. A. *et al.* Comparative leaves transcriptome analysis emphasizing on accumulation of anthocyanins in Brassica: Molecular regulation and potential interaction with photosynthesis. *Front. Plant Sci.* **7**, 1–15 (2016).
50. Park, S. J. *et al.* Response of leaf pigment and Chlorophyll fluorescence to light quality in soybean (Glycine max Merr. var Seoritae). *Korean J. Soil Sci. Fertil.* **43**, 400–406 (2010).
51. Mu, Q. *et al.* Photosynthesis of winter wheat effectively reflected multiple physiological responses under short-term drought–rewatering conditions. *J. Sci. Food Agric.* **102**, 2472–2483 (2022).
52. Bano, H., Athar, H., Zafar, Z. U., Ogbaga, C. C. & Ashraf, M. Peroxidase activity and operation of photo-protective component of NPQ play key roles in drought tolerance of mung bean [Vigna radiata (L.) Wilcziek]. *Physiol. Plant.* **172**, 603–614 (2021).
53. Nisa, Z. U. *et al.* A comparative metabolomic study on desi and kabuli chickpea (*Cicer arietinum* L.) genotypes under rainfed and irrigated field conditions. *Sci. Rep.* **10**, 13919 (2020).
54. Bellucci, E. *et al.* The INCREASE project: Intelligent collections of food-legume genetic resources for European agrofood systems. *Plant J.* **108**, 646–660 (2021).
55. Rocchetti, L. *et al.* Towards the development, maintenance and standardized phenotypic characterization of single-seed-descent genetic resources for chickpea. *Curr. Protoc.* **2**, 1–16 (2022).
56. Rocchetti, L. *et al.* The development of a European and Mediterranean Chickpea Association Panel (EMCAP). *Agronomy* **10**, 1417 (2020).
57. Klukas, C., Chen, D. & Pape, J.-M. Integrated analysis platform: An open-source information system for high-throughput plant phenotyping. *Plant Physiol.* **165**, 506–518 (2014).
58. Bernal-Vasquez, A.-M., Utz, H.-P. & Piepho, H.-P. Outlier detection methods for generalized lattices: A case study on the transition from ANOVA to REML. *Theor. Appl. Genet.* **129**, 787–804 (2016).

Acknowledgements
Klara Panzarova (PSI), Jens Bauernfeind (IPK Gatersleben) for supporting the image analysis, Annett Berge, Ute Krajewski, and the gardener team of Kathrin Gramel-Koch.

Author contributions
M.L. and H.T. conceived ideas and designed methodology; I.M., M.L. and H.T. collected data; M.L. and Y.Z. analysed data; M.L., H.T. and M.K. led writing of the manuscript. All authors contributed critically to drafts and gave final approval for publication.

Funding
Open Access funding enabled and organized by Projekt DEAL. This work was conducted as part of the STARGATE project funded by the European Union's Horizon 2020 research and innovation program under grant agreement No. 952339 and as part of the INCREASE project funded by the European Union's Horizon 2020 research and innovation program under grant agreement No. 862862.

Competing interests
The authors declare no competing interests.

Additional information

Supplementary Information The online version contains supplementary material available at https://doi.org/10.1038/s41598-024-63372-6.

Correspondence and requests for materials should be addressed to K.N.

Reprints and permissions information is available at www.nature.com/reprints.

Publisher's note Springer Nature remains neutral with regard to jurisdictional claims in published maps and institutional affiliations.

3. General Discussion

3.1 Can we use High-throughput Phenotyping for breeding drought tolerant crops?

The global mean temperature is increasing in the coming decades. This rise in temperature will have a strong impact on agricultural production. For example, a loss of 6 % in wheat yield is expected for each degree of global warming (Asseng et al., 2015). There are greater uncertainties regarding the precipitation in future than for the forecasted temperature change (Shiogama et al., 2022). Drought events are becoming more frequent and more severe, especially in southern Europe (Grillakis, 2019; Spinoni et al., 2018). To counteract the yield losses caused by the abiotic stress of drought stress, there is a need to breed cultivars that are drought tolerant and can ensure a realization of yield potential.

Genetic variance is required for breeding (Becker, 2019). PGR can bring such genetic variance and can be used for improving plant breeding (Hoisington et al., 1999; Zamir, 2001). The availability of low-cost genotypic data can facilitate the accessibility of genbank material (Schulthess et al., 2022). However, phenotypic evaluation remains time-consuming and cost-intensive.

HTP is proposed to overcome the phenotyping bottleneck (Furbank & Tester, 2011). HTP can take place at different scales. For example, as a screening for powdery mildew infection (Hinterberger et al., 2022), in field experiments (Kirchgessner et al., 2017) or in a controlled greenhouse (Lauterberg et al., 2022, 2023). In the greenhouse in particular, environment scenarios such as salinity, cold stress or fluctuating light, can be simulated in a targeted manner and phenotypic data of the PGRs or diverse genotypes can be recorded (Atieno et al., 2017; Humplík et al., 2015; Meyer et al., 2023). Drought stress and subsequent re-watering, as it occurs in nature, can be specifically simulated by irrigating individual pots with one plant each (Dhanagond et al., 2019). In a controlled scenario, the wilting point or the relative growth rate can be used as an indicator of drought stress. (Dhanagond et al., 2019; Lauterberg et al., 2023). Drought stress is reflected in various traits of plant growth and physiology (Varshney et al., 2021). Most important is the maintenance of biomass and yield under drought stress a coefficient of correlation of r=0.92 between biomass and grain yield was measured for wheat (Lauterberg et al., 2022). This emphasizes the relevance of analyzing PGRs in terms of biomass (Lauterberg et al., 2022). Additionally to biomass, color values and color ratios, HTP can capture photosynthesis by measuring chlorophyll fluorescence (Lauterberg et al., 2022, 2023, 2024). In greenhouse experiments, 60 genotypes of chickpea were analyzed with HTP (Lauterberg et al., 2023). Between these genotypes, significant differences in the maintenance of biomass could be recognized and superior genotypes identified. Data sets over 42 days and with high heritabilities could be created. For biomass, the heritability in drought stress was 0.81 and in control 0.56. Heritabilities around 0.7 could also be calculated for the color change, described by the mean color value of the plant. Similarly, for the ΦPSII a heritability of 0.7 was calculated. For the estimated biovolume, a coefficient of variation about 20% was calculated under drought stress among the 60 genotypes. These genotypes of PGR could be identified in two experiments with specific environmental conditions and show traits with a high heritability.

Heritability is noted in the breeder's equation:

$R=i*h*\sigma G$

R = Expected response to selection
i = intensity of selection
h = root of heritability
σG = root of genotypic variance

In breeding, genetic variability and time are crucial (Becker, 2019). HTP has a time advantage because the desired environmental conditions can be specifically simulated in the greenhouse. Genetic variability has been narrowed down (Van De Wouw et al., 2010). With the description of PGR and genetic data, the genetic variability in breeding should be expanded. Here, HTP can close the gap in time-consuming phenotyping (Rebetzke et al., 2019). Taking these factors into account, HTP offers potential for breeding.

However, working with PGRs can be challenging. PGRs can be relatives of the same species/ genus as, for example, *Triticum*. Genotypes of wild emmer (*T. diccocoides*) were tested in Israel with two contrasting water regimes and selected for their drought stress tolerance based on dry matter productivity. The selected genotypes G18-16 has been crossed with the cultivar Langdon (T. *turgidum* ssp. *durum*) to generate 152 Recombinant Inbred Lines (RIL), with single seed descent method to F6 generation (Peleg et al., 2008). Linkage analysis has been done with 307 microsatellite and Diversity Arrays Technologie marker (DArT) with an average distance of 7.5 cM between adjacent markers. With this RIL population and linkage map, a QTL for grain yield and harvest index and another QTL for total and spike dry matter under drought have been identified with DArT markers on chromosome 2B and chromosome 7A, respectively (Peleg et al., 2009).

These beneficial QTLs could be valuable for breeding, but using the genotype G18-16 of *T.diccocoides* or the RIL is both not suitable for agriculture production. *T. dicoccoides* is an undomesticated wheat species and brings some drawbacks, such as brittle rachis, described as “linkage drag” (Feuillet et al., 2008). The QTLs can be introgressed into elite material engaging marker-assisted back crossing by developing Near-isogenic Lines (NIL) (Merchuk-Ovnat, Barak, et al., 2016; Merchuk-Ovnat, Fahima, et al., 2016). The NIL, which are derived from three cycles of backcrossing and four cycles of selfing (BC_3F_4) and BCF_5, were investigated in two field experiments showed better drought tolerance for grain yield and biomass. Especially the QTL on chromosome 7A in the cultivar BarNir (NIL-B-7A-2) was superior. To further dissect the NIL, a HTP greenhouse experiment was conducted, mimicking the growth conditions in Israel (Lauterberg et al., 2022). The experiment took place across the entire life cycle and the effects established in field experiments could have been confirmed in a greenhouse pot experiment by HTP. The NIL-B-7A-2 was again superior, under drought stress and under control treatment. This circumstances could be explained, as the material has been used to develop new and finer linkage map using genotypic data of 15K iSelect marker with 12,908 SNPs (Deblieck et al., 2020). It can be seen, that nearby the introgressed QTL on chromosome 7A of G18-16, which was done with DArT markers, genetic material of the parent Langdon of the Recombinant inbred Line 12 was remaining. This could be one reason for the superior performance of NIL-B-7A-2, and further analysis such as sequencing would give the clear answer.

Using HTP and the image-derived trait, the formation of the higher thousand kernel weight could have been observed (Lauterberg et al., 2022). Due to the significantly longer green color of NIL-B-7A-2, indicated by the image-derived mean color value, during the final stage of ripening, the stay-green effect was identified (Rebetzke et al., 2016). Because of this delayed senescence, grain filling was still going on and resulted in a higher thousand kernel weight (Thomas & Ougham, 2014). This effect could be due to changes in hormone metabolism and chlorophyll degradation, as indicated by the SGR1 gene in Arabidopsis (Ren et al., 2010).

A promising application of HTP could be in pre-breeding to increase the genetic variance of highly heritable traits such as biomass. The intensity of selection for certain growth conditions can improve breeding in early generations. As described as an example, drought tolerance can be further dissected into a spatio-temporal level with HTP and complemented by chlorophyll fluorescence and imaging color traits.

3.2 How can HTP be involved to adapt chickpea to different cultivation areas?

Adaptation is becoming increasingly important in view of the impacts of environmental changes on agricultural production. Adaptation is multifactorial; in addition to climate and soil, the factors include biotic and abiotic factors.

When adapting crops to different cultivation areas, the flowering time, the shift from the vegetative to generative phase, is essential (Jung & Müller, 2009). For flowering time, day length, temperature and stress are the main factors. There are crops, such as winter wheat, that require vernalization to switch to generative phase. Chickpea are predominantly undetermined and do not require vernalization.

Adaptation to the different duration, intensity and timing of drought stress is necessary, as drought stress is one of the major challenges and a crucial factor for yield losses worldwide. Physiological adaptations to drought stress are the improvement of water uptake, the limitation of water loss or osmotic adaptation (Varshney et al., 2021). NIL of wheat, carrying a QTL originating from *T. diccocoides*, showed higher thousand kernel weight and estimated biovolume, with a higher water use efficiency (WUE) based on a pot greenhouse experiment (Lauterberg et al., 2022). In addition, the same NIL were tested in root tubes under well-watered condition and in a seedling 'cigar-role' experiments, meaning in wet paper, under well-watered and water-limited conditions (Merchuk-Ovnat et al., 2017). The NIL showed a higher root tip number under drought stress and a higher dry matter of root for 40 – 100cm.

Osmotic adaptation refers to the adjustment of osmolytes. Proline and sugars are known osmoprotectant, as they maintain the osmotic potential, stabilize macromolecules and prevent oxidative damage (Farooq et al., 2018; Nisa et al., 2020). In a field experiment with 44 chickpea genotypes, it was found that the more drought tolerant genotypes had higher osmolytes (Nisa et al., 2020).

Chickpea cultivars, that are adapted to drought stress are needed for the cultivation in the Mediterranean region, as there is an extremely variable precipitation (Duarte, 2022; Shiogama et al., 2022). So far, chickpea production has been concentrated in India and Australia (FAOSTAT, 2024). In

traditional growing areas such as South Asia, chickpeas are planted after the monsoon or grow with the residual moisture in the soil. Drought stress in the terminal growth phase is most common, and research has focused on this (Berger et al., 2020; Krishnamurthy et al., 2010; Pang et al., 2016; Pappula-Reddy et al., 2024).

In the Mediterranean area, chickpeas can be planted in autumn or spring, with chickpeas sown in winter having a higher yield than those sown in spring (Duarte, 2022; Zaiter & Barakat, 1995).

When sown in late autumn, the climate is more favorable with sufficient precipitation and less heat, which leads to more flowers and more pods and therefore higher yields. The plants are also taller, which makes harvesting easier. A disadvantage, however, is the risk of infection with the fungal disease *Ascochyta blight*, which is the main pathogen of chickpeas (Bretag et al., 2008; Fanning et al., 2022). Three-years of multi-location-field experiments in southern Australia have shown, that the yield loss of partially resistant cultivars is 64% and in susceptible cultivars up to 96% without the use of fungicide.

Sowing in spring, means a lower soil moisture that comes along with poor stand establishment and germination (Duarte, 2022; Duarte et al., 2023). During flowering and pod formation, the chickpeas are likely to be exposed to drought stress, so that development is interrupted and yield losses are to be expected.

Adapting chickpea to drought stress during vegetative stress would give a higher yield potential for chickpeas sown in spring and avoid seasons with higher risk of *Ascochyta blight*.

When adapting to drought stress, it is common to consider the maintenance of biomass production or crop yield (Varshney et al., 2021). In addition, there was a high correlation of 0.6 to 0.7 between estimated biovolume, which is a proxy for biomass, and hundred seed yield recorded for chickpeas grown in pots in the greenhouse, which underlines the relevance of screening for biomass (Lauterberg et al., 2024). Similar to this, in field experiments over three years, a correlation of grain yield and dry matter production of 0.6 has been recorded for chickpea (López-Bellido et al., 2008). The heritability for estimated biovolume was between 0.55 and 0.8, that has been measured in greenhouse pot experiments under drought stress and under salinity (Atieno et al., 2021; Lauterberg et al., 2023).

Genetic variation is key for adaptation and HTP provides an option to give access to PGR to search specifically for potential material. 60 diverse genotypes of chickpea PGR have been screened under drought stress and well-watered condition during vegetative growth using HTP (Lauterberg et al., 2023). Traits such as estimated biovolume, plant height, color values and the ΦPSII have been investigated. The relative growth reduced with prolonged drought stress from 1 voxel per day to -1.3 voxel per day and drought stress was initiated 21 until 42 days after sowing. With this drought stress scenario, a reduction of 72-82 % of estimated biovolume was obtained and has also been reflected in the image-derived mean color value with 16-28% change. For the estimated biovolume, a coefficient of variation about 20% was calculated under drought stress for the diverse genotypes. For the image-derived color ratios red to green and yellow to green similar coefficient of variation have been calculated, giving a high phenotypic variation, captured by HTP. Furthermore, using chlorophyll fluorescence, the theoretical NPQ has been investigated and a coefficient of variation of 10.5% after 14 days of drought stress (Lauterberg et al., 2024).

In order to create an adaptation potential to drought stress during the vegetative growth, the recovery during re-watering also plays a role. After re-watering, growth is clearly reflected in the relative growth rate and the estimated biovolume. And the coefficient of variation of up to 28% reflects that there is a higher variation in the recovery than in the drought tolerance. The recovery is reflected in the mean color value. Here the chickpeas achieve the color of the control plants. It can also be seen that the ΦPSII reached the level of the control plants.

The genotypes that show good drought tolerance, i.e. low biomass losses, can now be selected for adaptation. Superior genotypes could be identified via water use efficiency, biomass maintenance in the drought phase and biomass maintenance in the recovery phase (Lauterberg et al., 2023).

There are two types of chickpea: *desi* and *kabuli*. It has been described based on several field and greenhouse experiments, that *desi* is more tolerant to drought stress than *kabuli*. The better tolerance to drought stress is partly because of the osmolytes or metabolomics such as proline and sugars as well as a higher mineral content (Farooq et al., 2018; Medeiros et al., 2023; Nisa et al., 2020). Furthermore, the drought tolerance is set in a better photosynthetic performance. Described in the ΦPSII and by the advantageous plasticity of theoretical non-photochemical quenching ($NPQ_{(T)}$)under drought stress (Lauterberg et al., 2023, 2024).

To further proceed towards adaptation, the QTL for drought tolerance have to be localized. Therefore, mapping or genome-wide association studies are necessary. It would also be possible to work with a larger population of about 200 genotypes and carry out a genome-wide association study with genotypic data to identify QTLs, as has already been done using HTP for barley for drought stress and well-watered conditions (Dhanagond et al., 2019; Neumann et al., 2017).

Creating a mapping population of Recombinant Inbred Lines by crossing a drought tolerant with a drought sensitive line, has been done for chickpea with Indian breeding material and Lebanese landrace (Varshney et al., 2014). A “QTL-hotspot” on chromosome 4, explaining 58% of the phenotypic variation, has been identified and located with seven simple sequence repeat (SSR) markers. The lines have been genotyped in more depth with genotyping-by-sequencing and with this fine-mapping, 49 SNPs integrated in the “QTL-hotspot” region, covering 14cM, were converted into cleaved amplified polymorphic sequences (Jaganathan et al., 2015). In further analysis 12 genes were identified, being involved in the drought tolerance and with RT-qPCR some were differentially expressed in the founder lines. For gene CA_04567 membrane proteins which is relevant for or ABA regulation, the expression in the drought tolerant founder line ICC 4958 from India was higher (Kale et al., 2015).

In addition, a QTL originating from the described RIL population was introgressed into an elite cultivar of chickpea (Varshney, Gaur, et al., 2013). Three SSR markers were selected for foreground selection and the AFLP markers for background selection. This resulted in BC_3F_2 Introgression lines, which showed an improved root system architecture and in multilocation trails, better drought tolerance.

Besides marker-assisted backcrossing and marker assisted selection, targeted introgression with *Agrobacterium tumefaciens* or with CRISPR/Cas are options. The tolerance to *Helicoverpa armigera* has been improved with *A. tumefaciens* and CRISPR/Cas has been applied to improve drought tolerance (Badhan et al., 2021; Indurker et al., 2010).

In summary, the process of using HTP for crop adaptation has been described and it can be useful to identify tolerant genotypes which could be used for further dissection with mapping populations, QTL analysis and gene expression analysis.

3.3 Do HTP pot experiments and field experiments contradict or complement each other?

Researchers perform experiments to determine the phenotype. The phenotype results from the genotypes and the environmental factors. There are several environmental factors of which light quantity, light quality, CO_2 concentration, nutrients, air humidity, water, temperature and salinity are the most important ones (Massonnet et al., 2010). Under the assumption of the equation P = G + E, the same phenotype will result if a genotype has been exposed to the same environmental factors. However, reproducing phenotypes is and remains a challenge.

The advantage of field experiments is that plants grow in their habitat, under natural growing conditions for soil, temperature, light and water (Poorter, Fiorani, et al., 2012). In addition to strong dynamics of abiotic factors, there are also extreme events such as drought stress or hail and biotic factors such as pest infestation. The disadvantage is that these conditions cannot be influenced under any circumstances.

Alternatively, experiments will be carried out under controlled conditions in the laboratory or greenhouse. To investigate the differences between field and greenhouse experiments, a meta-analysis based on more than 19,800 mean values from 1,540 publications and over 4,680 species, of which 550 species were tested in the field and in the greenhouse, was carried out (Poorter et al., 2016). This showed that the environmental factors under controlled conditions differ from the conditions in the field, particularly with regard to light intensity, temperature, rooting volume and plant density. Choosing the right pot size is important for the rooting volume (Poorter, Bühler, et al., 2012). A meta- analysis based on 65 studies was conducted (Poorter, Bühler, et al., 2012). It was found that doubling the pot size increased biomass production by 43 %. Pots that are too small caused less root growth and led to restrictions in net photosynthesis. In addition, the temperature of the soil in a pot is clearly higher than in the field.

In order to analyze the reproducibility of leaf growth, three *A. thaliana* genotypes were tested in 10 laboratories (Massonnet et al., 2010). To set a certain standard, the pots, soil substrate and nutrient solution were provided centrally for all laboratories. When analyzing the growth, up to 8-fold changes in leaf growth were observed. The challenge is therefore to describe, monitor and precisely control the environmental conditions (Massonnet et al., 2010). However, there are also factors that are almost impossible to simulate in the laboratory and these include plant density. Not only are the plants competing for light, via plant density, but phytochrome signals were also transmitted for the orientation of growth of the plants (De Wit et al., 2012).

HTP systems were designed to facilitate non-destructive phenotyping in the field and in the greenhouse. UAV or stationary systems can be used in the field (Z. Khan et al., 2018; Kirchgessner et al., 2017). Furthermore, HTP in the greenhouse can be used to validate and to further decipher phenotypic traits, recorded in the field (Lauterberg et al., 2022). Numerous NIL were tested in field

experiments with two different irrigation regimes (Merchuk-Ovnat, Barak, et al., 2016; Merchuk-Ovnat et al., 2017; Merchuk-Ovnat, Fahima, et al., 2016). There were four cultivars and derived NIL, each containing one of two described QTLs from *T. diccocoides.* One QTL was associated with higher total and spike dry matter under drought stress and the other QTL to higher grain yield and harvest index (Merchuk-Ovnat, Barak, et al., 2016). Based on these experiments, the most promising lines were selected to further decipher and understand the beneficial effect of the QTLs in an HTP greenhouse experiment.

The performance of the NIL was compared with the performance of the recurrent parent in the field and greenhouse. The most consistent results across the field and greenhouse experiment were obtained for harvest index and osmotic potential. For NIL-B-7A-2 and the recurrent elite parent BarNir, a comparable phenotype was observed in the field and in the greenhouse for culm length, thousand-kernel weight, flowering time and plant biomass. The difference between the NIL-B and the recurrent partent BarNir was greater in the greenhouse than in the field for plant biomass and culm length. This could be due to the ΦPSII or the difference in temperature between field and greenhouse, as this effect was described on the basis of a meta-analysis (Poorter et al., 2016). A difference in temperature has a greater impact than light on biomass formation. The maximum temperatures of over 40 °C, which were measured in the field experiment, was technically challenging. The temperature in the greenhouse was closer to the optimum growth temperature for wheat than 40 °C and at a lower light intensity than in the field, so growth was limited by the source, by lower light intensity (Körner, 2015; Poorter et al., 2013). In the field it is the opposite, usually the temperature is not optimal for growth and with a high light intensity this leads to sink limitation.

Additionally, the spatio-temporal effect of the lines was investigated. As mentioned above, the stay-green effect was identified for NIL-B-7A-2 (Lauterberg et al., 2022; Ren et al., 2010; Thomas & Ougham, 2014). A further effect that can occur in a comparison between field and greenhouse was observed. The NIL-U-2B-3 had more tillers in the greenhouse than in the field. This may be due to the lower plant density in the greenhouse (Poorter et al., 2016).

In the greenhouse, the natural fluctuations and the intensity of temperature and light throughout the day and seasons pose a challenge (Poorter et al., 2016). In more than 25% of the studies examined in the meta-analysis described above, the temperature was not changed between day and night, although the differences ranged from 7-12 °C. Clouds can reduce the light intensity by 85% within seconds. These fluctuations are not simulated in the greenhouse or in a growth chamber. In addition, the light intensity throughout the day in the greenhouse is only 30 % of the intensity outside (Cabrera-Bosquet et al., 2016). However, HTP experiments in controlled greenhouses are important to investigate precise for spatio-temporal plant response (Langstroff et al., 2022). A one-plant-one-pot set up can be easily manipulated, stresses can be combined and future scenarios simulated in the controlled system.

The PhenoSphere was developed to perform experiments in field-like conditions and thus, close the gap between field and greenhouse (Heuermann et al., 2023). Field-like dynamics can be simulated for temperature, light quality and quantity, relative humidity, wind and CO_2 up to 1200ppm.

Furthermore, the plants grow in containers with layers of soil, loess and gravel. Four field experiments, one greenhouse experiment and two experiments in the PhenoSphere were conducted with 11 maize inbred lines to investigate and compare the growth conditions. A field experiment and the correspondingly simulated experiment in the PhenoSphere showed the same growth dynamics for plant height, but the yield traits were significantly different, which could be due to the plasticity of flowering time in two different maize populations.

In addition to formulating scientific questions, planning, conducting, analyzing and interpreting experiments, it is crucial to document this data in accordance with FAIR-principles: Findable, Accessible, Interoperable, Reusable (Wilkinson et al., 2016). To access the data, data repositories, such as e!DAL has been developed to share the data (Arend et al., 2020). With HTP, very complex data is created on unique HTP systems. In order to describe this data more homogeneously, MIAPPE (Minimum Information About a Plant Phenotyping Experiment), has been developed as a meta data standard (Papoutsoglou et al., 2020).
Combining HTP pot experiments with field studies could be beneficial, especially for targeted validation and precisely decipher genotypes for certain question for screening populations to overcome the phenotyping bottleneck. There are drawbacks of the different environments, which are known and be handled with care. Still HTP, especially in field-like conditions, has great potential to phenotype for future scenarios.

3.4 Is HTP imaging for chlorophyll fluorescence indicative of yield potential in a changing climate scenario?

HTP is used to derive traits that can describe the plants from the images. These include biomass and plant height or the growth dynamics calculated from these (Heuermann et al., 2023; Roth et al., 2023). Color traits are also important, including color ratio, mean color value or fluorescence color traits. The color traits can be used to describe senescence even before it is visible or the stay-green effect (Lauterberg et al., 2022, 2023). This provides indications of the physiological state of the plant.
There are numerous reviews in which the non-invasive measurements of traits of chlorophyll fluorescence were described (Baker, 2008; Long et al., 2022; Murchie & Lawson, 2013). The most important and frequently used traits are the ΦPSII and the maximum quantum efficiency of photosystem II (F_v/F_m) (Table 1). There are always different requirements for the measurements. For the measurement of fluorescence levels in dark-adapted plants, a dark adaptation of at least one hour is necessary (Björkmann & Demming, 1987). Adaptation to certain light conditions can be expected to take between 5 min and 30 min. The ΦPSII is done with light-adapted plants; F_v/F_m is measured with dark-adapted plants. Measurements can be made with portable devices, SPAD meter or in boxes (Benedict & Swidler, 1961; Jansen et al., 2009; Kuhlgert et al., 2016). However, it became interesting when systems for measuring chlorophyll fluorescence are integrated into HTP systems for all sizes of plants, as it is inevitable for understanding the biomass gain (Furbank et al., 2019; Tschiersch et al., 2017). Depending on the size of the plant, 184 to 1080 plants per hour can be measured on the HTP systems, with the crop plants having a height of up to 1.8 meters.

The chlorophyll fluorescence imaging with HTP has been successfully applied for several experiments. In an experiment with NIL of wheat, chlorophyll fluorescence was also measured. The ΦPSII was measured with two consecutive different light intensities to measure the plasticity of ΦPSII under drought stress (Lauterberg et al., 2022). A NIL of the cultivar BarNir, which carried a QTL of wild emmer for total and spike dry matter under drought and was drought tolerant in terms of biomass production, showed higher ΦPSII under drought stress and greater plasticity when switching between light intensities. Experiments with 60 genotypes of chickpea demonstrated a heritability for ΦPSII between 0.5-0.8 among drought stress and control treatment and five imaging days (Lauterberg et al., 2023). Additionally, a correlation between the biomass and the ΦPSII under drought stress and control was 0.7 and 0.4 to hundred seed weight and weight of seeds (Lauterberg et al., 2023, 2024).

Measurements of ΦPSII can easily be done, as light-adapted plants are required and the measurement is quick. Measuring NPQ is technically more challenging then measuring F_v/F_m or ΦPSII. The maximal fluorescence form dark and light adapted leaves (F_m and F_m‘) have to be measured to calculate NPQ (Baker, 2008). These circumstances make measuring NPQ with HTP very time-consuming and technically demanding.
Tietz et al., (2017) has published how to measure NPQ as theoretical NPQ ($NPQ_{(T)}$) (Table 1). Since F_v/F_m of healthy crops is a stable value and only varies for the respective species, a fixed value was used (Björkmann & Demming, 1987). This avoids the need for dark adaptation. In addition, far-red light is used to determine the minimum dark-adapted fluorescence more quickly, as it oxidized plastoquinone A, the first electron acceptor of photosystem II (Diner, 1977). Thus, what remains is the species specific measurement of F_v/F_m and the measurement of F_m‘ and F_0’ of a light-adapted plant.

Table 1: Formula of non-photochemical-quenching (NPQ), theoretical NPQ ($NPQ_{(T)}$) and ΦPSII. Modified after and with explanations of: (Baker, 2008; Björkmann & Demming, 1987; Lauterberg et al., 2024; Tietz et al., 2017). QA: primary quinone electron acceptor of PSII: Plastoquinone A.

$NPQ = \left(\frac{\left(\frac{1}{\left(1-\left(\frac{Fv}{Fm}\right)\right)} \right)^{-1}}{\left(\frac{F'm}{F'_0}\right)-1} \right) - 1$		Formula (1)
$NPQ_{(T)} = \left(\frac{4.88}{\left(\frac{F'm}{F'_0}\right)-1} \right) - 1$		Formula (2)
Parameter	Definition	Physiological relevance
F_0, F_0'	Minimal fluorescence from dark- and light-adapted leaf, respectively	Level of fluorescence when QA is maximally *oxidized* (PSII centers *open*)
F_m, F_m'	Maximal fluorescence from dark- and light-adapted leaf, respectively	Level of fluorescence when QA is maximally *reduced* (PSII centers *closed*)
F_v, F_v'	Variable fluorescence from dark- and light-adapted leaves, respectively	Demonstrates the ability of PSII to perform photochemistry (QA reduction)
F_v/F_m	Maximum quantum efficiency of PSII photochemistry	Maximum efficiency at which light absorbed by PSII is used for reduction of QA.
F_q'	Difference in fluorescence between F_m' and F' ("steady-state" light adapted)	Photochemical quenching of fluorescence by open PSII centers.
F_q'/F_m'	PSII operating efficiency ΦPSII	Estimates the efficiency at which light absorbed by PSII is used for QA reduction. At a given photosynthetically active photon flux density (PPFD) this parameter provides an estimate of the quantum yield of linear electron flux through PSII.
4.88	$= 1 / (1 - (F_v/F_m))$	Assuming $F_v/F_m = 0.83$, as described by Björkmann & Demming (1987), average across 44 species

Following this idea of Tietz et al., (2017), the measurement of $NPQ_{(T)}$ has been implemented successfully for HTP (Lauterberg et al., 2024). F_v/F_m was initially measured for 60 genotypes PGR of chickpea under control conditions and was 0.856 ± 0.002. $NPQ_{(T)}$ and NPQ were then measured under control conditions or calculated from the individual measured parameters. A correlation of r = 0.9 was achieved with the values for NPQ and $NPQ_{(T)}$. Furthermore, the repeatability of NPQ was 0.7 and for $NPQ_{(T)}$ 0.5. The capacity for measuring NPQ with fully dark-adapted plants was 9.4 plants per hour. For $NPQ_{(T)}$ it was on average 38.8 fully light-adapted plants per hour. This difference in the capacity of measurement clearly showed that $NPQ_{(T)}$ is suitable for HTP.

$NPQ_{(T)}$ was measured two times under drought stress for the 60 genotypes of chickpea and on the day of re-watering and once more during the subsequent recovery (Lauterberg et al., 2024). Of the 60 genotypes, 30 belong to the *desi* type and 30 to the *kabuli* type. As already described, *desi* is more tolerant to drought stress than *kabuli* (Farooq et al., 2018; Lauterberg et al., 2022; Nisa et al., 2020). In drought stress treatment, there was no significant difference between the two types of chickpea,

but in control, *desi* showed significantly higher values for $NPQ_{(T)}$ then *kabuli*. This means that the two types differ in their plasticity for $NPQ_{(T)}$ and the better drought tolerance of *desi* could be due to the effective dissipation of excess excitation energy of photosystem II (Lauterberg et al., 2024).
In this study, it was successfully shown that $NPQ_{(T)}$ as a proxy for NPQ with HTP under drought stress can contribute to the revealing and screening of drought tolerance of different genotypes or types of chickpea.
NPQ is associated with strong light intensities and has attracted particular attention in recent publications in connection with fluctuating light (De Souza et al., 2022; Kromdijk et al., 2016; Müller et al., 2001). At high light intensity, the reaction centers close and ATP synthase is inhibited, which in turn leads to acidification in the thylakoid lumen and the fast relaxation component triggers energy-dependent quenching (qE) (Ghosh et al., 2023; Ruban et al., 2012). The xanthophyll cycle is also involved. Acidification of the lumen converts violaxanthin into zeaxanthin, which in turn releases the excess absorbed energy in the form of heat. Kromdijk et al., (2016) have overexpressed the enzymes involved in the xanthophyll cycle and photosystem II subunit S (PsbS) in tobacco. An accelerated response to shading events was observed, leading to a dry matter productivity increase of 15%. Soybean has been engineered in the same way and in replicated field experiments, an increased seed yield by up to 33% have been reported (De Souza et al., 2022). It was also found that tobacco with overexpressed PsbS showed higher NPQ under drought stress, resulting in better WUE with no change in biomass production (Turc et al., 2024).

Improved dry matter production in tobacco, improved seed yield in soybean under control conditions, better WUE in tobacco and better biomass maintenance in chickpea under drought stress are related to NPQ. This shows the potential of further analyses of mutants or PGR with respect to NPQ, and this is why the application of $NPQ_{(T)}$ is valuable for HTP.

4. Conclusion

The effect of wild emmer QTLs in wheat cultivars from field experiments could be confirmed in a pot greenhouse experiment and could be further subdivided into more detailed periods. Among PGR of chickpea, genotypes could be selected based on image-derived traits of growth dynamics and photosynthesis for their tolerance to drought stress. In the future, experiments can be conducted with more genotypes to perform a GWAS and supplement the experiments with metabolomics sampling on indicative days. However, intensive breeding is still necessary before a cultivar can be selected that offers the necessary yield potential in challenging climates.

References

Literature

Abbo, S., Berger, J., & Turner, N. C. (2003). Viewpoint: Evolution of cultivated chickpea: four bottlenecks limit diversity andconstrain adaptation. *Functional Plant Biology*, *30*(10), 1081. https://doi.org/10.1071/FP03084

Amitrano, C., Junker, A., D'Agostino, N., De Pascale, S., & De Micco, V. (2022). Integration of high-throughput phenotyping with anatomical traits of leaves to help understanding lettuce acclimation to a changing environment. *Planta*, *256*(4), 1–19. https://doi.org/10.1007/s00425-022-03984-2

Arend, D., König, P., Junker, A., Scholz, U., & Lange, M. (2020). The on-premise data sharing infrastructure e!DAL: Foster FAIR data for faster data acquisition. *GigaScience*, *9*(10), giaa107. https://doi.org/10.1093/gigascience/giaa107

Aslam, M., Waseem, M., Jakada, B. H., Okal, E. J., Lei, Z., Saqib, H. S. A., Yuan, W., Xu, W., & Zhang, Q. (2022). Mechanisms of Abscisic Acid-Mediated Drought Stress Responses in Plants. *International Journal of Molecular Sciences*, *23*(3), 1084. https://doi.org/10.3390/ijms23031084

Asseng, S., Ewert, F., Martre, P., Rötter, R. P., Lobell, D. B., Cammarano, D., Kimball, B. A., Ottman, M. J., Wall, G. W., White, J. W., Reynolds, M. P., Alderman, P. D., Prasad, P. V. V., Aggarwal, P. K., Anothai, J., Basso, B., Biernath, C., Challinor, A. J., De Sanctis, G., … Zhu, Y. (2015). Rising temperatures reduce global wheat production. *Nature Climate Change*, *5*(2), 143–147. https://doi.org/10.1038/nclimate2470

Atieno, J., Colmer, T. D., Taylor, J., Li, Y., Quealy, J., Kotula, L., Nicol, D., Nguyen, D. T., Brien, C., Langridge, P., Croser, J., Hayes, J. E., & Sutton, T. (2021). Novel Salinity Tolerance Loci in Chickpea Identified in Glasshouse and Field Environments. *Frontiers in Plant Science*, *12*, 667910. https://doi.org/10.3389/fpls.2021.667910

Atieno, J., Li, Y., Langridge, P., Dowling, K., Brien, C., Berger, B., Varshney, R. K., & Sutton, T. (2017). Exploring genetic variation for salinity tolerance in chickpea using image-based phenotyping. *Scientific Reports*, *7*(1), 1–11. https://doi.org/10.1038/s41598-017-01211-7

Avni, R., Nave, M., Barad, O., Baruch, K., Twardziok, S., Gundlach, H., et al. (2017): Wild emmer genome architecture and diversity elucidate wheat evolution and domestication. In: Science 357 (6346), S. 93–97. https://doi.org/10.1126/science.aan0032

Badhan, S., Ball, A. S., & Mantri, N. (2021). First Report of CRISPR/Cas9 Mediated DNA-Free Editing of 4CL and RVE7 Genes in Chickpea Protoplasts. *International Journal of Molecular Sciences*, *22*(1), 396. https://doi.org/10.3390/ijms22010396

Baker, N. R. (2008). Chlorophyll Fluorescence: A Probe of Photosynthesis In Vivo. *Annual Review of Plant Biology*, *59*(1), 89–113. https://doi.org/10.1146/annurev.arplant.59.032607.092759

Barzana, G., Rios, J. J., Lopez-Zaplana, A., Nicolas-Espinosa, J., Yepes-Molina, L., Garcia-Ibañez, P., & Carvajal, M. (2021). Interrelations of nutrient and water transporters in plants under abiotic stress. *Physiologia Plantarum*, *171*(4), 595–619. https://doi.org/10.1111/ppl.13206

References

Bayahi, K., & Rezgui, S. (2018). Improvement of Yields in Chickpea (Cicer Arietinum. L): Genetic Study of Heterosis in Hybrids Derived from Desi x Kabuli and Kabuli x Kabuli Crosses. *Journal of Advancements in Plant Science*, *1*(1), 1–7. https://doi.org/10.18875/2639-1368.1.101

Becker, H. (2019). *Pflanzenzüchtung*. UTB GmbH. https://books.google.de/books?id=KAGWDwAAQBAJ

Bellucci, E., Mario Aguilar, O., Alseekh, S., Bett, K., Brezeanu, C., Cook, D., De La Rosa, L., Delledonne, M., Dostatny, D. F., Ferreira, J. J., Geffroy, V., Ghitarrini, S., Kroc, M., Kumar Agrawal, S., Logozzo, G., Marino, M., Mary-Huard, T., McClean, P., Meglič, V., … Papa, R. (2021). The INCREASE project: Intelligent Collections of food-legume genetic resources for European agrofood systems. *The Plant Journal*, *108*(3), 646–660. https://doi.org/10.1111/tpj.15472

Benedict, H. M., & Swidler, R. (1961). Nondestructive Method for Estimating Chlorophyll Content of Leaves. *Science*, *133*(3469), 2015–2016. https://doi.org/10.1126/science.133.3469.2015

Berger, J., Pushpavalli, R., Ludwig, C., Parsons, S., Basdemir, F., & Whisson, K. (2020). Wild and Domestic Differences in Plant Development and Responses to Water Deficit in Cicer. *Frontiers in Genetics*, *11*, 607819. https://doi.org/10.3389/fgene.2020.607819

Björkmann, O., & Demming, Ba. (1987). Photon yield of 0 2 evolution and chlorophyll fluorescence characteristics at 77 K among vascular plants of diverse origins. *Planta*, *170*, 489–504.

Bretag, T. W., MacLeod, W. J., Kimber, R. B. E., Moore, K. J., Knights, E. J. C., & Davidson, J. A. (2008). Management of ascochyta blight in chickpeas in Australia. *Australasian Plant Pathology*, *37*(5), 486. https://doi.org/10.1071/AP08046

Brichet, N., Fournier, C., Turc, O., Strauss, O., Artzet, S., Pradal, C., Welcker, C., Tardieu, F., & Cabrera-Bosquet, L. (2017). A robot-assisted imaging pipeline for tracking the growths of maize ear and silks in a high-throughput phenotyping platform. *Plant Methods*, *13*(1), 96. https://doi.org/10.1186/s13007-017-0246-7

Buckley, T. N., & Mott, K. A. (2013). Modelling stomatal conductance in response to environmental factors. *Plant, Cell & Environment*, *36*(9), 1691–1699. https://doi.org/10.1111/pce.12140

Cabrera-Bosquet, L., Fournier, C., Brichet, N., Welcker, C., Suard, B., & Tardieu, F. (2016). High-throughput estimation of incident light, light interception and radiation-use efficiency of thousands of plants in a phenotyping platform. *New Phytologist*, *212*, 269–281. https://doi.org/10.1111/nph.14027

Charmet, G. (2011). Wheat domestication: Lessons for the future. *Comptes Rendus. Biologies*, *334*(3), 212–220. https://doi.org/10.1016/j.crvi.2010.12.013

Cullis, C., & Kunert, K. J. (2016). Unlocking the potential of orphan legumes. *Journal of Experimental Botany*, erw437. https://doi.org/10.1093/jxb/erw437

Das Choudhury, S., Samal, A., & Awada, T. (2019). Leveraging Image Analysis for High-Throughput Plant Phenotyping. *Frontiers in Plant Science*, *10*, 508. https://doi.org/10.3389/fpls.2019.00508

De Souza, A. P., Burgess, S. J., Doran, L., Hansen, J., Manukyan, L., Maryn, N., Gotarkar, D., Leonelli, L., Niyogi, K. K., & Long, S. P. (2022). Soybean photosynthesis and crop yield are improved by accelerating recovery from photoprotection. *Science*, *377*(6608), 851–854. https://doi.org/10.1126/science.adc9831

References

De Wit, M., Kegge, W., Evers, J. B., Vergeer-van Eijk, M. H., Gankema, P., Voesenek, L. A. C. J., & Pierik, R. (2012). Plant neighbor detection through touching leaf tips precedes phytochrome signals. *Proceedings of the National Academy of Sciences*, *109*(36), 14705–14710. https://doi.org/10.1073/pnas.1205437109

Deblieck, M., Fatiukha, A., Grundman, N., Merchuk-Ovnat, L., Saranga, Y., Krugman, T., Pillen, K., Serfling, A., Makalowski, W., Ordon, F., & Perovic, D. (2020). GenoTypeMapper: Graphical genotyping on genetic and sequence-based maps. *Plant Methods*, *16*(1), 123. https://doi.org/10.1186/s13007-020-00665-7

Dhanagond, S., Liu, G., Zhao, Y., Chen, D., Grieco, M., Reif, J., Kilian, B., Graner, A., & Neumann, K. (2019). Non-Invasive Phenotyping Reveals Genomic Regions Involved in Pre-Anthesis Drought Tolerance and Recovery in Spring Barley. *Frontiers in Plant Science*, *10*, 1–21. https://doi.org/10.3389/fpls.2019.01307

Diner, B. A. (1977). Dependence of the deactivation reactions of Photosystem II on the redox state of plastoquinone pool a varied under anaerobic conditions. Equilibria on the acceptor side of Photosystem II. *Biochimica et Biophysica Acta (BBA) - Bioenergetics*, *460*(2), 247–258. https://doi.org/10.1016/0005-2728(77)90211-0

Duarte, I. (2022). Chickpea breeding program and research in portugal. *Open Journal of Plant Science*, *7*(2), 025–033. https://doi.org/10.17352/ojps.000049

Duarte, I., Imtiaz, M., Pinheiro, C., & Chaves, M. (2023). Adaptation and Yield Stability for chickpea genotypes to the Mediterranean basin. *International Journal of Plant Biology & Research*, *11*(1134).

Eker, T., Sari, D., Sari, H., Tosun, H. S., & Toker, C. (2022). A kabuli chickpea ideotype. *Scientific Reports*, *12*(1), 1611. https://doi.org/10.1038/s41598-022-05559-3

Fàbregas, N., & Fernie, A. R. (2019). The metabolic response to drought. *Journal of Experimental Botany*, *70*(4), 1077–1085. https://doi.org/10.1093/jxb/ery437

Fanning, J., Brand, J., Munoz Santa, I., McDonald, L., Taylor, J., & Hollaway, G. (2022). Management of chickpea Ascochyta blight using fungicides and cultivar resistance improves grain yield, quality, and grower profitability. *Frontiers in Plant Science*, *13*, 942220. https://doi.org/10.3389/fpls.2022.942220

FAO. (1998). *The State of the World's Plant Genetic Resources for Food and Agriculture*. FAO. https://www.fao.org/3/w7324e/w7324e.pdf

FAOSTAT. (2024). *FAOSTAT* [Dataset]. http://www.fao.org/faostat/en/#home

Farooq, M. A., Ullah, A., Lee, D.-J., & Alghamdi, S. S. (2018). Desi chickpea genotypes tolerate drought stress better than kabuli types by modulating germination metabolism, trehalose accumulation, and carbon assimilation. *Plant Physiology and Biochemistry*, *126*, 47–54.

Farquhar, G. D., & Sharkey, T. D. (1982). Stomatal Conductance and Photosynthesis. *Annual Review of Plant Physiology*, *33*(1), 317–345. https://doi.org/10.1146/annurev.pp.33.060182.001533

Feuillet, C., Langridge, P., & Waugh, R. (2008). Cereal breeding takes a walk on the wild side. *Trends in Genetics*, *24*(1), 24–32. https://doi.org/10.1016/j.tig.2007.11.001

Fiorani, F., & Schurr, U. (2013). Future Scenarios for Plant Phenotyping. *Annual Review of Plant Biology*, *64*(1), 267–291. https://doi.org/10.1146/annurev-arplant-050312-120137

References

Foyer, C. H., Lam, H.-M., Nguyen, H. T., Siddique, K. H. M., Varshney, R. K., Colmer, T. D., Cowling, W., Bramley, H., Mori, T. A., Hodgson, J. M., Cooper, J. W., Miller, A. J., Kunert, K., Vorster, J., Cullis, C., Ozga, J. A., Wahlqvist, M. L., Liang, Y., Shou, H., … Considine, M. J. (2016). Neglecting legumes has compromised human health and sustainable food production. *Nature Plants*, *2*(8), 16112. https://doi.org/10.1038/nplants.2016.112

Furbank, R. T., Jimenez-Berni, J. A., George-Jaeggli, B., Potgieter, A. B., & Deery, D. M. (2019). Field crop phenomics: Enabling breeding for radiation use efficiency and biomass in cereal crops. *New Phytologist*, *223*(4), 1714–1727. https://doi.org/10.1111/nph.15817

Furbank, R. T., & Tester, M. (2011). Phenomics—Technologies to relieve the phenotyping bottleneck. *Cell Press*, *18*(12), 635–643.

Ghosh, D., Mohapatra, S., & Dogra, V. (2023). Improving photosynthetic efficiency by modulating non-photochemical quenching. *Trends in Plant Science*, *28*(3), 264–266. https://doi.org/10.1016/j.tplants.2022.12.016

Giorgi, F., Raffaele, F., & Coppola, E. (2019). The response of precipitation characteristics to global warming from climate projections. *Earth System Dynamics*, *10*(1), 73–89. https://doi.org/10.5194/esd-10-73-2019

Godfray, H. C. J., Beddington, J. R., Crute, I. R., Haddad, L., Lawrence, D., Muir, J. F., Pretty, J., Robinson, S., Thomas, S. M., & Toulmin, C. (2010). Food Security: The Challenge of Feeding 9 Billion People. *Science*, *327*(5967), 812–818. https://doi.org/10.1126/science.1185383

Grillakis, M. G. (2019). Increase in severe and extreme soil moisture droughts for Europe under climate change. *Science of The Total Environment*, *660*, 1245–1255. https://doi.org/10.1016/j.scitotenv.2019.01.001

Gupta, S., Nawaz, K., Parween, S., Roy, R., Sahu, K., Kumar Pole, A., Khandal, H., Srivastava, R., Kumar Parida, S., & Chattopadhyay, D. (2016). Draft genome sequence of *Cicer reticulatum* L., the wild progenitor of chickpea provides a resource for agronomic trait improvement. *DNA Research*, dsw042. https://doi.org/10.1093/dnares/dsw042

Heuermann, M. C., Knoch, D., Junker, A., & Altmann, T. (2023). Natural plant growth and development achieved in the IPK PhenoSphere by dynamic environment simulation. *Nature Communications*, *14*(1), 5783. https://doi.org/10.1038/s41467-023-41332-4

Hinterberger, V., Douchkov, D., Lueck, S., Reif, J. C., & Schulthess, A. W. (2022). High-throughput imaging of powdery mildew resistance of the winter wheat collection hosted at the German Federal ex situ Genebank for Agricultural and Horticultural Crops. *GigaScience*, *12*, giad007. https://doi.org/10.1093/gigascience/giad007

Hoisington, D., Khairallah, M., Reeves, T., Ribaut, J.-M., Skovmand, B., Taba, S., & Warburton, M. (1999). Plant genetic resources: What can they contribute toward increased crop productivity? *Proceedings of the National Academy of Sciences*, *96*(11), 5937–5943. https://doi.org/10.1073/pnas.96.11.5937

References

Humplík, J. F., Lazár, D., Fürst, T., Husičková, A., Hýbl, M., & Spíchal, L. (2015). Automated integrative high-throughput phenotyping of plant shoots: A case study of the cold-tolerance of pea (Pisum sativum L.). *Plant Methods*, *11*(1), 1–11. https://doi.org/10.1186/s13007-015-0063-9

Indurker, S., Misra, H. S., & Eapen, S. (2010). Agrobacterium-mediated transformation in chickpea (Cicer arietinum L.) with an insecticidal protein gene: Optimisation of different factors. *Physiology and Molecular Biology of Plants*, *16*(3), 273–284. https://doi.org/10.1007/s12298-010-0030-x

Jaganathan, D., Thudi, M., Kale, S., Azam, S., Roorkiwal, M., Gaur, P. M., Kishor, P. B. K., Nguyen, H., Sutton, T., & Varshney, R. K. (2015). Genotyping-by-sequencing based intra-specific genetic map refines a ''QTL-hotspot" region for drought tolerance in chickpea. *Molecular Genetics and Genomics*, *290*(2), 559–571. https://doi.org/10.1007/s00438-014-0932-3

Jahnke, S., Roussel, J., Hombach, T., Kochs, J., Fischbach, A., Huber, G., & Scharr, H. (2016). phenoSeeder—A Robot System for Automated Handling and Phenotyping of Individual Seeds. *Plant Physiology*, *172*(3), 1358–1370. https://doi.org/10.1104/pp.16.01122

Jansen, M., Gilmer, F., Biskup, B., Nagel, K. A., Rascher, U., Fischbach, A., Briem, S., Dreissen, G., Tittmann, S., Braun, S., De Jaeger, I., Metzlaff, M., Schurr, U., Scharr, H., & Walter, A. (2009). Simultaneous phenotyping of leaf growth and chlorophyll fluorescence via GROWSCREEN FLUORO allows detection of stress tolerance in Arabidopsis thaliana and other rosette plants. *Functional Plant Biology*, *36*(11), 902. https://doi.org/10.1071/FP09095

Jung, C., & Müller, A. E. (2009). Flowering time control and applications in plant breeding. *Trends in Plant Science*, *14*(10), 563–573. https://doi.org/10.1016/j.tplants.2009.07.005

Kale, S. M., Jaganathan, D., Ruperao, P., Chen, C., Punna, R., Kudapa, H., Thudi, M., Roorkiwal, M., Katta, M. A., Doddamani, D., Garg, V., Kishor, P. B. K., Gaur, P. M., Nguyen, H. T., Batley, J., Edwards, D., Sutton, T., & Varshney, R. K. (2015). Prioritization of candidate genes in "QTL-hotspot" region for drought tolerance in chickpea (Cicer arietinum L.). *Scientific Reports*, *5*(1), 15296. https://doi.org/10.1038/srep15296

Khan, A. W., Garg, V., Sun, S., Gupta, S., Dudchenko, O., Roorkiwal, M., Chitikineni, A., Bayer, P. E., Shi, C., Upadhyaya, H. D., Bohra, A., Bharadwaj, C., Mir, R. R., Baruch, K., Yang, B., Coyne, C. J., Bansal, K. C., Nguyen, H. T., Ronen, G., … Varshney, R. K. (2024). Cicer super-pangenome provides insights into species evolution and agronomic trait loci for crop improvement in chickpea. *Nature Genetics*, *56*(6), 1225–1234. https://doi.org/10.1038/s41588-024-01760-4

Khan, Z., Rahimi-Eichi, V., Haefele, S., Garnett, T., & Miklavcic, S. J. (2018). Estimation of vegetation indices for high-throughput phenotyping of wheat using aerial imaging. *Plant Methods*, *14*(1), 20. https://doi.org/10.1186/s13007-018-0287-6

Kirchgessner, N., Liebisch, F., Yu, K., Pfeifer, J., Friedli, M., Hund, A., & Walter, A. (2017). The ETH field phenotyping platform FIP: A cable-suspended multi-sensor system. *Functional Plant Biology*, *44*(1), 154. https://doi.org/10.1071/FP16165

References

Klukas, C., Chen, D., & Pape, J.-M. (2014). Integrated Analysis Platform: An Open-Source Information System for High-Throughput Plant Phenotyping. *Plant Physiology*, *165*(2), 506–518. https://doi.org/10.1104/pp.113.233932

Knoch, D., Werner, C. R., Meyer, R. C., Riewe, D., Abbadi, A., Lücke, S., Snowdon, R. J., & Altmann, T. (2021). Multi-omics-based prediction of hybrid performance in canola. *Theoretical and Applied Genetics*, *134*(4), 1147–1165. https://doi.org/10.1007/s00122-020-03759-x

Kooyers, N. J. (2015). The evolution of drought escape and avoidance in natural herbaceous populations. *Plant Science*, *234*, 155–162. https://doi.org/10.1016/j.plantsci.2015.02.012

Körner, C. (2015). Paradigm shift in plant growth control. *Current Opinion in Plant Biology*, *25*, 107–114. https://doi.org/10.1016/j.pbi.2015.05.003

Kosma, D. K., Bourdenx, B., Bernard, A., Parsons, E. P., Lü, S., Joubès, J., & Jenks, M. A. (2009). The Impact of Water Deficiency on Leaf Cuticle Lipids of Arabidopsis. *Plant Physiology*, *151*(4), 1918–1929. https://doi.org/10.1104/pp.109.141911

Krishnamurthy, L., Kashiwagi, J., Gaur, P. M., Upadhyaya, H. D., & Vadez, V. (2010). Sources of tolerance to terminal drought in the chickpea (Cicer arietinum L.) minicore germplasm. *Field Crops Research*, *119*(2–3), 322–330. https://doi.org/10.1016/j.fcr.2010.08.002

Kromdijk, J., Głowacka, K., Leonelli, L., Gabilly, S. T., Iwai, M., Niyogi, K. K., & Long, S. P. (2016). Improving photosynthesis and crop productivity by accelerating recovery from photoprotection. *Science*, *354*(6314), 857–861. https://doi.org/10.1126/science.aai8878

Kuhlgert, S., Austic, G., Zegarac, R., Osei-Bonsu, I., Hoh, D., Chilvers, M. I., Roth, M. G., Bi, K., TerAvest, D., Weebadde, P., & Kramer, D. M. (2016). MultispeQ Beta: A tool for large-scale plant phenotyping connected to the open PhotosynQ network. *Royal Society Open Science*, *3*(10), 1–17. https://doi.org/10.1098/rsos.160592

Kurepa, J., & Smalle, J. A. (2022). Auxin/Cytokinin Antagonistic Control of the Shoot/Root Growth Ratio and Its Relevance for Adaptation to Drought and Nutrient Deficiency Stresses. *International Journal of Molecular Sciences*, *23*(4), 1933. https://doi.org/10.3390/ijms23041933

Langstroff, A., Heuermann, M. C., Stahl, A., & Junker, A. (2022). Opportunities and limits of controlled-environment plant phenotyping for climate response traits. *Theoretical and Applied Genetics*, *135*(1), 1–16. https://doi.org/10.1007/s00122-021-03892-1

Lauterberg, M., Saranga, Y., Deblieck, M., Klukas, C., Krugman, T., Perovic, D., Ordon, F., Graner, A., & Neumann, K. (2022). Precision phenotyping across the life cycle to validate and decipher drought-adaptive QTLs of wild emmer wheat (Triticum turgidum ssp. Dicoccoides) introduced into elite wheat varieties. *Frontiers in Plant Science*, *13*, 965287. https://doi.org/10.3389/fpls.2022.965287

Lauterberg, M., Tschiersch, H., Papa, R., Bitocchi, E., & Neumann, K. (2023). Engaging Precision Phenotyping to Scrutinize Vegetative Drought Tolerance and Recovery in Chickpea Plant Genetic Resources. *Plants*, *12*(15), 2866. https://doi.org/10.3390/plants12152866

Lauterberg, M., Tschiersch, H., Zhao, Y., Kuhlmann, M., Mücke, I., Papa, R., Bitocchi, E., & Neumann, K. (2024). Implementation of theoretical non-photochemical quenching (NPQ(T)) to investigate NPQ of chickpea

under drought stress with High-throughput Phenotyping. *Scientific Reports*, *14*(1), 13970. https://doi.org/10.1038/s41598-024-63372-6

Long, S. P., Taylor, S. H., Burgess, S. J., Carmo-Silva, E., Lawson, T., De Souza, A. P., Leonelli, L., & Wang, Y. (2022). Into the Shadows and Back into Sunlight: Photosynthesis in Fluctuating Light. *Annual Review of Plant Biology*, *73*(1), 617–648. https://doi.org/10.1146/annurev-arplant-070221-024745

López-Bellido, F. J., López-Bellido, R. J., Khalil, S. K., & López-Bellido, L. (2008). Effect of Planting Date on Winter Kabuli Chickpea Growth andYield under Rainfed Mediterranean Conditions. *Agronomy Journal*, *100*(4), 957–964. https://doi.org/10.2134/agronj2007.0274

López-Bellido, L., Benítez-Vega, J., García, P., Redondo, R., & López-Bellido, R. J. (2011). Tillage system effect on nitrogen rhizodeposited by faba bean and chickpea. *Field Crops Research*, *120*(1), 189–195. https://doi.org/10.1016/j.fcr.2010.10.001

Lynch, J. P. (2013). Steep, cheap and deep: An ideotype to optimize water and N acquisition by maize root systems. *Annals of Botany*, *112*(2), 347–357. https://doi.org/10.1093/aob/mcs293

Maccaferri, M., Harris, N. S., Twardziok, S. O., Pasam, R. K., Gundlach, H., Spannagl, M., Ormanbekova, D., Lux, T., Prade, V. M., Milner, S. G., Himmelbach, A., Mascher, M., Bagnaresi, P., Faccioli, P., Cozzi, P., Lauria, M., Lazzari, B., Stella, A., Manconi, A., … Cattivelli, L. (2019). Durum wheat genome highlights past domestication signatures and future improvement targets. *Nature Genetics*, *51*(5), 885–895. https://doi.org/10.1038/s41588-019-0381-3

Massonnet, C., Vile, D., Fabre, J., Hannah, M. A., Caldana, C., Lisec, J., Beemster, G. T. S., Meyer, R. C., Messerli, G., Gronlund, J. T., Perkovic, J., Wigmore, E., May, S., Bevan, M. W., Meyer, C., Rubio-Díaz, S., Weigel, D., Micol, J. L., Buchanan-Wollaston, V., … Granier, C. (2010). Probing the Reproducibility of Leaf Growth and Molecular Phenotypes: A Comparison of Three Arabidopsis Accessions Cultivated in Ten Laboratories. *Plant Physiology*, *152*(4), 2142–2157. https://doi.org/10.1104/pp.109.148338

Medeiros, J. S., Nunes Da Silva, M., Carvalho, S. M. P., Santos, C. S., & Vasconcelos, M. W. (2023). Low water supply differentially affects the growth, yield and mineral profile of kabuli and desi chickpeas (Cicer arietinum). *Annals of Applied Biology*, 1–13. https://doi.org/10.1111/aab.12835

Merchuk-Ovnat, L., Barak, V., Fahima, T., Ordon, F., Lidzbarsky, G. A., Krugman, T., & Saranga, Y. (2016). Ancestral QTL Alleles from Wild Emmer Wheat Improve Drought Resistance and Productivity in Modern Wheat Cultivars. *Frontiers in Plant Science*, *7*. https://doi.org/10.3389/fpls.2016.00452

Merchuk-Ovnat, L., Fahima, T., Ephrath, J. E., Krugman, T., & Saranga, Y. (2017). Ancestral QTL Alleles from Wild Emmer Wheat Enhance Root Development under Drought in Modern Wheat. *Frontiers in Plant Science*, *8*, 703. https://doi.org/10.3389/fpls.2017.00703

Merchuk-Ovnat, L., Fahima, T., Krugman, T., & Saranga, Y. (2016). Ancestral QTL alleles from wild emmer wheat improve grain yield, biomass and photosynthesis across enviroinments in modern wheat. *Plant Science*, *251*, 23–34. https://doi.org/10.1016/j.plantsci.2016.05.003

Meyer, R. C., Weigelt-Fischer, K., Tschiersch, H., Topali, G., Altschmied, L., Heuermann, M. C., Knoch, D., Kuhlmann, M., Zhao, Y., & Altmann, T. (2023). Dynamic growth QTL action in diverse light

environments: Characterization of light regime-specific and stable QTL in Arabidopsis. *Journal of Experimental Botany*, *74*(17), 5341–5362. https://doi.org/10.1093/jxb/erad222

Müller, P., Li, X.-P., & Niyogi, K. K. (2001). Non-Photochemical Quenching. A Response to Excess Light Energy. *Plant Physiology*, *125*(4), 1558–1566. https://doi.org/10.1104/pp.125.4.1558

Murchie, E. H., & Lawson, T. (2013). Chlorophyll fluorescence analysis: A guide to good practice and understanding some new applications. *Journal of Experimental Botany*, *64*(13), 3983–3998. https://doi.org/10.1093/jxb/ert208

Nadeem, M., Li, J., Yahya, M., Sher, A., Ma, C., Wang, X., & Qiu, L. (2019). Research Progress and Perspective on Drought Stress in Legumes: A Review. *International Journal of Molecular Sciences*, *20*(10), 2541. https://doi.org/10.3390/ijms20102541

Neumann, K., Zhao, Y., Chu, J., Keilwagen, J., Reif, J. C., Kilian, B., & Graner, A. (2017). Genetic architecture and temporal patterns of biomass accumulation in spring barley revealed by image analysis. *BMC Plant Biology*, *17*(1), 1–12. https://doi.org/10.1186/s12870-017-1085-4

Nevo, E., & Chen, G. (2010). Drought and salt tolerances in wild relatives for wheat and barley improvement. *Plant, Cell & Environment*, *33*(4), 670–685. https://doi.org/10.1111/j.1365-3040.2009.02107.x

Nigam, S. N., Chaudhari, S., Deevi, K. C., Saxena, K. B., & Janila, P. (2021). Trends in Legume Production and Future Outlook. In *Genetic Enhancement in Major Food Legumes*. Springer, Cham.

Nisa, Z. U., Arif, A., Waheed, M. Q., Shah, T. M., Iqbal, A., Siddiqui, A. J., Choudhary, M. I., El-Seedi, H. R., & Musharraf, S. G. (2020). A comparative metabolomic study on desi and kabuli chickpea (Cicer arietinum L.) genotypes under rainfed and irrigated field conditions. *Scientific Reports*, *10*(1), 13919. https://doi.org/10.1038/s41598-020-70963-6

Pang, J., Turner, N. C., Khan, T., Du, Y.-L., Xiong, J.-L., Colmer, T. D., Devilla, R., Stefanova, K., & Siddique, K. H. M. (2016). Response of chickpea (*Cicer arietinum* L.) to terminal drought: Leaf stomatal conductance, pod abscisic acid concentration, and seed set. *Journal of Experimental Botany*, erw153. https://doi.org/10.1093/jxb/erw153

Papoutsoglou, E. A., Faria, D., Arend, D., Arnaud, E., Athanasiadis, I. N., Chaves, I., Coppens, F., Cornut, G., Costa, B. V., Ćwiek-Kupczyńska, H., Droesbeke, B., Finkers, R., Gruden, K., Junker, A., King, G. J., Krajewski, P., Lange, M., Laporte, M., Michotey, C., … Pommier, C. (2020). Enabling reusability of plant phenomic datasets with MIAPPE 1.1. *New Phytologist*, *227*(1), 260–273. https://doi.org/10.1111/nph.16544

Pappula-Reddy, S.-P., Kumar, S., Pang, J., Chellapilla, B., Pal, M., Millar, A. H., & Siddique, K. H. M. (2024). High-throughput phenotyping for terminal drought stress in chickpea (Cicer arietinum L.). *Plant Stress*, *11*, 100386. https://doi.org/10.1016/j.stress.2024.100386

Peleg, Z., Cakmak, I., Ozturk, L., Yazici, A., Jun, Y., Budak, H., Korol, A. B., Fahima, T., & Saranga, Y. (2009). Quantitative trait loci conferring grain mineral nutrient concentrations in durum wheat × wild emmer wheat RIL population. *Theoretical and Applied Genetics*, *119*(2), 353–369. https://doi.org/10.1007/s00122-009-1044-z

References

Peleg, Z., Saranga, Y., Suprunova, T., Ronin, Y., Röder, M. S., Kilian, A., Korol, A. B., & Fahima, T. (2008). High-density genetic map of durum wheat × wild emmer wheat based on SSR and DArT markers. *Theoretical and Applied Genetics*, *117*(1), 103–115. https://doi.org/10.1007/s00122-008-0756-9

Poorter, H., Anten, N. P. R., & Marcelis, L. F. M. (2013). Physiological mechanisms in plant growth models: Do we need a supra-cellular systems biology approach? *Plant, Cell & Environment*, *36*, 1673–1690. https://doi.org/10.1111/pce.12123

Poorter, H., Bühler, J., Van Dusschoten, D., Climent, J., & Postma, J. A. (2012). Pot size matters: A meta-analysis of the effects of rooting volume on plant growth. *Functional Plant Biology*, *39*(11), 839. https://doi.org/10.1071/FP12049

Poorter, H., Fiorani, F., Pieruschka, R., Wojciechowski, T., Van Der Putten, W. H., Kleyer, M., Schurr, U., & Postma, J. (2016). Pampered inside, pestered outside? Differences and similarities between plants growing in controlled conditions and in the field. *New Phytologist*, *212*(4), 838–855. https://doi.org/10.1111/nph.14243

Poorter, H., Fiorani, F., Stitt, M., Schurr, U., Finck, A., Gibon, Y., Usadel, B., Munns, R., Atkin, O. K., Tardieu, F., & Pons, T. L. (2012). The art of growing plants for experimental purposes: A practical guide for the plant biologist. *Functional Plant Biology*, *39*(11), 821. https://doi.org/10.1071/FP12028

Ray, D. K., Ramankutty, N., Mueller, N. D., West, P. C., & Foley, J. A. (2012). Recent patterns of crop yield growth and stagnation. *Nature Communications*, *3*(1), 1293. https://doi.org/10.1038/ncomms2296

Rebetzke, G. J., Jimenez-Berni, J. A., Bovill, W. D., Deery, D. M., & James, R. A. (2016). High-throughput phenotyping technologies allow accurate selection of stay-green. *Journal of Experimental Botany*, *67*(17), 4919–4924. https://doi.org/10.1093/jxb/erw301

Rebetzke, G. J., Jimenez-Berni, J., Fischer, R. A., Deery, D. M., & Smith, D. J. (2019). Review: High-throughput phenotyping to enhance the use of crop genetic resources. *Plant Science*, *282*, 40–48. https://doi.org/10.1016/j.plantsci.2018.06.017

Ren, G., Zhou, Q., Wu, S., Zhang, Y., Zhang, L., Huang, J., Sun, Z., & Kuai, B. (2010). Reverse Genetic Identification of CRN1 and its Distinctive Role in Chlorophyll Degradation in *Arabidopsis*. *Journal of Integrative Plant Biology*, *52*(5), 496–504. https://doi.org/10.1111/j.1744-7909.2010.00945.x

Roth, L., Fossati, D., Krähenbühl, P., Walter, A., & Hund, A. (2023). Image-based phenomic prediction can provide valuable decision support in wheat breeding. *Theoretical and Applied Genetics*, *136*(7), 162. https://doi.org/10.1007/s00122-023-04395-x

Ruban, A. V., Johnson, M. P., & Duffy, C. D. P. (2012). The photoprotective molecular switch in the photosystem II antenna. *Biochimica et Biophysica Acta (BBA) - Bioenergetics*, *1817*(1), 167–181. https://doi.org/10.1016/j.bbabio.2011.04.007

Rubio, J., Flores, F., Moreno, M. T., Cubero, J. I., & Gil, J. (2004). Effects of the erect/bushy habit, single/double pod and late/early flowering genes on yield and seed size and their stability in chickpea. *Field Crops Research*, *90*(2–3), 255–262. https://doi.org/10.1016/j.fcr.2004.03.005

Saglam, A., Saruhan, N., Terzi, R., & Kadioglu, A. (2011). The relations between antioxidant enzymes and chlorophyll fluorescence parameters in common bean cultivars differing in sensitivity to drought

stress. *Russian Journal of Plant Physiology*, *58*(1), 60–68. https://doi.org/10.1134/S102144371101016X

Sahrawat, A. K., Becker, D., Lütticke, S., & Lörz, H. (2003). Genetic improvement of wheat via alien gene transfer, an assessment. *Plant Science*, *165*(5), 1147–1168. https://doi.org/10.1016/S0168-9452(03)00323-6

Schoen, A., Saripalli, G., Hosseinirad, S., Sharma, P. K., Kajla, A., Yadav, I. S., & Tiwari, V. (2024). Genome Sequences from Diploids and Wild Relatives of Wheat for Comparative Genomics and Alien Introgressions. In R. Appels, K. Eversole, C. Feuillet, & D. Gallagher (Eds.), *The Wheat Genome* (pp. 241–263). Springer International Publishing. https://doi.org/10.1007/978-3-031-38294-9_12

Schreiber, U., Schliwa, U., & Bilger, W. (1986). Continuous recording of photochemical and non-photochemical chlorophyll fluorescence quenching with a new type of modulation fluorometer. *Photosynthesis Research*, *10*(1–2), 51–62. https://doi.org/10.1007/BF00024185

Schulthess, A. W., Kale, S. M., Liu, F., Zhao, Y., Philipp, N., Rembe, M., Jiang, Y., Beukert, U., Serfling, A., Himmelbach, A., Fuchs, J., Oppermann, M., Weise, S., Boeven, P. H. G., Schacht, J., Longin, C. F. H., Kollers, S., Pfeiffer, N., Korzun, V., … Reif, J. C. (2022). Genomics-informed prebreeding unlocks the diversity in genebanks for wheat improvement. *Nature Genetics*, *54*(10), 1544–1552. https://doi.org/10.1038/s41588-022-01189-7

Semba, R. D., Ramsing, R., Rahman, N., Kraemer, K., & Bloem, M. W. (2021). Legumes as a sustainable source of protein in human diets. *Globall Food Security*, *28*.

Shi, R., Seiler, C., Knoch, D., Junker, A., & Altmann, T. (2023). Integrated phenotyping of root and shoot growth dynamics in maize reveals specific interaction patterns in inbreds and hybrids and in response to drought. *Frontiers in Plant Science*, *14*, 1–16. https://doi.org/10.3389/fpls.2023.1233553

Shiogama, H., Watanabe, M., Kim, H., & Hirota, N. (2022). Emergent constraints on future precipitation changes. *Nature*, *602*(7898), 612–616. https://doi.org/10.1038/s41586-021-04310-8

Singh, R., Kumar, K., Purayannur, S., Chen, W., & Verma, P. K. (2022). *Ascochyta rabiei*: A threat to global chickpea production. *Molecular Plant Pathology*, *23*(9), 1241–1261. https://doi.org/10.1111/mpp.13235

Spinoni, J., Vogt, J. V., Naumann, G., Barbosa, P., & Dosio, A. (2018). Will drought events become more frequent and severe in Europe? *International Journal of Climatology*, *38*(4), 1718–1736. https://doi.org/10.1002/joc.5291

Tanksley, S. D., & McCouch, S. R. (1997). Seed Banks and Molecular Maps: Unlocking Genetic Potential from the Wild. *Science*, *277*(5329), 1063–1066. https://doi.org/10.1126/science.277.5329.1063

Tanno, K., & Willcox, G. (2006). The origins of cultivation of Cicer arietinum L. and Vicia faba L.: Early finds from Tell el-Kerkh, north-west Syria, late 10th millennium b.p. *Vegetation History and Archaeobotany*, *15*(3), 197–204. https://doi.org/10.1007/s00334-005-0027-5

Tardieu, F., Cabrera-Bosquet, L., Pridmore, T., & Bennett, M. (2017). Plant Phenomics, From Sensors to Knowledge. *Current Biology*, *27*(15), R770–R783. https://doi.org/10.1016/j.cub.2017.05.055

References

Tardieu, F., Simonneau, T., & Muller, B. (2018). The Physiological Basis of Drought Tolerance in Crop Plants: A Scenario-Dependent Probabilistic Approach. *Annual Review of Plant Biology*, *69*(1), 733–759. https://doi.org/10.1146/annurev-arplant-042817-040218

Tester, M., & Langridge, P. (2010). Breeding Technologies to Increase Crop Production in a Changing World. *Science*, *327*(5967), 818–822. https://doi.org/10.1126/science.1183700

The International Wheat Genome Sequencing Consortium (IWGSC) et al. Shifting the limits in wheat research and breeding using a fully annotated reference genome.Science361,eaar7191(2018).DOI:10.1126/science.aar7191

Thomas, H., & Ougham, H. (2014). The stay-green trait. *Journal of Experimental Botany*, *65*(14), 3889–3900. https://doi.org/10.1093/jxb/eru037

Tietz, S., Hall, C. C., Cruz, J. A., & Kramer, D. M. (2017). NPQ(T): A chlorophyll fluorescence parameter for rapid estimation and imaging of non-photochemical quenching of excitons in photosystem-II-associated antenna complexes: New, rapid probe of non-photochemical quenching. *Plant, Cell & Environment*, *40*(8), 1243–1255. https://doi.org/10.1111/pce.12924

Tschiersch, H., Junker, A., Meyer, R. C., & Altmann, T. (2017). Establishment of integrated protocols for automated high throughput kinetic chlorophyll fluorescence analyses. *Plant Methods*, *13*(1), 1–16. https://doi.org/10.1186/s13007-017-0204-4

Turc, B., Sahay, S., Haupt, J., De Oliveira Santos, T., Bai, G., & Glowacka, K. (2024). Up-regulation of non-photochemical quenching improves water use efficiency and reduces whole-plant water consumption under drought in *Nicotiana tabacum*. *Journal of Experimental Botany*, *75*(13), 3959–3972. https://doi.org/10.1093/jxb/erae113

Uga, Y., Sugimoto, K., Ogawa, S., Rane, J., Ishitani, M., Hara, N., Kitomi, Y., Inukai, Y., Ono, K., Kanno, N., Inoue, H., Takehisa, H., Motoyama, R., Nagamura, Y., Wu, J., Matsumoto, T., Takai, T., Okuno, K., & Yano, M. (2013). Control of root system architecture by DEEPER ROOTING 1 increases rice yield under drought conditions. *Nature Genetics*, *45*(9), 1097–1102. https://doi.org/10.1038/ng.2725

Van De Wouw, M., Van Hintum, T., Kik, C., Van Treuren, R., & Visser, B. (2010). Genetic diversity trends in twentieth century crop cultivars: A meta analysis. *Theoretical and Applied Genetics*, *120*(6), 1241–1252. https://doi.org/10.1007/s00122-009-1252-6

Varshney, R. K., Barmukh, R., Roorkiwal, M., Qi, Y., Kholova, J., Tuberosa, R., Reynolds, M. P., Tardieu, F., & Siddique, K. H. M. (2021). Breeding custom-designed crops for improved drought adaptation. *Advanced Genetics*, *2*(3), e202100017. https://doi.org/10.1002/ggn2.202100017

Varshney, R. K., Gaur, P. M., Chamarthi, S. K., Krishnamurthy, L., Tripathi, S., Kashiwagi, J., Samineni, S., Singh, V. K., Thudi, M., & Jaganathan, D. (2013). Fast-Track Introgression of "QTL-hotspot" for Root Traits and Other Drought Tolerance Traits in JG 11, an Elite and Leading Variety of Chickpea. *The Plant Genome*, *6*(3), 1–9. https://doi.org/10.3835/plantgenome2013.07.0022

Varshney, R. K., Song, C., Saxena, R. K., Azam, S., Yu, S., Sharpe, A. G., Cannon, S., Baek, J., Rosen, B. D., Tar'an, B., Millan, T., Zhang, X., Ramsay, L. D., Iwata, A., Wang, Y., Nelson, W., Farmer, A. D., Gaur, P. M., Soderlund,

C., … Cook, D. R. (2013). Draft genome sequence of chickpea (Cicer arietinum) provides a resource for trait improvement. *Nature Biotechnology*, *31*(3), 240–246. https://doi.org/10.1038/nbt.2491

Varshney, R. K., Thudi, M., Nayak, S. N., Gaur, P. M., Kashiwagi, J., Krishnamurthy, L., Jaganathan, D., Koppolu, J., Bohra, A., Tripathi, S., Rathore, A., Jukanti, A. K., Jayalakshmi, V., Vemula, A., Singh, S. J., Yasin, M., Sheshshayee, M. S., & Viswanatha, K. P. (2014). Genetic dissection of drought tolerance in chickpea (Cicer arietinum L.). *Theoretical and Applied Genetics*, *127*(2), 445–462. https://doi.org/10.1007/s00122-013-2230-6

Varshney, R. K., Thudi, M., Roorkiwal, M., He, W., Upadhyaya, H. D., Yang, W., Bajaj, P., Cubry, P., Rathore, A., Jian, J., Doddamani, D., Khan, A. W., Garg, V., Chitikineni, A., Xu, D., Gaur, P. M., Singh, N. P., Chaturvedi, S. K., Nadigatla, G. V. P. R., … Liu, X. (2019). Resequencing of 429 chickpea accessions from 45 countries provides insights into genome diversity, domestication and agronomic traits. *Nature Genetics*, *51*(5), 857–864. https://doi.org/10.1038/s41588-019-0401-3

Walter, A., Liebisch, F., & Hund, A. (2015). Plant phenotyping: From bean weighing to image analysis. *Plant Methods*, *11*(1), 14. https://doi.org/10.1186/s13007-015-0056-8

Wilkinson, M. D., Dumontier, M., Aalbersberg, Ij. J., Appleton, G., Axton, M., Baak, A., Blomberg, N., Boiten, J.-W., Da Silva Santos, L. B., Bourne, P. E., Bouwman, J., Brookes, A. J., Clark, T., Crosas, M., Dillo, I., Dumon, O., Edmunds, S., Evelo, C. T., Finkers, R., … Mons, B. (2016). The FAIR Guiding Principles for scientific data management and stewardship. *Scientific Data*, *3*(1), 160018. https://doi.org/10.1038/sdata.2016.18

Zait, Y., Shemer, O. E., & Cochavi, A. (2024). Dynamic responses of chlorophyll fluorescence parameters to drought across diverse plant families. *Physiologia Plantarum*, *176*(5), e14527. https://doi.org/10.1111/ppl.14527

Zaiter, H. Z., & Barakat, S. G. (1995). Flower and pod abortion in chickpea as affected by sowing date and cultivar. *Canadian Journal of Plant Science*, *75*(2), 321–327. https://doi.org/10.4141/cjps95-056

Zamir, D. (2001). Improving plant breeding with exotic genetic libraries. *Nature*, *2*, 983–989.

List of abbreviations

ABA	abscisic acid (plant hormone)
BC_2F_3	two cycles of back-crossing with the elite parent followed by three generations of selfing
DArT	diversity arrays technologie marker
E	environmental influence
FAO	Food and Agriculture Organization
F_v/F_m	maximal quantum efficiency photosystem ii
G	genotype
GWAS	genome wide association study
HTP	High-throughput Phenotyping
NIL	near isogenic line
NIL-B-7A -2	near isogenic line, elite parent BarNir, carrying introgressed QTL on chromosome 7a, 2 is the number of line
NPQ	non-photochemical quenching
$NPQ_{(T)}$	theoretical non-photochemical quenching
P	phenotype
PAM	pulse amplitude modulation
PGR	plant genetic resources
PsbS	photosystem II subunit S
PSII	photosystem II
QA	plastoquinon A
QTL	quantitative trait loci
r	coefficient of correlation
RIL	recombinant inbred line
RT-qPCR	real-time quantitative polymerase chain reaction
SPAD	soil plant analysis development (SPAD) chlorophyll meter
SSR	simple sequence repeats
UAV	unmanned aerial vehicle
WUE	water use efficiency
ΦPSII	operating efficiency of photosystem II

List of figures

List of tables

Appendix

Declaration under oath / Eidesstattliche Erklärung

I declare under penalty of perjury that this thesis is my own work entirely and has been written without any help from other people. I used only the sources mentioned and included all the citations correctly both in word and in content.

Ich erkläre an Eides statt, dass ich die Arbeit selbstständig und ohne fremde Hilfe verfasst, keine anderen als die von mir angegebenen Quellen und Hilfsmittel benutzt und die den benutzten Werken wörtlich oder inhaltlich entnommenen Stellen als solche kenntlich gemacht habe.

Gatersleben, 25.02.2025

Madita Lauterberg

Acknowledgments / Danksagung

Bei Prof. Dr. Klaus Pillen, meinem Doktorvater und Leiter der Professur für Pflanzenzüchtung der Martin-Luther-Universität Halle-Wittenberg (MLU) möchte ich mich für die Möglichkeit der Promotion und der Zusammenarbeit mit Dr. Kerstin Neumann, meiner Betreuerin am Leibniz-Institut für Pflanzengenetik und Kulturpflanzenforschung (IPK) in Gatersleben, bedanken.

Besonders möchte ich mich bei Dr. Henning Tschiersch und Dr. Kerstin Neumann bedanken. Wir haben viele interessante und konstruktive Diskussionen führen können. Die Möglichkeit meine eigenen Ideen einzubringen und Hennings unerschöpflichen und vielfältigen Wissensschatz werde ich in sehr guter Erinnerung behalten.

Zudem gilt mein Dank Prof. Dr. Andreas Graner, Ute Krajewski und Ingo Mücke für all die Zeit und Geduld die Ihr euch genommen habt um mir vieles zu erklären und greifbarer zu machen; sowie den Gärtnern und technischen Mitarbeitern ohne die die Durchführung der Versuche und unmöglich gewesen wäre.

Mein Dank gilt auch meinen Projektpartnern von STARGATE, sowie den INCREASE Projektpartnern Prof. Dr. Roberto Papa, Prof. Dr. Luis Guasch, Dr. Elena Bitocchi sowie Dr. Elisa Bellucci.

Abschließend gilt mein Dank meinem Partner, meiner Familie, meinen Freunden, Feodora und meinen Trainingspartnern. Ohne Euch hätte ich das alles nicht schaffen können.

Curriculum vitae

Madita Maria Lauterberg

Professional Experience

02/2021 – 08/2024 PhD student at Leibniz-Institute for Plant Genetics and Crop Plant Research (IPK) Gatersleben, Germany
Working group "Automated Plant Phenotyping", Dr. Kerstin Neumann
PhD thesis: „Utilizing High-throughput Phenotyping to dissect Plant Genetic Resources of Wheat and Chickpea under Drought Stress".

Publications

Lauterberg, M., Tschiersch, H., Zhao, Y., Kuhlmann, M., Mücke, I., Papa, R., Bitocchi, E., & Neumann, K. (2024). Implementation of theoretical non-photochemical quenching ($NPQ_{(T)}$) to investigate NPQ of chickpea under drought stress with High-throughput Phenotyping. *Scientific Reports*, 14(1), 13970. https://doi.org/10.1038/s41598-024-63372-6

Lauterberg, M., Tschiersch, H., Papa, R., Bitocchi, E., & Neumann, K. (2023). Engaging Precision Phenotyping to Scrutinize Vegetative Drought Tolerance and Recovery in Chickpea Plant Genetic Resources. *Plants* 12, 2866. https://doi.org/10.3390/plants12152866

Lauterberg, M., Saranga, Y., Deblieck, M., Klukas, C., Krugman, T., Perovic, D., Ordon, F., Graner, A., & Neumann, K. (2022). Precision phenotyping across the life cycle to validate and decipher drought-adaptive QTLs of wild emmer wheat (*Triticum turgidum* ssp. *dicoccoides*) introduced into elite wheat varieties. *Frontiers in Plant Science*, 13. https://doi.org/10.3389/fpls.2022.965287

Conference Contributions

28.04.2021 INCREASE Annual Meeting, Ancona, Italy
Talk: Progress of the chickpea High-throughput Phenotyping experiments

05.11.2021 Cereal Biotechnology and Breeding 5 (CBB5) (online),
Talk: Precision phenotyping for root and shoot development under contrasting water regimes to characterize wild emmer (*Triticum turgidum* ssp. *dicoccoides*) QTL that improve grain yield under drought in durum (*T. turgidum* ssp. *durum*) and bread wheat (*T. aestivum*)

12.-15.09.2022 INCREASE Annual Meeting, Ancona, Italy
Talk: Evaluation of genetic resources of chickpea (*Cicer arietinum* L.) using non-invasive phenotyping under drought stress to describe and exploit the diversity of biomass accumulation

09.2022 Institute's day IPK Gatersleben

Poster: Evaluation of chickpea (*Cicer arietinum* L.) genetic resources for drought tolerance by precision phenotyping

13.-14.03.2023 GPZ Meeting, Genome Analysis, MLU Halle

Talk: Searching for donor genotypes in chickpea (*Cicer arietinum* L.): utilizing precision phenotyping to scrutinize vegetative drought tolerance throughout plant genetic resources

08.10.2022 Crops4Future, IPK Gatersleben

Speaker of the discussion with pupils

06.04.2022 Bioökonomiekongress, Metropolregion Mitteldeutschland

Poster: Präzisionsphänotypisierung zur Erfassung der Diversität von Kichererbsen (*Cicer arietinum* L.) unter Trockenstress

17.08.2022 Botaniker Tagung, Universität Bonn

Talk: Evaluation of genetic resources of chickpea (*Cicer arietinum* L.) using non-invasive phenotyping under drought stress to describe and exploit the diversity of biomass accumulation

24.05.2023 Early career scientist symposium, Gregor-Mendel-Institute Vienna

Poster: Searching for donor genotypes in chickpea (*Cicer arietinum* L.): utilizing precision phenotyping to scrutinize vegetative drought tolerance throughout plant genetic resources

03.07.2023 Plant Science Student Conference, IPK Gatersleben

Co-Chair of the Conference, organized by PhD Board

Poster: Precision Phenotyping across the life cycle to validate and decipher drought-adaptive QTLs of wild emmer wheat (*T. dococcoides*) introduced into elite wheat varieties

Talk: Searching for donor genotypes in chickpea (*Cicer arietinum* L.): utilizing precision phenotyping to scrutinize vegetative drought tolerance throughout plant genetic resources

23.11.2023 Cereal Biotechnology and Breeding 7 (CBB7), Werningerode

Poster: Deciphering the effect of wild emmer (*T. dococcoides*) QTL introduced into elite wheat varieties on root growth by precision phenotyping

07.-10.05.2024 INCREASE Annual Meeting, FAO, Rome, Italy

Talk: Comparison of the photoprotective mechanism of *desi* and *kabuli* under drought stress

Gatersleben, 25.02.2025